Planar Cell Polarity Pathways in Breast Development

A submission to the Faculty of Science, University of Sheffield for the degree of Master of Philosophy

Michael Nesbit

2016

Abstract

Epithelial cells are the building blocks of tissues which line surfaces throughout the body. These cells are robustly arranged into patterns and structures depending on the specialised functions of various organs. How single cells arrange into these structures is a fundamental question in biology. The mammary gland provides an ideal system to study epithelial morphogenesis as it develops post-natally and remodels during adult life. Like many internal organs, mammary epithelia are assembled into a branched network of ducts, with milk producing alveoli developing during pregnancy and lactation. However, the mechanisms which regulate the organisation of epithelial cells into distinct morphological structures remain to be uncovered. This study investigated the hypothesis that ductal morphogenesis could be induced by the following 3 ways: a) collective cell migrations along the length of the duct, b) oriented cell divisions and c) regulated cell shape and intercellular adhesions.

Collective cell behaviours are commonly regulated by Planar Cell Polarity (PCP) proteins, the phenomenon by which cells are polarised in the 2D plane of an epithelium.

When cultured in 3D matrix, mouse mammary epithelial cells form the ducts and branches of the mammary gland. Here we investigated alternative 3D mammary culture techniques and designed tools to analyse PCP pathways in primary organoid cultures. These include shRNA knockdown of Vangl2 and insertion of H2B-RFP to analyse oriented cell division in organoids. PCP in the pubertal developing mammary gland was investigated and reveals Vangl2 protein expression mirrors increased ductal elongation and branching, and Vangl2 localisation to some cell membranes, which suggests that Vangl2 plays roles in the development of mammalian mammary epithelia.

Mammary gland morphology was investigated using a 3D immunofluorescence and microscopy technique of whole mount tissue, and we showed a distinct organisation of myoepithelial cells around elongating ducts. By understanding the mechanisms of epithelial morphogenesis under normal conditions, we understand more how these processes could function abnormally in disease states such as cancer.

Declaration

I hereby declare that this thesis has been composed by the undersigned Michael Nesbit for the degree of MPhil at the University of Sheffield. This work has not been presented in any previous application for a degree and all work was performed by the undersigned unless otherwise dictated in the text. All sources of information used have been specifically acknowledged in the text.

Michael Nesbit, September 2016

Acknowledgements

I would like to thank my supervisors Dr. Nasreen Akhtar and Professor David Strutt for allowing me to work in their labs and their guidance throughout this project. I would also like to thank past and present members of the Strutt Lab for their support. Thanks to Dr Darren Robinson and Dr Nick Van-Hateren for imaging assistance in the Light Microscopy Facility, and Professor Gillian Tozer and The Department of Oncology for allowing me to use their space and equipment. Thanks to the Biomedical Science Department staff and students for creating a pleasant working environment and Interval Café Bar for obvious reasons. Thanks also to Nathaniel Baldwin and John C Moss for inventing headphones.

Contents

Introduction

Between the first and last moment in the life of every organism on Earth, an extraordinarily complex yet flawless cascade of molecular processes occur. A significant proportion of these events have changed very little from the earliest living beings up to humans, elephants or jellyfish of today, most of all the pathways which facilitate basic survival, growth and metabolism. However with the development of complex multicellular life about 1.5 billion years ago, cells started working together, creating structures which performed specific functions to serve the organism as a whole. Consider humans, who have a massive branched network of tubes which supply our blood with oxygen so that every cell in our body has the opportunity to thrive; a 30ft long digestive tract to convert our food into nutrients; and waste treatment plants in our liver and kidneys. All ultimately developed from one fertilised egg cell, which housed the blueprint to become over 30 trillion cells working in synergy to provide opportunity of survival of each person, and pass on these instructions for the next generation. However, how cells collectively produce patterns and structure essential for the correct function of tissues is a fundamental question of biology. By focussing on the mechanisms which may regulate these processes, we hope to provide some answers to this question.

Epithelial Morphogenesis

Most organs in the mammalian body are a network of tubes which are lined by epithelial cells, single components of which act as both structural building blocks and functional units. Epithelial tissues develop from a relatively small number of cells which follow intrinsic rules to divide, specialise and rearrange to produce specific patterns largely conserved across individuals and species, which also rearrange and recycle during adulthood. Understanding how epithelial organs develop, and what happens when things go wrong in disease, requires us to dissect the cellular and molecular mechanisms which drive these changes.

Three events occur in the formation of some tubular mammalian epithelial structures, for example a placode in the embryo in mammary gland development: Firstly, cells need to be specified to an epithelial lineage; then they will generate a single central lumen, and finally they will elongate and branch. Branching is essential to increase surface area for absorption, secretion or exchange within limited 3D space.

There are many cellular mechanisms and physical forces which regulate the formation of tubular organs. A common mechanism of tube formation is ‘budding’, in which cell migration and proliferation from existing tubular epithelia drive growth, for example in angiogenesis (Chung and Andrew, 2008).

It is important to note that some tubular organs form by other methods, as shown in **Figure 1**. For example, the neural tube arises after cellular 'wrapping' of an epithelial sheet into a tube, which then detaches from the sheet (Lubarsky and Krasnow, 2003; Sawyer et al., 2010). Lumens are also generated where two cells generate a lumen between themselves which expands. This method, observed in Drosophila heart formation is known as 'entrapment' (Medioni et al., 2008; Santiago-Martínez et al., 2008). It is also important that lumens are kept clear of debris to allow unobstructed flow, requiring maintenance such as ‘cavitation’, the apoptosis of cells detached from the epithelium (Humphreys et al., 1996; Jaskoll and Melnick, 1999), though this process is thought to play no role in establishing apicobasal polarity. It is unclear whether tubular epithelium development is directionally driven by polarity established within and across groups of epithelial cells as well as apicobasal polarity, which may be important to regulate correct growth in large multicellular tissues.

Mammary Gland Development

The study of epithelial morphogenesis in the past has mostly been achieved through the imaging of fixed tissues at various stages, or live imaging of ‘lower’ organisms such as Drosophila. However with the advent of new techniques in live imaging and the culture of live organoids, it is now possible to observe the behaviours of cells and their proteins in real time. The mammary gland is favoured as a model to study morphogenesis as unlike other organs which develop a) within the body cavity and b) during embryonic growth, most mammary gland development occurs a) under the skin, b) during puberty and c) remodels during adult life in pregnant individuals.

Early mammary gland development occurs between E11-18 in the mouse with the formation of mammary placodes along the milk lines. Epithelial buds begin to invade into the fat pad and the first lumens are formed (Veltmaat et al., 2003). Little mammary growth occurs until puberty, when under control of growth hormone and oestrogen, terminal end

i) Budding

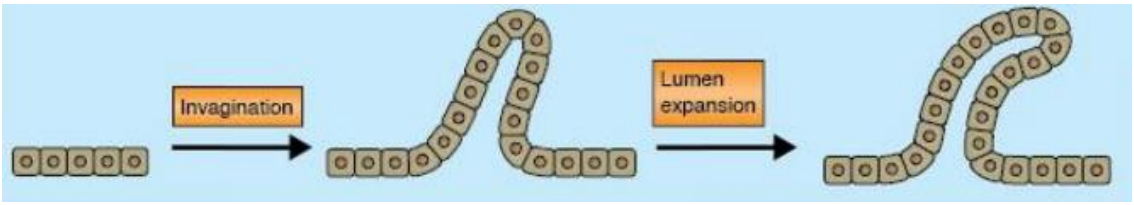

ii) Wrapping

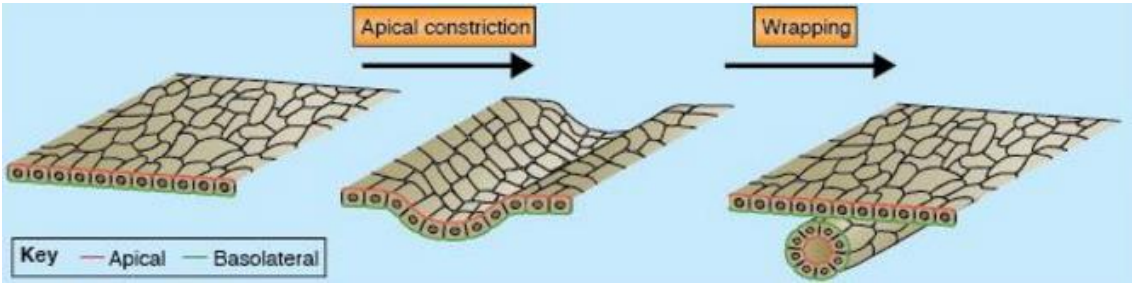

iii) Entrapment

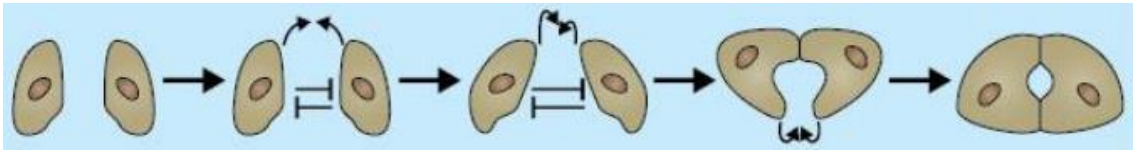

Figure 1 Modes of tubulogenesis

Diagrams depicting how some tubular organs develop from non-tubular arrangements (images taken from a poster by Irulea-Arispe and Bietel, 2013). i) In budding, cells in a tube or sheet invaginate to produce a new tubular structure. ii) during neural tube formation, a line of cells in a sheet constrict their apical membranes producing a tube before pinching off. iii) cells can come together, producing a lumen in a gap between them, for example during Drosophila embryonic heart formation.

buds (TEBs) at the end of the ducts invade into the fat pad, branching to create an extensive mammary tree (Ball, 1998).

The function of the mammary gland is to produce and secrete milk to feed young offspring. These take many different forms, from the breasts of a human to the udders of a cow. During pregnancy, mammary epithelia undergo a rapid transformation due to increased growth and branching, leading to formation of alveoli along and at the termini of the ducts. Luminal epithelial cells, which make up the apical layer of the ducts, synthesise milk proteins and secrete milk into the lumen during lactation. Milk is then squeezed through the duct towards the nipple by contractile myoepithelial cells which lie basally to luminal epithelial cells, to be received by the suckling infant. After the infant is weaned, luminal cells cease milk secretion and the mammary gland returns to its pre-pregnant state through the involution process (reviewed by Macias & Hinck, 2012). These stages are reviewed in **Figure 2**.

The mammary gland consists of a double layer of epithelial cells as shown in **Figure 3**. Luminal epithelial cells have a typical cuboidal/columnar shape, apico-basal polarity and are joined by adherens junctions. Basally is a layer of contractile myoepithelial cells, which do not form tight junctions between themselves or luminal cells and are known to be cellular tumour suppressors (Sternlicht et al., 1997). How myoepithelial cells contribute to the structural development of the mammary gland is unclear, whether through mechanical force or intercellular signalling, however they are required to form functional mammary epithelia and establishing apico-basal polarity of luminal cells. Both luminal and myoepithelial cells differentiate from the highly proliferative multi-layered terminal end bud (TEB) at the tip of the duct. The TEB invades the fat pad as the duct elongates, leaving behind layers of polarised epithelial cells (Pechoux et al., 1999). TEB morphology is shown in **Figure 4**. The mechanisms which drive moulding of the duct into its characteristic tube shape in the wake of the TEB are not known, however it may be caused by force exerted by myoepithelial cells wrapping around the duct. Secreted by the myoepithelial cells is a laminin-rich basement membrane, which forms a divide between mammary epithelia and the extracellular matrix. The basement membrane plays an important role in signalling to mammary epithelial cells, including induction of milk protein expression (Streuli et al., 1991).

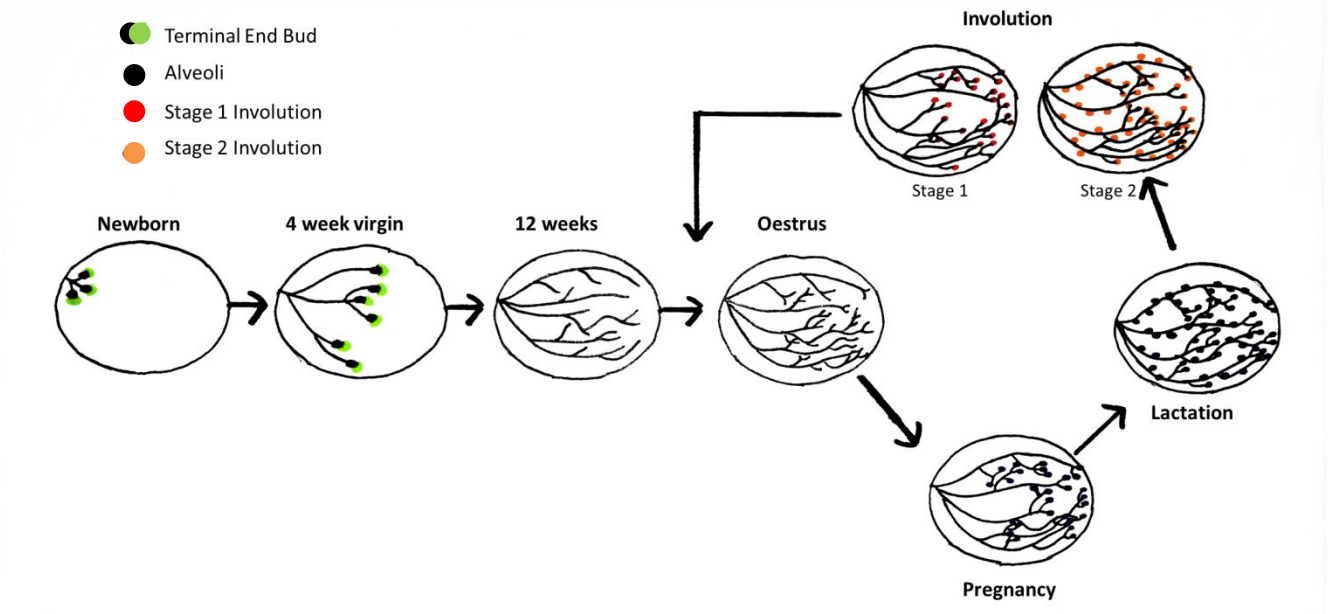

Figure 2 Stages of mammary gland development

Most mammary gland proliferation and branching occur during puberty at weeks 4-12 under influence of hormones including oestrogen. When a mouse is pregnant, oestrogen and progesterone drive increased proliferation and branching and the formation of secretory alveoli throughout the glandular tree. In late pregnancy, prolactin mediates further alveogenesis and milk production. After infants are weaned, milk production ceases and the mammary gland is remodelled during the involution stage. The mammary gland is capable of repeating this cycle during later pregnancies.

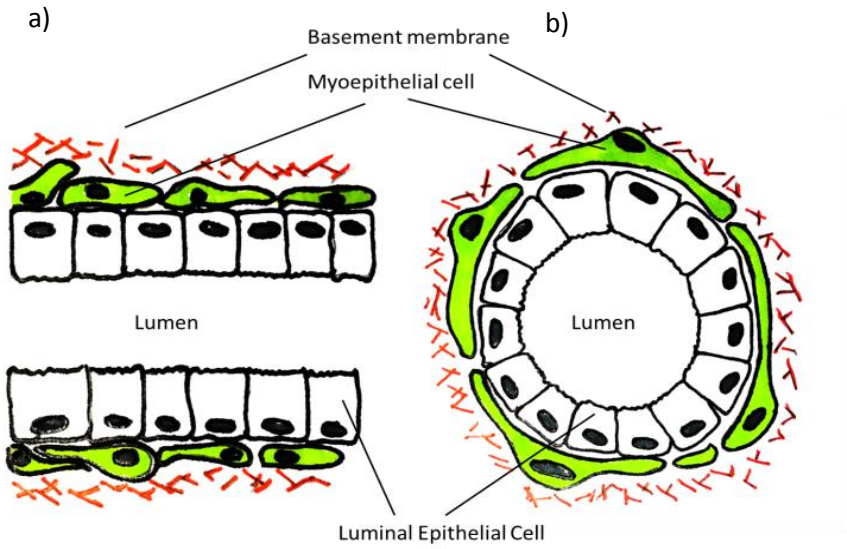

Figure 3 Schematic Diagram of the Quiescent Mammary Gland Duct

Luminal epithelial cells (white) are subtended by myoepithelial cells (green), which secrete and sit on a laminin basement membrane (red). Luminal epithelial cells make up a single layer joined at the apical face by tight and adherens junctions. The lumen is kept clear of cells.
Views are a) longitudinal section and b) cross section of the duct.

The branching of tubular organs is essential to provide enough surface area for gas and fluid movement, transfer and secretion. Branching of tubes can occur by different modes, including lateral branching as in the pancreas (Puri and Hebrok, 2007), two way branching (bifurcation) and planar branching as in the lung (Metzger et al., 2008), and three way branching (trifurcation). However, branching in the breast has no stereotypic repeating pattern. Evidence from 3D organoid cultures suggest that mammary branching in part relies on mechanical constraints imposed by surrounding myoepithelial cells and interactions with the extracellular matrix (Ewald et al., 2008). Growth and branching of mammary epithelium is also driven by stresses exerted by the tissue itself outward towards the extracellular matrix (Gjorevski and Nelson, 2010, 2012). Other factors which may direct mammary branching include fibrils of collagen already present within the stroma, which may lay out a path for development to follow (Brownfield et al., 2013; Guo et al., 2012) and the secretion of metalloproteinases by the cells of the terminal end bud are suggested to overcome resistance of the extracellular matrix along this path (Alcaraz et al., 2011).

Experiments in other organ models suggest some of the cell shape changes epithelia may undergo to initiate branching. Live imaging of pancreas explants shows that branching is preceded by apical membrane constriction of some cap cells producing a furrow, with two branches developing either side. This activity seems to be initiated by cues from the basement membrane through integrins (Shih et al., 2015). Whether apical constriction events prior to branching occur in development of other organs is unclear, however this could be analysed using organoid cultures of other tissues, for example the mammary gland.

Live imaging of mammary organoids show that elongation is driven by division of luminal cells which grow into gaps in myoepithelial cell coverage. Division of single ducts into multiple branches is observed in places where myoepithelial cells obstruct the TEB (Ewald et al., 2008) as shown in **Figure 5**. As luminal and myoepithelial cells differentiate from progenitors in the tip of the TEB, it is possible that myoepithelial differentiation reduces growth in the middle of the TEB resulting in branching into two ducts.

It is clear that epithelial cells are capable of producing these tubular structures by following a defined set of rules, which result in repeated patterns across various organs and species. To do this effectively, cells are required to alter their behaviour to suit the context of the

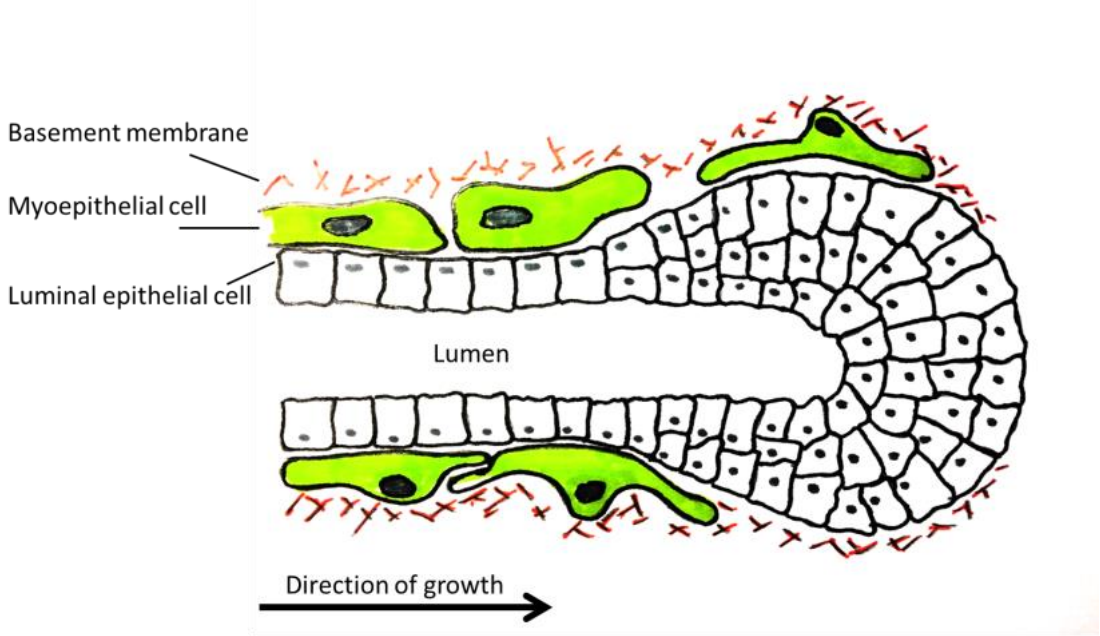

Figure 4 Schematic view of the Terminal End Bud (TEB) during pubertal development

The TEB consists of a multi-layered epithelium of luminal epithelial cells at the distal end. These cells are highly proliferative and contain stem cell populations which differentiate into both luminal and myoepithelial cells. Proximal to the TEB is the single layered duct, where the luminal cells display apico-basal polarity. Establishment of apico-basal polarity is set up as cells contact the extracellular matrix (ECM) and transduce signals through integrins. Luminal epithelial cells (white), myoepithelial cells (green), basement membrane (red).

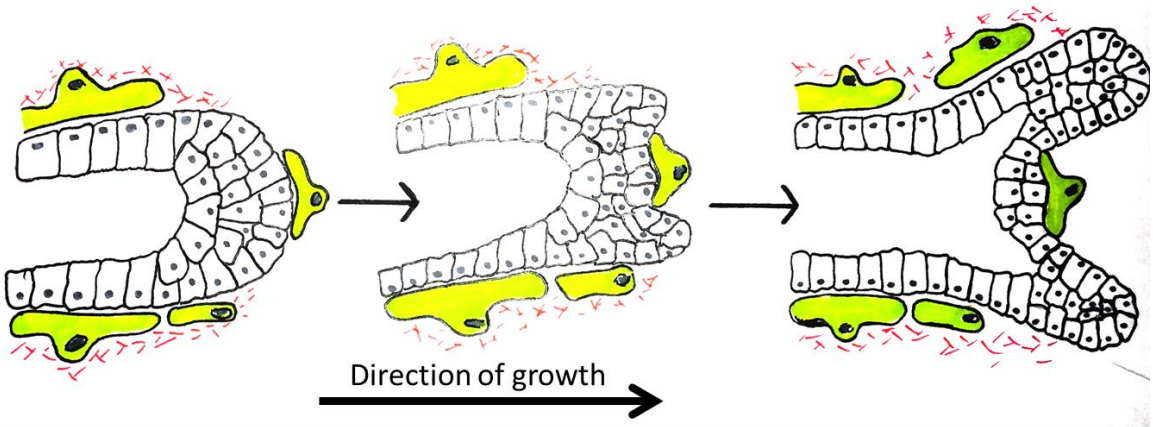

Figure 5 Schematic diagram showing TEB branching due to myoepithelial cell coverage

Evidence in live organoid cultures suggest that branching may occur where the growing TEB is obstructed by myoepithelial (ME) cells. This is as the duct usually grows in gaps in ME cell coverage.

overall tissue, whether in direction of collective cell migration, orientation of cell division, or tight control of their shape. We hypothesise that Planar Cell Polarity pathways are active in developing mammary epithelia and are required to produce proper morphology.

Planar Cell Polarity

Planar cell polarity (PCP) describes the phenomenon by which cells are organised in a 2-dimensional plane perpendicular to the apicobasal axis. PCP pathways and their homologues have been identified in several tissues and to control several important developmental mechanisms in morphogenesis. Loss or mutation of PCP proteins often results in viable but misshapen tissues, from the fly wing to the mouse lung, heavily suggesting that PCP pathways play essential roles in the patterning of organisms.

The hairs (or trichomes) on a Drosophila wing usually orientate pointing distally. The observation that some Drosophila mutants displayed abnormal hair polarity (Gubb and Garcia-Bellido, 1982) led to the identification and characterisation of proteins organising polarity at a cellular level over the last 32 years. There are two PCP protein pathways which establish planar polarity in *Drosophila:* the 'core' pathway consists of *frizzled, dishevelled, strabismus, prickle* and *diego;* and the *fat/dachsous* system. The first planar cell polarity protein to be identified was Frizzled, a 7-pass transmembrane receptor (Vinson et al., 1989) which also functions as a Wnt receptor in canonical Wnt signalling (Bhanot et al., 1996). The mutation or loss of *frizzled* results in significant polarity defects, with trichomes initiating in centre of cells (Wong and Adler, 1993). Importantly, the protein products of these genes are localised asymmetrically in developing wing cells (Strutt, 2001; Bastock et al., 2003) shortly before planar polarity is manifested in localisation of the actin-rich trichome in the pupal wing, as shown in **Figure 6**. Asymmetric localisation of core proteins is thought to result from feedback interactions between proximally and distally localising components (Strutt, 2001). In the *Drosophila* wing, these result in the distal localisation of the transmembrane protein Frizzled (Strutt, 2001) and the cytoplasmic proteins Dishevelled (Axelrod, 2001) and Diego (Feguin et al., 2001). Contrastingly, on the proximal cell edges are the transmembrane protein Strabismus (Bastock et al., 2003) and cytoplasmic Prickle (Tree et al., 2002). The cadherin protein Starry night/ Flamingo is localised both proximally and distally and adheres homophilically (Usui et al., 1999) across cell junctions (**Figure 7**). Flamingo is localised stably

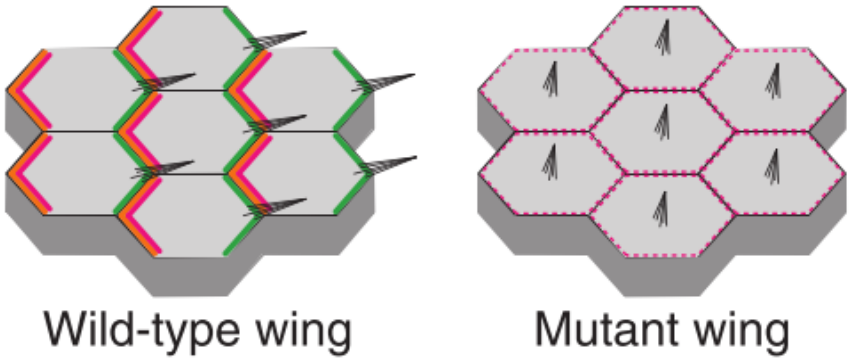

Figure 6 Schematic representations of PCP in the pupal wing

In the wild type wing, *frizzled, dishevelled and diego* (green) are localised distally, with *strabismus*, *prickle* (orange) and effectors which repel trichome initiation: *fuzzy, fritz and multiple wing hairs* (red) recruited proximally. The trichome initiates distally. In PCP mutant wings, core protein localisation is lost and the trichome initiates in the cell centre. (Diagram taken from Goodrich and Strutt, 2011)

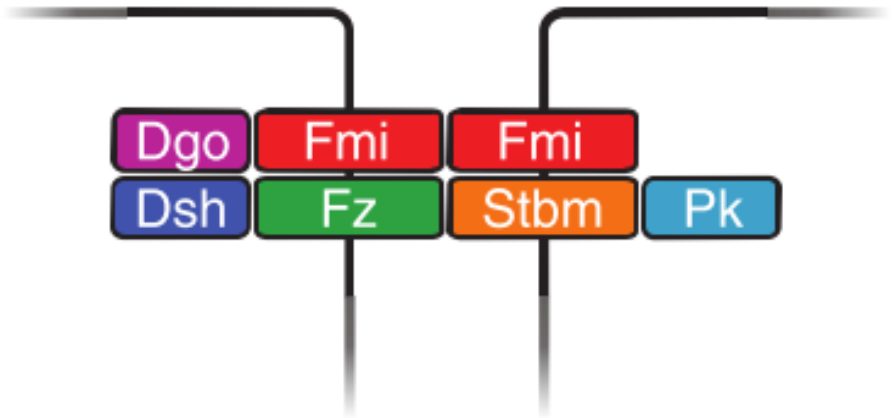

Figure 7 Core protein asymmetry at D*rosophila* wing cell boundaries

At vertical cell junctions of pupal *Drosophila* wing, core PCP proteins localise asymmetrically in puncta. Both cell junctions have the cadherin *flamingo* which homophilically binds across the junction, but associate with different proteins in each cell. In the distal cell, transmembrane *frizzled* interacts with *flamingo* and the intracellular proteins *dishevelled* and *diego.* On proximal membranes (right), *strabismus* interacts with *flamingo* and its intracellular binding partner *prickle*.

at junctions in complexes with Frizzled and Strabismus (Usui et al., 1999). In their absence, Flamingo is found in the apical plasma membrane. This may be as Flamingo at proximal and distal junctions is endocytosed at a higher rate when not bound in complexes with Frizzled and Strabismus (Strutt and Strutt, 2008).

Asymmetry is retained from cell to cell over a large area, suggesting these interactions dictate overall tissue polarity, and a polarised cell can define the polarity of its neighbours. This is evident in *Drosophila* wings, as patches of cells lacking *frizzled* activity in a wildtype background cause trichomes of non-mutant cells to point towards the *frizzled* mutant clones instead of pointing distalward normally (Vinson and Adler, 1987), shown schematically in **Figure 8**. *Van Gogh/strabismus* functions in the opposite way, as in *strabismus* mosaic mutants surrounding host cell trichromes point away from mutant cells (Taylor et al., 1998).

In *Drosophila* wing cells, PCP core proteins localise at vertical junctions in a punctate pattern (Strutt and Strutt, 2011). These punctae are reduced in size and stability in core polarity gene mutants. The intracellular proteins Dishevelled, Prickle and Diego are not required for the initial association of Frizzled, Strabismus and Flamingo into complexes (Lawrence et al., 2004). They may however amplify asymmetry by negative feedback mechanisms. For example, Prickle localises to the proximal side of cells where it inhibits Dishevelled membrane binding, consequently antagonising Frizzled accumulation at the proximal cell edge (Tree et al., 2002). Further negative interactions are observed between Diego and Prickle (Das et al., 2004), and between Strabismus and Dishevelled (Bastock et al., 2003). It is unknown whether PCP mechanisms produce such asymmetry and propagate as efficiently in development of mammalian epithelial tissues.

Planar polarity is promoted by ‘effector’ genes, which act downstream of the core planar polarity genes. One of the most obvious readouts is the formation of a trichrome on a fly wing, a process regulated by the effector multiple wing hairs (*mwh*) (Wong and Adler, 1993). mwh encodes a protein with a GTPase binding/formin-homology domain (GBD/FH3) (Strutt and Warrington, 2008) which localises proximally and inhibits actin polymerisation in the proximal part of the cell (Yan et al., 2008). Planar polarity pathway effectors which act upstream of *mwh* include *inturned* (Adler et al., 2004), *fuzzy* (Lee and Adler, 2002) and *fritz* (Collier et al., 2005).

The *fat/dachsous* pathway is another regulator of planar polarity. These genes encode cadherins which asymmetrically interact between neighbouring cells (Brittle et al., 2010, 2012). Like the core proteins, *fat/dachsous* mutations cause cell-nonautonomous disruption to the polarity of neighbouring cells (Adler et al., 1998). It is suggested that the *fat/dachsous* system orientates core planar cell polarity proteins by transducing tissue level directional cues encoded by expression gradients of the golgi protein Four-jointed (Zeidler et al., 2000; Strutt et al., 2004). The Fat/Dachsous pathway may establish polarity upstream of the core pathway (Harumoto et al., 2010), however both pathways largely work autonomously so are most likely independent.

Evidence for PCP in Fish, Frogs and Mice

Planar Cell Polarity pathways are important in patterning tissues throughout the animal kingdom, with increasing evidence implicating PCP homologues in processes as diverse as gastrulation in fish, to lung development in mice.

Strabismus has two highly conserved mammalian homologues: Van Gogh-like proteins 1 and 2 (Vangl1 and Vangl2). All homologues contain 4 transmembrane spanning regions and PDZ protein interaction domains at the C-terminus (Wolff and Rubin, 1998). Vangl2 function has been studied in various tissues by analysis of Looptail mouse mutants, a naturally occurring strain (Strong and Hollander, 1949) which has a mutation in the cytoplasmic domain of Vangl2, resulting in protein sequestration in the endoplasmic reticulum. Whereas homozygous mutants do not survive due to failed neural tube closure (Kibar et al., 2001), in surviving Lp+/- mice, Vangl2 interacts with other PCP proteins in the protein synthesis pathway, including Vangl1, exacerbating mutant phenotypes (Yin et al., 2012).

Similarly to the fly wing, asymmetric localisation of PCP proteins is observed in some mammalian tissues, for example in arranging polarity of hair cells in the mouse inner ear. This is important as hair cells are excited or inhibited depending on the direction of mechanical stimulation by vibrations through air which allow accurate hearing (Hudspeth et al., 1977). In wild type E18.5 mouse inner ears, the outer hair cells are arranged in rows with stereocilia all pointing in one direction, however in lp+/- mice or mice expressing mutant Vangl2 lacking a transmembrane domain, (Vangl2 $_{\Delta TMs/Lp}$), stereocilia polarity is lost (**Figure 9**). This polarity is preceded by the asymmetric localisation of Vangl2 along the axis of

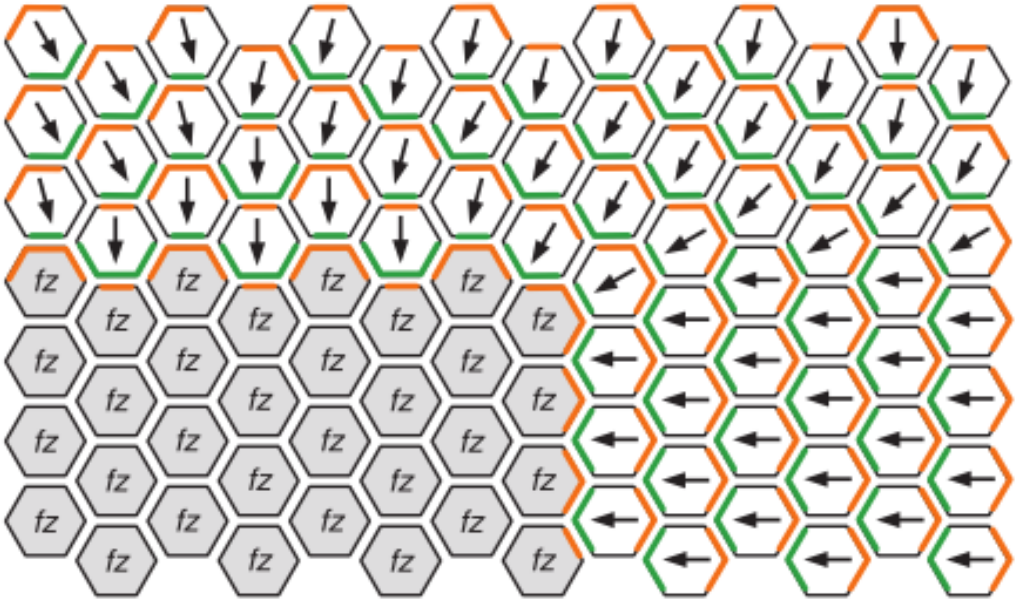

Figure 8 Schematic representation tissue polarity in mutant *frizzled* clone wings

Trichome polarity (arrows) in wild type wings goes from proximal to distal (left to right on this diagram). Cells lacking *frizzled* (grey) only express *strabismus* (orange), which interacts with *frizzled* (green) on neighbouring wild type cells. This propagates throughout neighbouring cells and results in orientation of trichromes towards the *frizzled* clones. (Goodrich and Strutt, 2011).

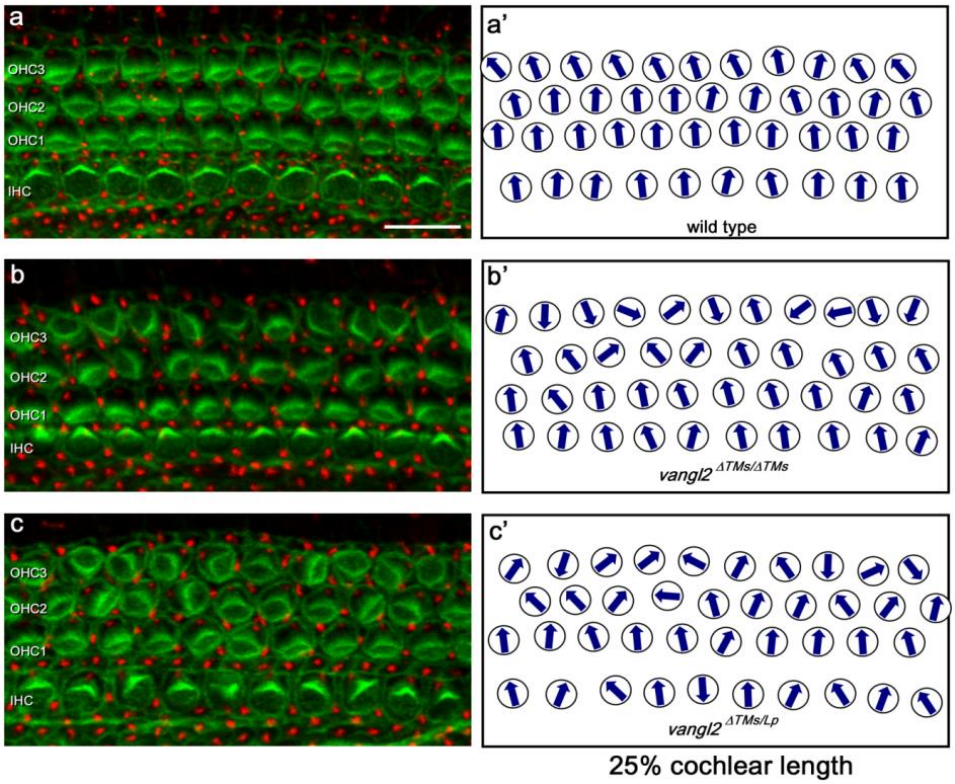

Figure 9 Planar cell polarity phenotypes in the inner ear

Planar cell polarity phenotypes in Vangl2 mutant mouse inner ears. Stained for phalloidin (green) and pericentrin (red), E18.5 b) and b') show that in a *Vangl2* total mutant (which has lost its TM domain exon via Cre/Lox deletion), significant polarity defects occur. c) and c') show that when this mutant is crossed with a looptail mouse, polarity is disturbed even further, perhaps due to further sequestration of Vangl1. (Yin et al., 2012).

polarity, to the inner edge of inner hair cells and the distal edge of supporting cells (Montcouquiol, 2006). Similar polarity defects in the inner ear occur in mutants for a mammalian *flamingo* homologue, *Celsr1* (Curtin et al., 2013) in both mice and chick (Davies et al., 2005). Asymmetric localisation of Vangl1 and Frizzled6 is observed in the mouse trachea during development (Vladar et al., 2012), as well as at apical junctions between multicilliated cells in lung epithelium, prior to polarised ciliary orientation (Vladar et al., 2015).

As well as regulating planar polarity of hairs on a fly wing, PCP pathways play an important role in orienting mammalian epidermal hairs, first observed in the swirling hair pattern on the back of Frizzled6 null mice (Guo et al., 2004). In mouse epidermis, Frizzled6, Vangl2 and Celsr1 display specific asymmetric localisation within basal epidermal cells and are required to establish hair follicle polarity (Devenport et al., 2008). In looptail and crsh mutant mice, asymmetry of these proteins is lost resulting in development of unpolarised hair follicles.

Intriguingly, planar cell polarity pathways are an essential part of some morphogenetic events in development, including roles in collective cell migration, oriented cell division and cell shape, driving pattern formation in epithelial tissues.

An early event in embryo development is convergent extension, a morphogenetic process in which cells converge medially to extend the tissue at the long axis. In PCP mouse mutants and in Xenopus and zebrafish with knocked down PCP activity, convergent extension fails and the neural tube fails to close, resulting in lethality. In wildtype zebrafish embryos, a plate of unpolarised cells converge on the dorsal midline and divide along the medio-lateral axis (Kimmel et al., 1994), with one cell crossing the midline and gaining apicobasal polarity (Tawk et al., 2007). In PCP mutants, cell divisions occur on both sides of the midline resulting in two duplicate neural tubes (Ciruna et al., 2006). To intercalate, cells usually display protrusive activity; however this is lost if strabismus is overexpressed in Xenopus embryos (Goto and Keller, 2002). Further studies in Xenopus showed that Vangl2 is enriched along anterior cell borders, which drives medio-lateral folding through feedback with Myosin II (Ossipova et al., 2015).

This event highlights how planar polarisation of cells during a morphogenetic process must be tightly controlled by PCP pathways to result in correct patterning of tissues early in development.

Oriented cell divisions are an important aspect of tubular organ development and elongation, as demonstrated in the mouse kidney (Karner et al., 2009; Saburi et al., 2008) and chick neural tube (Sausedo et al., 1997). This is important as most tubes must retain a constant diameter and single epithelial layers, restricting cell divisions to only the long axis. A good model for studying circumferential polarity is in polycystic kidneys, where deregulation of cell division orientation and proliferation result in large cysts and enlarged luminal spaces (Fischer et al., 2006). To maintain a tubular structure, cells divide along the axis of the renal tube, suggesting some sort of intrinsic polarity is required. This may be regulated via polarisation of cell-cell contacts to the lateral edges of epithelial cells, resulting in polarisation of centrosomes, leading to oriented cell division (Taylor et al., 2010; Zovein et al., 2010).

Loss of planar polarised cell division resulting in disrupted tissue morphogenesis is a contributing factor to polycystic kidney disease. Evidence suggests that mitotic orientation is disrupted in polycystic kidney models, with Pkd mutants showing increased cell division at angles perpendicular to the tube length (Luyten et al., 2010). Frizzled3, a mammalian homologue of the Drosophila protein Frizzled, is upregulated and localised to primary cilia in cystic kidneys, suggesting involvement of planar cell polarity mechanisms in kidney epithelial morphology and cell division polarisation. However, it is unclear whether PCP pathways are involved in orienting cell divisions in development of other mammalian organs.

Both the core and *fat/dachsous* PCP pathways have been shown to affect oriented cell divisions in *Drosophila.* Localisation of *frizzled* and *strabismus* to opposite poles of *Drosophila* SOP cells results in planar polarised asymmetric cell division (Bellaiche et al., 2001, 2004), and mutant clones of *fat, dachsous and dachs* show misoriented mitotic spindles (Baena-Lopez, 2005).

PCP and Cell Shape

All epithelial tissues are structures made up of thousands of cells which control their shape to collectively form a structure, in the same way which cuboidal bricks make up straight wall while wedge shaped bricks would build a tunnel. During development, this is a tightly controlled process to ensure that tissues do not grow too large or too small. This is clearly evident in the *Drosophila* trachea, as even if the trachea develops with only half the normal number of cells, the cells adjust their shape and size to form a fully formed organ with the correct dimensions (Beitel and Krasnow, 2000).

Cells can control their shape by regulation of their actin cytoskeleton, for example by building acto-myosin networks below the apical membrane to drive constriction which can also be transmitted across cells, mediated by adhesion receptors.

Remodelling of intercellular adhesions is important in epithelial morphogenesis through increase or decrease of contacts between neighbouring cells, or restricting adherens junctions to only lateral membranes. Evidence shows that PCP pathways play regulatory roles in adhesions junctions in various tissues.

Endocytosis of e-cadherin can break cell contacts, and the polarisation of this process could drive the direction of tubular elongation, as studied in Drosophila trachea. Localised e-cadherin endocytosis is dependent on asymmetric RhoGEF2 distribution, which is in turn dependent on asymmetric frizzled activity (Warrington and Strutt, 2013). This results in planar polarised e-cadherin mediated adhesion which is lost in PCP mutants.

Planar cell polarity pathway regulation of adherens junctions is also evident in mouse models. In renal epithelial cultures, e-cadherin co-immunoprecipitates with Vangl2, and Vangl2 overexpression increases e-cadherin internalisation (Nagaoka et al., 2014). In lp/+ cultures, surface e-cadherin levels are higher, heavily implicating a role for Vangl2 in e-cadherin endocytosis in mammals.

Regulation of adherens junctions is also suggested to be due to Vangl2 mediated Rac1 localisation. RNAi knockdown of Vangl2 impaired cell-cell adhesion in Madin-Darby Canine Kidney (MDCK) Epithelial Cells and cytoskeletal integrity in HEK293T cells in a Rac1 dependent manner (Lindqvist et al., 2010).

Impaired neural tube adherens junctions were present in both Lp/+ mouse embryos and in mouse embryos overexpressing Vangl2 (Torban et al., 2007). Immunofluorescence of the neural tube at E9.5 shows that in lp/lp, the distribution of Rac1 to the neural tube apical surface is lost, leading to random Rac1 distribution. Studies in human keratinocytes showed that activated Rac1 influences adherens junctions via regulation of clathrin independent endocytosis of e-cadherin, resulting in destabilisation of cell junctions (Akhtar and Hotchin, 2001).

Actomyosin networks are an important regulator of cell and tissue shape, and evidence suggests their interaction with PCP pathways. In *Ciona* notochord, both myosin and *strabismus* colocalise at anterior cell boundaries, however PCP protein polarisation is reliant on myosin, and not vice versa (Smith et al., 2015).

PCP in Epithelial Morphogenesis

Evidence shows that in mammals, PCP pathways play important roles in the development of some epithelial organs. Analysis of looptail and crsh mouse strains shows significant differences in the branching and cell morphology of lungs (Yates et al., 2010). Vangl2 and Celsr1 mutant mice have lung tubes of smaller diameter, with fewer branches and larger lung buds during development. Whereas wildtype E14.5 lungs have a cytoskeletal ring of actin round the lumen, actin in mutants is more diffuse and less organised; however this is not due to defects in apico-basal polarity. These results suggest that PCP pathways may be important in both regulation of cell shape during development or the linking of actin cables between cells across junctions.

Defects may arise early in lung development. Lung explants in culture media show Vangl2 localisation to the tips of growing epithelial buds; however in $lp^{+/-}$ cultures, explants develop with larger and fewer buds (Yates et al., 2010). These results collectively implicate PCP pathways in formation of multicellular actin cables which regulate the diameter of epithelial tubes, although a direct link has not been identified.

PCP in Cancer

Planar Cell Polarity pathways play roles in pathways during the development of tissues and organs, at times when cells are dividing, migrating and rearranging. Most cancers occur as a result of these developmental pathways activating in the wrong time and place, rendering the investigation into human development an integral part of cancer research.

Analysis of human cancer tissue samples show that Vangl2 is consistently upregulated in breast, ovarian and uterine carcinomas and others. Cancer genomics databases show Vangl2 is overexpressed in 24%, and amplified in 13% of invasive breast carcinomas (Cerami et al. 2012, Gao et al. 2013) and Vangl1 overexpression is implicated in shorter overall survival in ER+ breast cancer patients (Gyorffy et al., 2010).

Vangl2 has recently been directly implicated in a subset of basal breast cancers, relatively rare forms of breast cancers which arise from myoepithelial cells. Due to the lack of clear drug targets like oestrogen or progesterone receptors, these cancers are more difficult to treat and have worse prognosis for patients. Increased Vangl2 mRNA and DNA copy number is observed in basal breast cancer samples compared to controls, a trend which increases in larger and higher grade tumours (Puvirajesinghe et al., 2016). Experiments in SUM149 cells, a basal breast cancer cell line, showed that Vangl2 signals through the Wnt-JNK pathway to increase proliferation (Puvirajesinghe et al., 2016). Signalling occurs through an endosomal scaffolding protein, p62/SQSTM1, a newly identified Vangl2 interacting protein.

Cell migration and invasion is a key stage of the transformation of a tumour from benign to metastatic, and it is important to understand the processes driving this behaviour. Breast adenocarcinoma cells migrate in culture, with Frizzled-Dishevelled and Vangl2-Prickle complexes identified at the leading protrusions (Luga et al., 2012). Knockdown of PCP proteins by siRNA reduces both number of protrusions and speed of cell migration, suggesting that the asymmetric localisation of PCP proteins promotes migratory behaviours, possibly through activation of RhoA promoting cytoskeletal remodelling driving polarised migration (Habas et al., 2001).

Conclusion

It is clear that Planar Cell Polarity pathways play essential roles in the morphogenesis of various tissues from fruit flies to humans, including directing collective cell migration in patterning the body axis in the early embryo, directing cell polarity in the auditory system and in the formation of epithelial organs such as the mouse lung. Through dissection of the mechanisms by which PCP activity translates into morphogenetic changes, we now know that planar cell polarity pathways act through directing polarised cell migration, asymmetrically distributing effector proteins to localise dynamic processes and modulation of cell shape through effects on the cytoskeleton and adhesions.

However, the mechanisms by which PCP pathways coordinate the development of tubular structures are unclear. There is also no evidence of whether PCP protein expression changes during development, an important point to establish to suggest when these mechanisms function. Although some evidence suggests that they localise to the leading edge of developing epithelial tubules and Vangl1/Fz6 localise asymmetrically in multiciliated lung cells, Vangl2 localisation has not been observed in vivo in tubular mammalian epithelia.

Hypothesis

The complex task of building epithelial tissues can be dissected if the discrete changes in the behaviour of cells are characterised on an individual basis. We put forward 3 hypotheses which may explain how multiple epithelial cells can coordinate their behaviour to produce tubular structures: 1) cells in the developing epithelia are collectively polarised to extend the tissue in only one direction; 2) cell divisions are oriented to extend only along the length of the axis, maintaining single cell layers and tube diameter; 3) cell shapes are collectively established and maintained via control over intracellular adhesions and cortical actin networks which may be regulated by PCP pathways.

Aims

The aim of this project was to investigate the role of PCP pathway activity in driving the morphogenesis of tubular epithelial tissues, using the mammary gland as a model. This would be achieved by the real time observation of epithelial morphogenesis in mammary organoid cultures; and analysis of morphogenesis after PCP pathway knockdown.

Furthermore, analysis of PCP expression and localisation in mouse mammary tissue throughout puberty aimed to highlight where and when pathway activity contributes to the development of the mammary gland.

The advantages of studying epithelial morphogenesis using a mammary gland model are that it develops during puberty and pregnancy, allowing analysis at various stages of development, rather than other epithelial organs which develop in the embryo. Furthermore real time mammary gland development can be imaged using primary 3D cultures: Improvement in organoid technology allows researchers to observe the epithelial morphogenesis of mammary tissue from unpolarised cell masses into structures similar to the branched ducts present in vivo. Briefly, this involves the culture of mammary epithelial cells isolated from fresh mouse mammary glands in 3D Matrigel matrix. Cells establish apicobasal polarity to generate a single central lumen before dividing to elongate and branch, while differentiating into both luminal and myoepithelial cells. Organoid growth can be imaged in real time using confocal microscopy by addition of cell dyes and fluorescent-tagged proteins or reporters. Targeted genes can also be knocked down using RNA interference, showing how specific pathways regulate morphogenesis.

Using this method we aimed to:

1) Analyse collective cell movements driving epithelial tubulogenesis, e.g. do migrating cells in elongating ducts predominantly move together in one direction, and are these movements regulated by PCP pathways?

2) Measure oriented cell division by incorporating fluorescent histones into organoid cultures, allowing us to observe whether division is polarised along the long ductal axis.

These aims would be supplemented by observing effects of PCP protein knockdown on development using lentiviral delivered shRNAs.

3) Analyse the expression and localisation of PCP proteins in vivo to suggest their functional importance in development, using mammary tissue dissected from mice at various developmental stages.

We also aimed to investigate mammary gland morphogenesis by developing a 3D whole mount imaging protocol. Normal mammary gland tissue consists of two major cell types, with myoepithelial cells polarising along the length of the mature duct. How this organisation is manifested, and its functional importance, is unclear. By reconstructing whole pieces of mammary gland tissue using immunostaining and confocal microscopy, we aimed to deduce how this organisation is produced in developing ducts and alveoli.

In summary we provide a new insight into the 3D biology of the mammary gland and its multicellular structure, and progressed towards optimising conditions allowing future 3D organoid experiments. We also generated the tools required to knock down PCP pathways in these cultures, and provided evidence to suggest that PCP protein activity increases along with pubertal mammary development.

Methods

1. Immunofluorescence staining and imaging
    1. Whole mount mammary glands preparation
    2. Frozen sections preparation and staining
    3. Cell cultures (2D and 3D)
    4. Confocal Microscopy
    5. Widefield Microscopy
    6. Light Sheet Fluorescence Microscopy
2. Tissue analysis
    1. Mouse culling and mammary gland dissection
    2. Tissue lysis
    3. Western blot
3. Cell culture
    1. 3T3s and Eph4 cell culture
    2. 3D cell culture
    3. cDNA transfection
    4. Cell culture lysis
4. Molecular Biology
    1. Competent cell production
    2. cDNA preparation
    3. PCR
        i. Colony PCR
        ii. cDNA PCR
    4. RNA isolation

1. Immunofluorescence Staining and Imaging

1.1 Whole Mount Mammary Gland Preparation

All studies were approved by the Local Ethics Committee and were conducted according to the Home Office Animals (Scientific Procedures, UK) Act 1986. Female C57BL/6J mice were culled by cervical dislocation at stages of either adult virgin, pregnancy day 5 or 12. Glands 2 and 3 or 4 were immediately removed and stretched onto Poly-L-Lysine slides (Thermo Scientific P4981). Small sections (2-5^{2}mm) were either a) placed onto new Poly-L-Lysine slides then immediately immersed in 10% formalin solution (Sigma HT501128) for up to 1 hour, or b) into 4% paraformaldehyde for up to 1 hour. Samples were washed in phosphate-buffered saline (PBS) (Thermo Fisher Scientific 18912014) x3 then permeabilised in 0.2% Triton in PBS for 30 minutes at room temperature. Samples were washed in PBS 3x and blocked in 10% goat serum in PBS for 2-3 hours at room temperature. Primary antibodies (1:1000 dilution) or TritC-Phalloidin (Sigma-Aldrich) in 5% goat serum in PBS were added to samples over night at 4°C. Samples were washed in PBS x5 at room temperature and fluorescent secondary antibodies (1:500 dilution) in 5% goat serum were added for 2-3 hours at room temperature with DAPI (1:10,000 dilution). Samples were washed 5x in PBS and mounted in ProLong Gold Antifade Mountant (Thermo Fisher Scientific P36930) and imaged within a few days.

1.2 Frozen sections preparation and staining

Mammary glands were removed from 4-12 week old CD1 mice and immediately embedded in optimal-cutting temperature compound (OCT), frozen in liquid nitrogen and stored at -80°C. Samples were cut into 10uM sections on Poly-L-Lysine slides (Thermo Scientific P4981) using a cryostat and stored at -80°C. For immunofluorescence staining, sections were drawn around in wax and fixed in 4% paraformaldehyde for 10 minutes on ice. Slides were washed in PBS 3x and blocked in 10% goat serum for 1 hour at room temperature. Primary antibodies were added either 1 hour at room temperature or overnight at 4°C. Slides were washed in PBS x5 and secondary antibodies in 5% goat serum were added for 1 hour at room temperature in the dark. Slides were washed 1x in PBS and DAPI (1:10,000 dilution) in

PBS was added for 2-3 minutes. Slides were washed 5x in PBS and mounted in ProLong Gold Antifade Mountant (Thermo Fisher Scientific P36930) under coverslips.

1.3 Cell culture (2D and 3D) immunofluorescence

Cells were grown on 10mm round coverslips previously treated in nitric acid. Media was washed off in PBS x3 and cells were fixed in 4% paraformaldehyde for 10 minutes. If cells expressed GFP, all following stages were carried out in low light. Cells were then washed in PBS 3x and blocked in 10% goat serum on Parafilm (Sigma P7793) in a moisture chamber for 1 hour at room temperature. Primary antibodies were added in 5% goat serum for 1 hour on Parafilm in a moisture chamber at room temperature and washed in PBS 3x. Secondary antibodies were added in 5% goat serum for 1 hour and washed 1x in PBS. DAPI (1:10,000 dilution in PBS) was added for 2-3 minutes and washed in PBS 3x. Slides were mounted on glass slides in either Dako mounting medium (S3023) for 2D cultures or ProLong Gold Antifade Mountant (Thermo Fisher Scientific P36930) for 3D cultures.

1.4 Confocal Microscopy

Samples were imaged on either an inverted Nikon A1R GaAsP confocal using a Nikon 60× oil or a Nikon A1 TIRF confocal microscope. Sample regions and pixel sizes were adjusted depending on regions of interest with pinhole size maintained at 1.2AU. Most images were captured at a resolution of 512x512 or 1024x1024 pixels. For multi-stack images, Z-intervals were set at 200nM. Lasers used were 403nm, 488, 568 and 604nm. Files were saved as .nd2 format and processed on Imaris image processing software (Bitplane) to produce 2D colour and 3D images or ImageJ to take measurements.

1.5 Widefield Microscopy

Samples were imaged using an Olympus upright fluorescence system through Volocity imaging software (PerkinElmer) using either 10x or 20x objectives.

1.6 Light Sheet Fluorescence Microscopy

After staining, samples were immediately kept in phosphate-buffered saline at 4°C until imaging. Samples were secured in 0.8% agarose in a glass capillary tube and acquired using a Zeiss Z1 light sheet microscope on a PC running Zen Black 2014 software. Z-stacks were taken at the minimum interval of 375nm.

2. Tissue Analysis

2.1 Mouse culling and mammary gland dissection

All studies were approved by the Local Ethics Committee and were conducted according to the Home Office Animals (Scientific Procedures, UK) Act 1986. Female CD1 mice were culled by cervical dislocation at ages 4, 6, 8, 10 and 12 weeks, n=3, or at 5 or 12 days pregnant. Glands 2 and 3 were immediately dissected placed into an Eppendorf tube. Samples were frozen in liquid nitrogen and stored at -80°C.

2.2 Tissue Lysis

All equipment was pre-chilled on dry ice before procedure. Frozen mammary glands were crushed into powder and lysed in 1x Lysis buffer (10%w/v glycerol, 50mM Tris-HCL, 100mM NaCl, 1% nonidet-p40, 2nM MgCL2, pH 7.5) plus 1mM PMSF (in 100mM stock in propan-2-ol), 1x protease cocktail inhibitor and 1mM sodium orthovanadate (Sigma Aldrich S6508). Samples were homogenised and passed through a 25 gague needle and stored at -80°C.

2.3 Western Blot

Tissue samples were made up in 2x Laemelli buffer (30% urea (Sigma-Aldrich 208884), 5% Sodium dodecyl sulphate (Sigma-Aldrich L3771), 6% Dithiothreitol (Sigma-Aldrich D0632), 50mM Tris pH8.0, 2mg bromophenol blue (Sigma-Aldrich B0126)), vortexed and heated at 90°C for 5 minutes. Mammary tissue lysates were passed through a 25 gauge needle and heated again directly prior to loading. 15-30µl per sample was loaded onto a 10% polyacrylamide SDS-page gel. Blank lanes were filled with 50/50 water and sample buffer. 5ul ladders were used including HyperPAGE Prestained Protein Marker (Bioline 33065) and Colourplus Prestained Protein Ladder (NEB P7712). Gels were run at 25mA for ~1hour 20 minutes in running buffer (1L ddH20, 14.4g glycine (Sigma-Aldrich G8898), 3g Tris (Sigma-

Aldrich T1503), 1g Sodium dodecyl sulphate (Sigma-Aldrich L3771)). Gels were transferred onto Immobilon-P PVDF membrane (Roth T831.1) in transfer buffer (14.4g Glycine (Sigma-Aldrich G8898), 3g Tris (Sigma-Aldrich T1503), Sodium Dodecyl Sulphate (Sigma-Aldrich L3771)) at 100V for 1 hour 15 minutes. The membrane was blocked in 5% milk in Tris Buffered Saline (TBS)-0.1% Tween 20 (Sigma-Aldrich P1379) for 1 hour at room temperature, agitating. Primary antibodies were added at various dilutions in 1% milk over night at 4°C, agitated and washed 5x in TBS-0.1% Tween 20. Secondary HRP bound antibodies were added at 1-500 to 1-10,000 dilutions in 1% milk for 1 hour at room temperature, agitated and washed 5x in PBS. Signal was detected using ECL detection kit (ThermoFisher Scientific 32106) and manually developed onto X-ray film in a dark room. Films were scanned onto a PC running HP scanning software and enhanced using ImageJ imaging software. Band size quantification was performed using protocols previously described at http://lukemiller.org/index.php/2010/11/analyzing-gels-and-western-blots-with-image-j/.

3. Cell Culture

3.1 Swiss 3T3, Eph4 and HeLa Cell Culture

All cell lines were kept in 37°C incubators at 5% CO2 and passaged at 1/10 every 3-4 days using Trypsin-EDTA (ThermoFisher 25200056). Swiss 3T3 and HeLa cell lines were grown in Dulbecco's Modified Eagle's Medium (DMEM) (Lonza BE12-604F) with 1% ultraglutamine (Lonza BE17-605E), 1% Penacillin-Streptomyocin, 10% heat inactivated foetal bovine serum (FBS) (Sigma-Aldrich). FBS was heat inactivated in a waterbath for 30 minutes at 56°C. Eph4 cells were grown in DMEM-F12 medium (Lonza BE12-719F) with with 1% ultraglutamine (Lonza BE17-605E), 1% Penacillin-Streptomyocin, 5% heat inactivated foetal bull serum (FBS) and 5ug/ml insulin (Sigma-Aldrich I0516). Multiwell experiments were performed on Corning Costar cell culture plates.

3.2 3D Eph4 Cell Culture

3D EPh4 cell culture experiments were performed on 12 well or 24 well Corning Costar Cell Culture Plates (Sigma-Aldrich I0516). Corning Matrigel Basement Membrane Matrix, *LDEV-Free, 10mL (Corning#354234) was thawed on ice prior to plating. Eph4 cells were dissociated using Trypsin-EDTA (ThermoFisher 25200056) for 20 minutes at 37°C.

Meanwhile 100ul of matrigel per well was spread onto round coverslips and set for 30 minutes at 37°C. Eph4 cells were resuspended in minimal media (DMEM-F12 medium (Lonza BE12-719F) plus 1% Penacillin-Streptomyocin. Cells were seeded at a density of $2.5x10^4$ cells per well 500ul minimal media, or media with added FGF2 (Sigma-Aldrich F0291-25UG). Cells were incubated at 37°C for 5-6 days until fixing, with media changed at day 3.

3.3 cDNA transfection

Cells were seeded on the previous day at 20-30% confluency on 12 or 24 well Corning Costar Cell Culture Plates (Sigma-Aldrich I0516). On day of transfection, media was removed and blank Dulbecco's Modified Eagle's Medium (DMEM) (Lonza BE12-604F) was added for 1 hour. Cells were transfected using Lipofectamine 2000 (Invitrogen) according to the manufacturer's instructions. Briefly, for 1 well of a 12 well plate, 2ug of DNA and 4ul Lipofectamine 2000 was added to blank 100ul DMEM or Optimem (ThermoFisher Scientific 31985062) separately, mixed and incubated for 15 minutes. Both solutions were then mixed and incubated for a further 15 minutes before being added drop wise to the cells. After 3 hours, media was removed and complete media (Dulbecco's Modified Eagle's Medium (DMEM) (Lonza BE12-604F) with 1% ultraglutamine (Lonza BE17-605E), 1% Penacillin-Streptomyocin and 10% heat inactivated foetal bull serum (FBS) was added. Cells were harvested or fixed 24 or 48 hours after transfection.

3.4 Cell Culture Lysis

All solutions and equipment was pre-chilled on ice. Cells were removed from the incubator, media removed and immediately washed x3 in cold PBS phosphate-buffered saline (PBS) (Thermo Fisher Scientific 18912014). Cells were lysed in 1x Lysis buffer (10%w/v glycerol, 50mM Tris-HCL, 100mM NaCl, 1% nonidet-p40, 2nM MgCL2, pH 7.5) plus 1mM PMSF (in 100mM stock in propan-2-ol), 1x protease cocktail inhibitor, and 1mM sodium orthovanadate (Sigma Aldrich S6508) and immediately scraped into a cold Eppendorf tube using a cell scraper. Samples were centrifuged at 14,000rpm for 10 minutes at 4°C and the supernatant was carefully moved into a new chilled tube. Samples were stored at -80°C until use.

4. Molecular Biology

4.1 Competent Cell Production

DH5α cells (ThermoFisher Scientific 18258012) were thawed and cultured overnight in 5ml Luria-Bertani (LB) Medium (0.5% Bacto-Tryptone (Sigma-Aldrich T9410), 0.25% Yeast extract (Sigma-Aldrich Y0375), 0.5% Sodium Chloride (Sigma-Aldrich), pH7.5 at 37°C shaking. 500ul over overnight culture was inoculated to 50ml LB medium and incubated at 37°C shaking for 2 hours. Cultures were centrifuged at 4000rpm for 5 minutes. Supernatant was discarded and cell pellets were resuspended in 10ml of 100mM $CaCl_2$ (Sigma-Aldrich C1016, autoclaved) and incubated on ice for 20 minutes. Cells were centrifuged at 4000rpm for 5 minutes and resuspended in 5ml freeze-thaw buffer (100mM $CaCl_2$, 15% glycerol (Sigma-Aldrich G5516, autoclaved), ddH20). 200ul aliquots were stored at -80°C and thawed on ice before use.

4.2 cDNA preparation

2.5ul of ligated DNA or 0.5ul of cDNA was added to 30-50ul of thawed DH5α cells or a-select silver cells (Bioline 85027) and incubated for 20 minutes on ice under sterile conditions. Cells were heat shocked for 90 seconds at 45°C and incubated on ice for 60 seconds, then topped up with 800ul LB media and incubated for 2 hours at 37°C, shaking. Cells were centrifuged for 4 minutes at 5000rpm and the pellet was resuspended in 100ul LB media. Samples were then spread onto agar plates (0.5% NaCl, 0.5% bacto-tryptone (Sigma-Aldrich T9410), 0.25% yeast extract (Sigma-Aldrich Y0375), 0.75% agar (Sigma-Aldrich A1296) with ampicillin (Sigma-Aldrich A9518) at 100ug/ml and incubated overnight at 37°C. Colonies were picked and inoculated in 5ml LB media with ampicillin (Sigma-Aldrich A9518) at 100ug/ml overnight at 37°C, shaking. The following morning, cultures were centrifuged at 7,500rpm for 3 minutes and the supernatant removed. cDNA was isolated by following the protocol laid out in the GeneJET Plasmid Midiprep Kit (ThermoFisher Scientific K0502). cDNA concentrations were measured on a nanodrop (ThermoFisher Scientific) and stored at -20°C.

4.3 Polymerase Chain Reaction

i. colony PCR

Colonies were picked with a pipette tip, added to 50ul ddH_2O and mixed by vortex for 10 seconds. 5ul was used as a template for PCR. PCR reactions were set up under the following conditions in 50ul PCR tubes: 12.5ul Biomix Red (Bioline 25006), 1ul forward primer 10uM, 1ul reverse primer 10uM, 5ul colony PCR mix, Ultrapure DNase/RNase-Free Distilled Water (ThermoFisher Scientific 10977035) up to 25ul. PCR cycle, gel loading and imaging was carried out as described in Methods 4.3.ii.

ii. cDNA PCR

PCR reactions were set up under the following conditions: 12.5ul Biomix Red (Bioline 25006), 1ul forward primer 10uM, 1ul reverse primer 10uM, 500ng cDNA, Ultrapure DNase/RNase-Free Distilled Water (ThermoFisher Scientific 10977035) up to 25ul. PCR cycle: 95°C, 1m30s, 60°C 1m, 72°C 1m, (95°C 30s, 60°C 1m, 72°C 1m)x30, 72°C 10m. PCR products were immediately loaded onto a 2% 35ml agarose gel (Sigma-Aldrich A5304) with 0.25% SYBR-Safe (ThermoFisher Scientific S33102) at 100v for 20 minutes. Gels were imaged, printed and scanned onto a PC using HP Scanning software. Gel images were enhanced using ImageJ imaging software.

4.4 RNA isolation

Cells were lysed directly in a 12 well culture plate (Corning) by addition of 190ul trifast (peqGOLD) using a cell scraper. Samples were kept for 5 minutes at room temperature. 38ul chloroform (Sigma-Aldrich) per sample was added, shaken vigorously for 15 seconds and kept for 3-10 minutes at room temperature. Samples were centrifuged for 5 minutes at 12,000g at room temperature. The top RNA-containing aqueous phase was moved to a new tube and 95ul isopropanol was added. Samples were kept on ice for 5-15 minutes and centrifuged for 10 minutes at 12,000g at 4°C. The supernatant was removed and the RNA pellet washed twice with 75% ethanol by vortex and centrifugation for 10 minutes at 12,000g at 4°C. Excess isopropanol was removed by air drying and the pellet was resuspended in Ultrapure DNase/RNase-Free Distilled Water (ThermoFisher Scientific 10977035). RNA concentrations were measured on a nanodrop (ThermoFisher Scientific).

i. DNAse treatment

Excess DNA was removed using RNAse-free DNAse set (Qiagen 79254) and RNeasy Mini kit (Qiagen 74104). In a sterile microcentrifuge tube, the following were mixed: <87.5ul RNA solution, 10ul Buffer RDD, 5ul DNAse I stock solution, Ultrapure DNase/RNase-Free Distilled Water (ThermoFisher Scientific 10977035) up to 100ul and incubated at room temperature for 20-25 minutes. RNA was isolated from the mixture following page 56 of the RNeasy Mini kit (Qiagen 74104) handbook. RNA concentrations were measured on a nanodrop.

Results

1. Immunofluorescent Imaging of Whole Mount Mammary Epithelia

We hypothesise that epithelial morphogenesis is in part controlled by planar cell polarity pathways, which may drive proper development through polarised collective cell movements, oriented cell divisions and regulation of cell shape. As previously described, dynamic processes can be studied by real time imaging of organoid cultures; however it is important to consider the differences between ex vivo cultures and true development in vivo. We sought to investigate PCP pathways in vivo by imaging whole pieces of mammary tissue at various stages of development. Developing a good quality method to visually analyse mammary gland morphology would provide the framework to investigate, using immunofluorescence, a variety of planar polarised events including oriented cell division, trends in cell shape and localisation of PCP proteins. We decided to develop an imaging protocol to produce high quality 3D images of mammary gland structures, with a view to analysing localisation of PCP proteins in mature and developing structures. We also aimed to use this method in analysis of mammary tissue in PCP mutant mice.

There is a clear lack of high quality images of the mammary ductal tree in published literature because of the limitations posed by the nature of mammary tissue. Traditionally, immunofluorescent staining and imaging on tissue has been carried out on thin (10um) sections of tissue which have been embedded in cutting media or wax. Advantages of this technique include the limited distance antibodies are required to penetrate, and the high resolution of imaging possible due to reduced light scattering. However, thin sections are not ideal to study all aspects of morphology as only narrow 3D slices of the whole tissue can be acquired. By staining and imaging whole pieces of tissue, it is possible to capture detailed 3D data which can be reconstructed in whole or as a series of 2D stacks. Only 3D reconstruction allows observation of the surface organisation of tissues, which is important to investigate cellular arrangements produced by planar polarised processes. However, 3D whole mount imaging of mammary tissue poses its own limitations. The mammary gland develops within a stroma composed of adipocytes which cause light scattering within the tissue when attempting to analyse by fluorescence microscopy. The thickness of the tissue

also limits penetrance and diffusion of primary and secondary antibodies. Therefore even the highest quality mammary tissue images which can be acquired need to be close to the coverslip, with relatively little covering from adipose tissue. Here we stained mouse mammary tissues at various developmental stages using different cell markers, and collected images using either confocal microscopy or light sheet fluorescence microscopy (LSFM).

1.2 Rendering mammary gland morphology in 3D

Immunofluorescent staining and confocal imaging of whole mount mammary tissue rendered high quality images of mammary tissue which provide new insights into its morphogenesis at both quiescent stages and during increased development in pregnant animals. Dissected mammary tissues were incubated with trit-c conjugated phalloidin, a diffusible fluorescent dye which binds to actin; and DAPI, which stains cell nuclei.

Figure 1a shows 3D rendering of a mammary duct taken from a 19 week old virgin female mouse. The striated actin arrangement along the length of the duct shows the elongated morphology of ME cells. i) shows a 3D reconstruction of a piece of the duct, as it would appear from the outside. As we penetrate deeper into the tissue luminal epithelial (LE) cell shapes appear. ii) shows a cross section of the LE cell layer, with each cell contacting 5-7 other cells at their lateral boundaries. iii) LE cells arrange into a single layer (white arrows), with an apical membrane facing the lumen (into which they secrete milk proteins) and a basal membrane which contacts ME cells (yellow arrow).

It is unknown how and when ME cell polarisation is established, however it is not yet established in developing ducts undergoing morphogenesis, as shown in the branching structure in **Figure1b**. This image also shows that at the branch site, the ME cells alter their polarity to follow the long axis of side branch duct.

During the involution stage of mammary remodelling, alveoli which secreted milk during lactation undergo apoptosis and the gland returns to its pre pregnant state. **Figure 1c** shows a wide view of mammary epithelia which had been through the pregnancy and involution cycle. We chose to investigate a mouse at this stage as side branches are more numerous

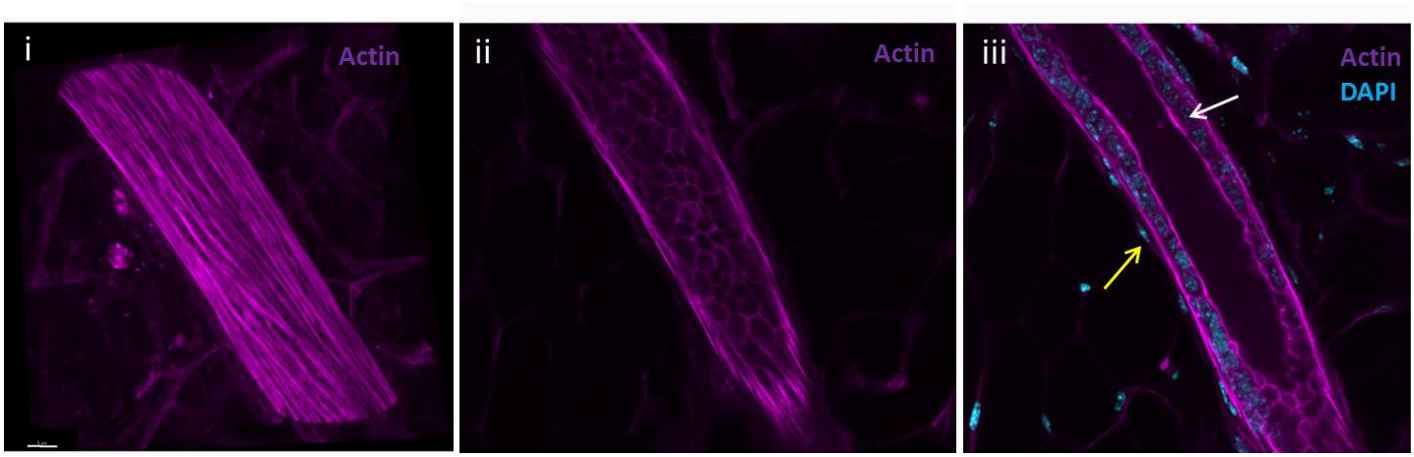

Figure 1a Actin Staining of a 19wk virgin mammary duct

Actin (magenta) staining shows morphology of cellular cytoskeletons in the mammary gland duct of a 19 week old C57 female mouse. i) 3D reconstruction of all z-stack sections showing whole duct ii) single slice image through epithelial cells cortical actin iii) cross section of duct showing single layer of luminal epithelial cells (white arrow) around a central lumen, subtended by myoepithelial cells (yellow arrow) which can be observed by staining of cortical actin. Image acquired on x60 lens, pixel size 0.41um, Z-step size 200nM. Scale bar 5um.

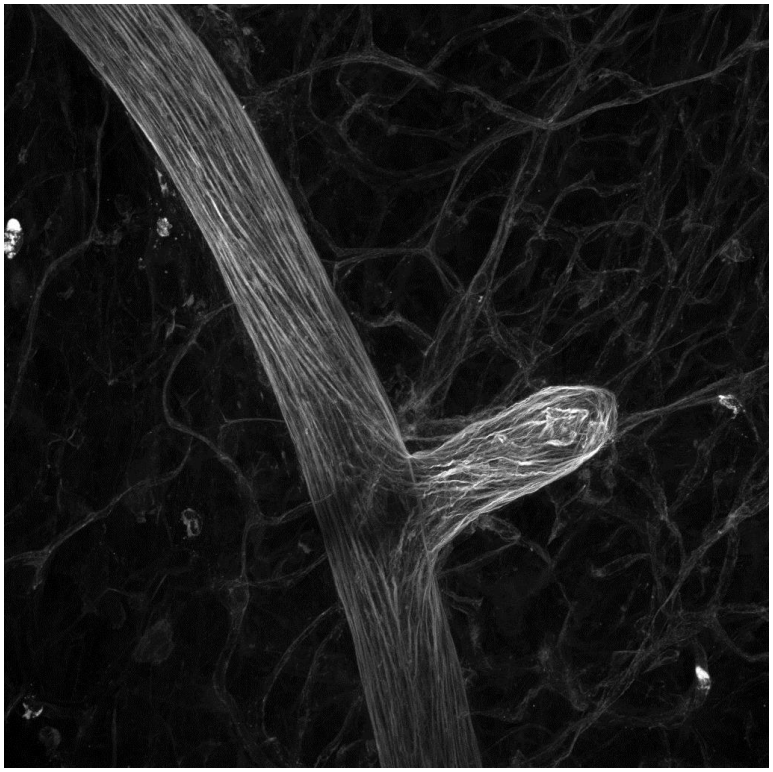

Figure 1b Myoepithelial cell alignment is continuous between branch sites

Actin (white) stained using tritc-phalloidin. Image shows a branching mammary gland of a 19 week old female C57 mouse. Image is 3D rendered using Imaris software.

than in a nulliparous mouse, therefore increasing probability of acquiring good quality data of full ducts. ME cells are clearly polarised along the length of the duct but not at the alveoli.

1.3 Myoepithelial cell arrangements in ducts, bifurcating ducts and alveoli

ME cells are smooth muscle actin (SMA) containing cells which surround mammary ducts, located between the luminal epithelial cells and the basement membrane. ME cells function during lactation to contract to squeeze milk through the duct. In most invasive epithelial breast cancers, there is an absence of ME cells, and 3D organoid cultures lacking ME cells show loss of tissue architecture, including loss of lumen and elongation (reviewed in Gudjonsson et al., 2009). How ME cells contribute to building structure of the mammary gland is unclear.

Here we optimised whole mount mammary gland staining to visualise different cell types and structures by using specific antibodies. Antibody staining against SMA specifically recognised ME cells, while Keratin 8/18 (K8/18) and e-cadherin (e-cad) antibodies were used to mark luminal epithelial (LE) cells, as LE cells express e-cadherin at a much higher level than ME cells (Daniel et al., 1995). In the quiescent duct, ME cells are all polarised along the length of the duct, with very little error, and do not leave any large gaps, thus concealing LE cells from the basement membrane (**Figure 1d**). Due to antibody and light penetrance limitations of staining and imaging thick mammary gland tissue, some mice were put through an entire pregnancy cycle before staining experiments. This is as during pregnancy, smaller ducts develop in order to increase milk production, which are therefore easier to stain and allowing capture of higher resolution images, for example **Figure 1d.**

ME cells differentiate from precursors in the terminal end bud (TEB), the developing end of the duct. **Figure 1e** shows a section of a single duct (white arrow) branching into 4 ducts in a 5 day pregnant mouse. Development of new ducts at this stage of pregnancy increases opportunities to capture images of developing ducts to observe their morphology. Note how the ends of the ducts have a bulbous morphology (yellow arrow), with LE cells of various shapes and sizes within the bulb. Contrastingly, further up the duct, LE cells have more cuboidal morphology and less layers.

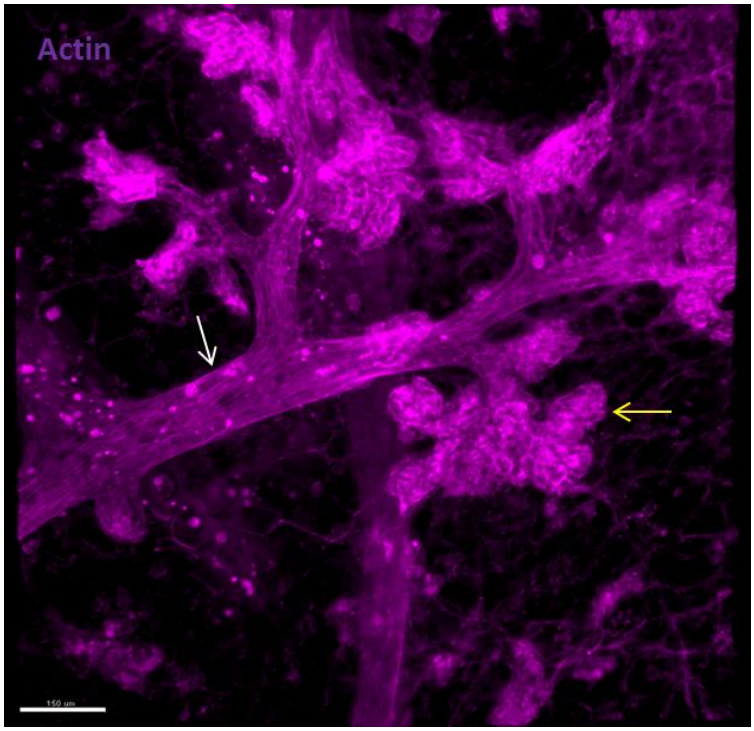

Figure 1c Mammary gland of post-partum mouse after involution cycle

Actin (magenta) stained with tritc-phalloidin. Arrows point out anatomical features including ducts (white) and alveoli (yellow). Image acquired on x20 lens, scale bar 150um, pixel size 2.51um, Z-step size 200nM.

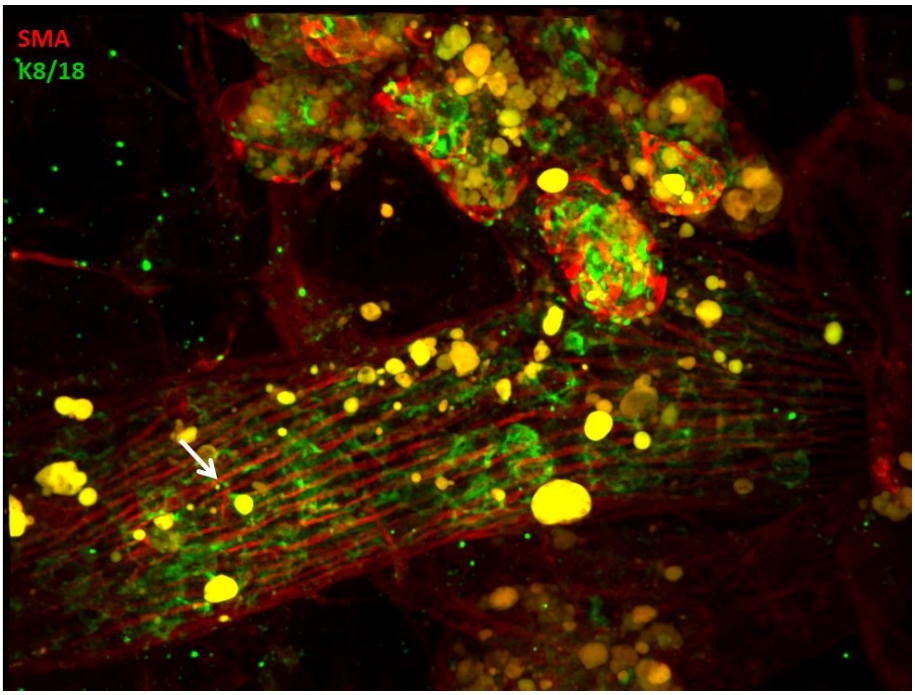

Figure 1d Myoepithelial cells are polarised along the length of mammary ducts

Mammary gland of a mouse which has been through the pregnancy cycle and fully involuted to a pre-pregnant state stained for smooth muscle actin (SMA) (red) showing ME cells (white arrow) and keratin 8/18 (green) specifically staining LE cells. The duct runs from right to left, note all smooth muscle actin staining is oriented in the same direction along the length of the duct, suggesting that ME cells are also elongated. Image acquired on x60 lens, pixel size 0.41um, Z-step size 200nM.

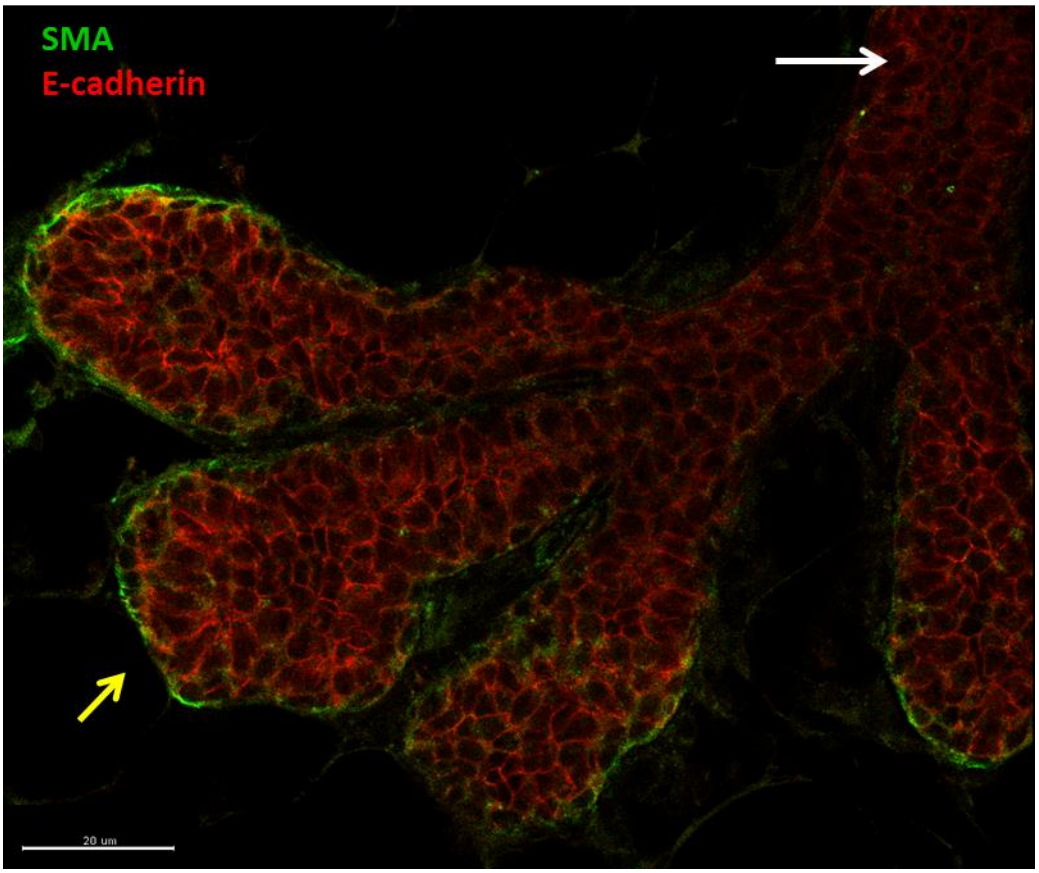

Figure 1e Developing mammary ducts have a bulbous terminus

Mammary gland of a 5 day pregnant c57 mouse stained for smooth muscle actin (green) and e-cadherin (red). This image shows a single z-section of a duct splitting from one (white arrow) into 4 branches. Duct TEBs have a bulbous morphology (yellow arrow). Scale bar 20um.

How the duct is moulded into its tubular shape from the bulbous TEB is not known. However, images of developing buds taken from 5 or 12 day pregnant mice suggest that ME cells may be organised orthogonally to the length of the duct as shown in **Figure 1f**.

Whereas ME cells along the duct all adopt a linear morphology along the duct, at the TEB they adopt a more stellate morphology (**Figure 1g**). Stellate ME cells may be advantageous in the TEB as increased surface area and reach could mould the round morphology into a tubular shape by force as smooth muscle actin contracts.

Unpolarised arrangement of ME cells is also a feature of bifurcating ducts, as shown in **Figure 1h**. This suggests that ME cells adopt a linear polarisation along the duct at the time when ducts reach maturity, an indicator of which is the full apicobasal polarisation and single layered arrangement of LE cells. Quantification of ME cell angles in relation to the long ductal axis shows that ME cells orientate along the duct in mature tissue, are unpolarised around alveoli and appear partially polarised (around 45°) in elongating ducts (**Figure 1i**).

The origins of ME cells is of great interest as they play an important role in mammary gland development. ME cells differentiate from luminal cell compartments in the TEB during development (reviewed in Gudjonsson et al., 2009). Analysis of cells derived from mammary tissue showed that bipotent human breast epithelial cells are positive for epithelial specific antigen (ESA) and negative for MucI (Stingl et al., 1998). Stem cells in the mammary gland are thought to be located suprabasally, nearer the ECM to the lumen (Gudjonsson et al., 2002), however analysis of single sections from Z-stacks taken of bifurcating ducts show smooth muscle actin positive cells in the centre of the TEB contacting the lumen, surrounded by SMA-, e-cadherin+ luminal cells, as shown in **Figure 1j.** Indeed studies in organoid cultures suggest that ME cells differentiate from vertically dividing apical luminal cells (Heubner et al., 2014). After division, the apical luminal cell retains tight junctions backing onto the lumen, while the basally located daughter became unpolarised with the potential for ME cell differentiation.

In order to confirm bifurcating and developing buds were correctly identified, and not in growth arrest, samples were co-stained for ki67, a cellular marker for proliferation. Ki67 can

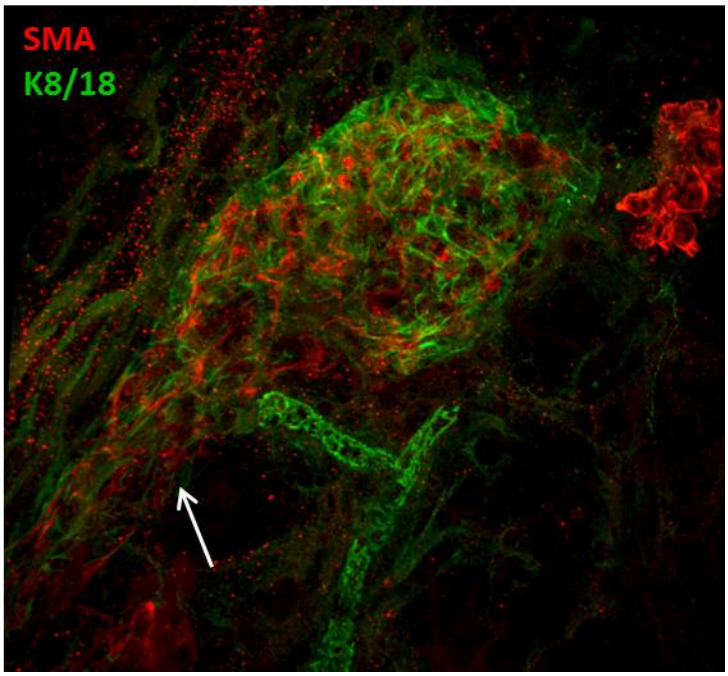

Figure 1f Myoepithelial cells are arranged differently in the developing duct of a P12 c57 mouse

Mammary gland of a p5 c57 mouse stained for smooth muscle actin (green) marking ME cells and keratin8/18 (red) marking LE cells. The duct is growing from left to right. Note further down the duct, the diameter decreases and ME cells become more elongated (white arrow). Image acquired on x60 lens, pixel size 0.41um, Z-step size 200nM.

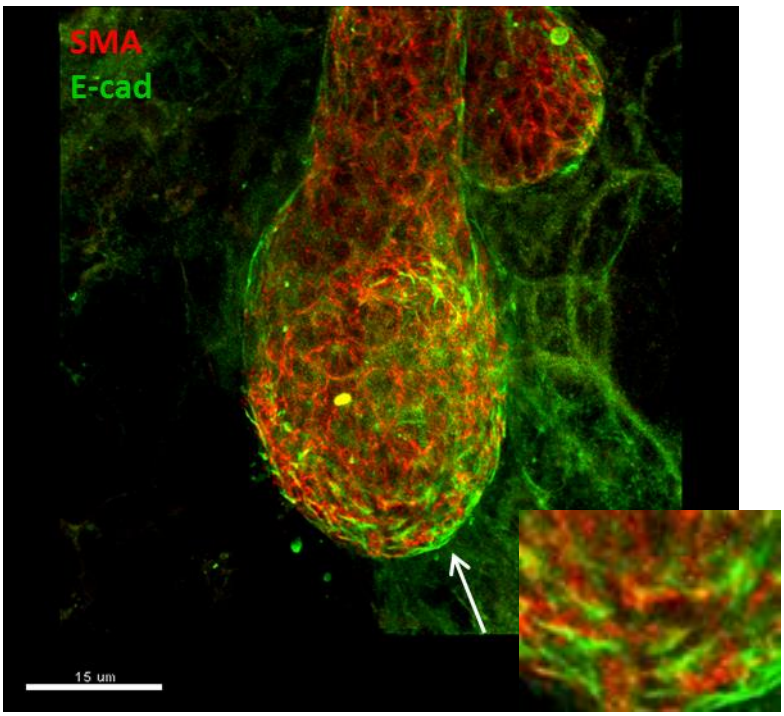

Figure 1g Myoepithelial cells in developing buds have a stellate morphology

Mammary gland of a mouse a p5 c57 mouse stained for smooth muscle actin (green) and e-cadherin (red). Direction of growth is top to bottom. ME cells have a stellate morphology at the growing tip (white arrow and insert). Image acquired on x60 lens, scale bar 15um, pixel size 0.41um, Z-step size 200nM.

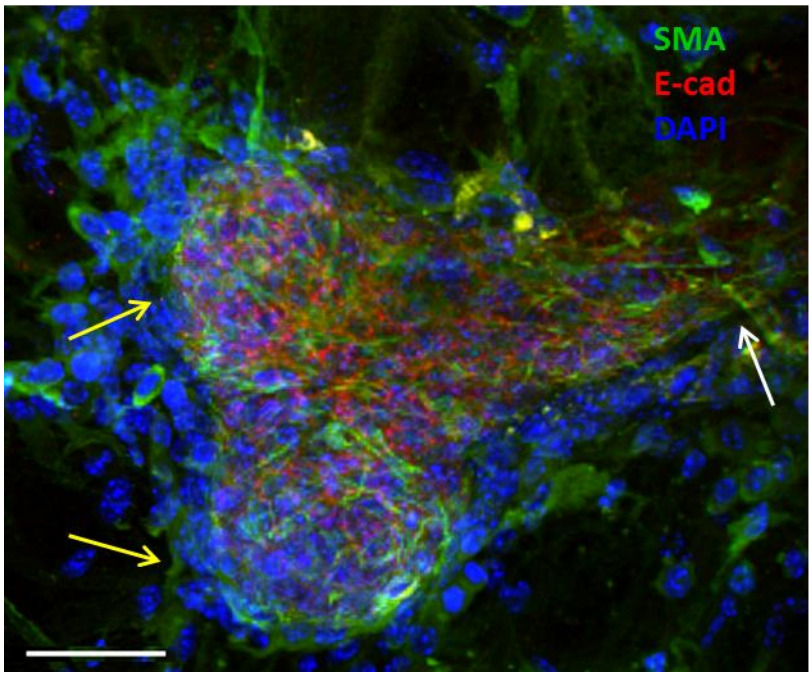

Figure 1h Myoepithelial cells are unpolarised and elongated in bifurcating ducts

3D rendered mammary gland of a 5 day pregnant c57 mouse stained for smooth muscle actin (green), e-cadherin (red) and nuclei (blue). Direction of growth is right to left, with one duct (white arrow) branching into two (yellow arrows). Image acquired on x60 lens, scale bar 33um, pixel size 0.41um, Z-step 200nM.

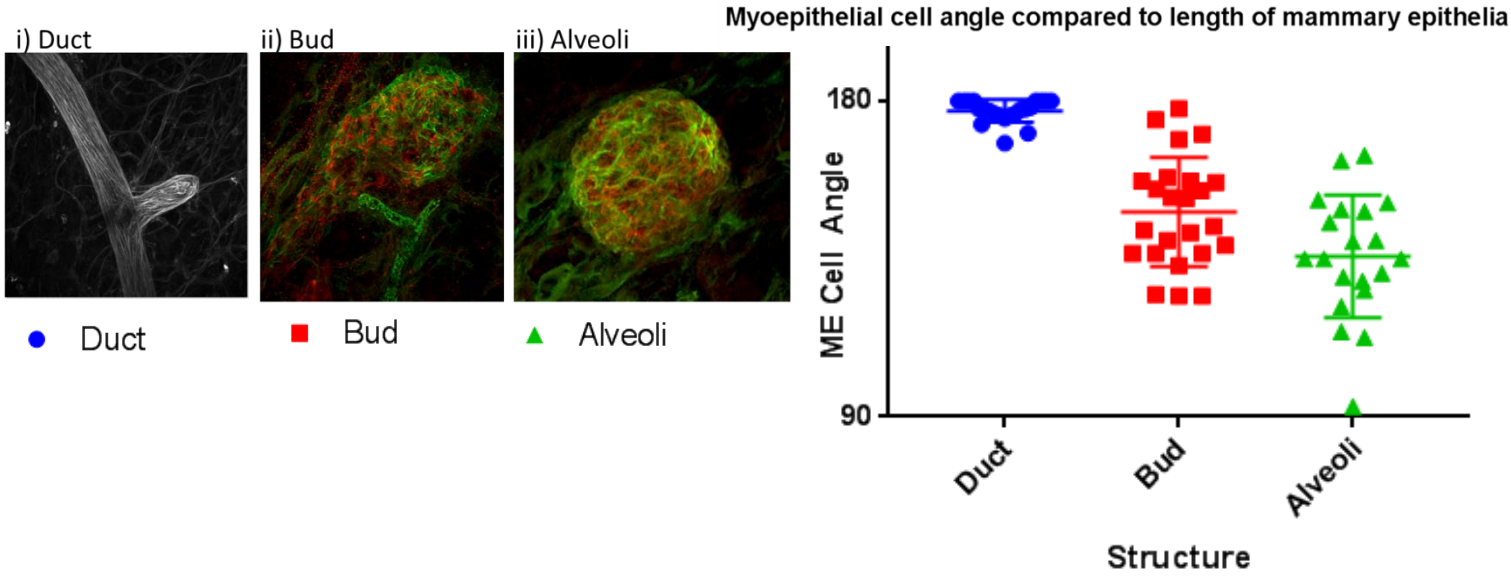

Figure 1i Quantification of myoepithelial cell polarisation in ducts, elongating buds and alveoli

ME cell angles (inferred from actin and SMA staining) in relation to the long ductal axis was measured using ImageJ in i) mature mammary duct stained for actin (white), ii) elongating mammary epithelia stained for SMA (green) and K8/18 (red) and iii) alveoli (stained for SMA (green) and K8/18). Each plot shows indicates one image, and each data point indicates an individual ME cell. This scatter graph shows that all ME cells are polarised along the length of a mature duct, which is reduced in buds and widely varied around alveoli. Bars show the mean with standard error of the mean.

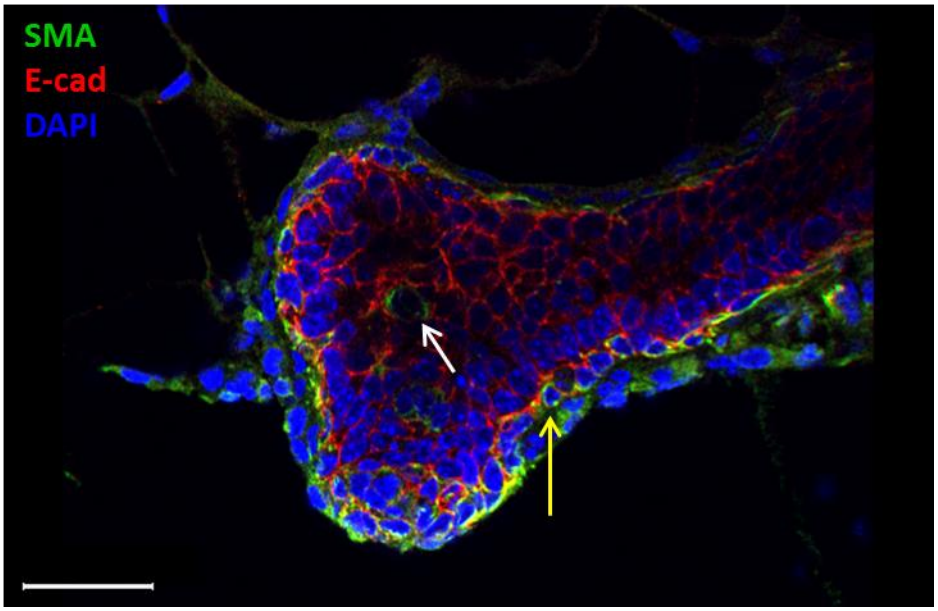

Figure 1j Differentiated myoepithelial cells are present both basally and apically in the TEB

Mammary gland of a p5 c57 mouse stained for smooth muscle actin (green), e-cadherin (red) and nuclei (blue). Direction of growth is right to left. Note the green, SMA+ cell in the centre of the bud (white arrow). Also note the rounded SMA+ cells at the bottom right of the duct (yellow arrow), which have not yet flattened to the normal ME cell morphology. Image acquired on x60 lens, scale bar 33um, pixel size 0.41um, Z-step size 200nM.

be identified in the nucleus during interphase, or at the chromosomes during mitosis. Therefore, developing buds have higher levels of Ki67 positive cells than ducts (**Figure 1k**).

During pregnancy, there is a massive expansion of epithelial cells which form side branches and alveoli at the termini of branches. Whereas the mammary ducts are tubular, alveoli are spherical and all join on to the single central lumen, where milk proteins are secreted into. **Figure 1l** shows whole mount immunostaining of a mammary gland which has been through the pregnancy cycle and is undergoing the involution process. To the right the linear ME cells are clearly polarised along the length of the duct, whereas alveolar ME cells (white arrow) have a stellate morphology and are not collectively polarised in any direction.

1.4 Basement membrane morphology

ME cells secrete the basement membrane which forms a physical barrier between the epithelial and stromal compartments. This barrier is significant in cancer, as epithelial tumours can be contained within the basement membrane, known as ductal carcinoma in situ (DCIS). However, when they break through the basement membrane they can become invasive and metastatic. The nature of physical contact and signalling between luminal epithelial cells and the basement membrane is an area of debate in breast development and cancer. We therefore used this whole mount imaging technique to analyse the morphology of the mammary basement membrane in virgin and pregnant mice in relation to the epithelial compartments by staining for basement membrane protein laminin-a. **Figure 1m** shows that in the duct, the basement membrane fits closely with ME cell coverage, which appears as striations along the length of the duct. This close-knit conformation is also apparent in the developing ducts of a pregnant mouse, where the basement membrane shows striations at angles perpendicular to the duct (**Figure 1n**). In contrast, we captured a point during the morphogenesis of an alveolus before complete basement membrane deposition. It is clear in **Figure 1o** that although there is partial ME coverage of the luminal cells, some luminal cells are exposed to the ECM, whereas most of the duct with ME cell coverage is subtended by basement membrane. However, it is possible that this phenomenon is due to mechanical damage to mammary tissue during processing, and has not been observed in other examples.

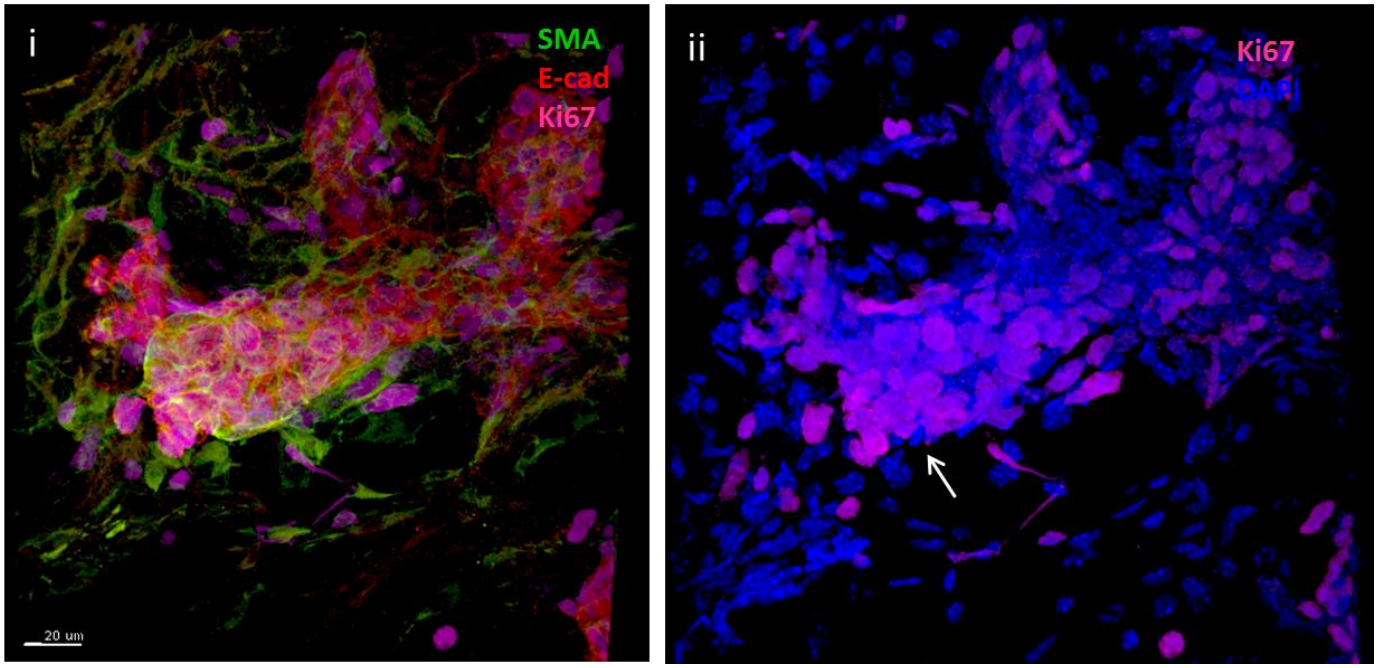

Figure 1k Ki67 staining for cellular proliferation in a developing p12 mammary gland

Mammary gland of a mouse a p12 c57 mouse stained for i) smooth muscle actin (green), e-cadherin (red) and ki67 (magenta) and ii) Ki67 (magenta) and nuclei (blue). Direction of growth is right to left. Note the high density of ki67 staining around the ends (white arrow) compared to the central duct. Image acquired on x60 lens, scale bar 20um, pixel size 0.41um, Z-step size 200nM.

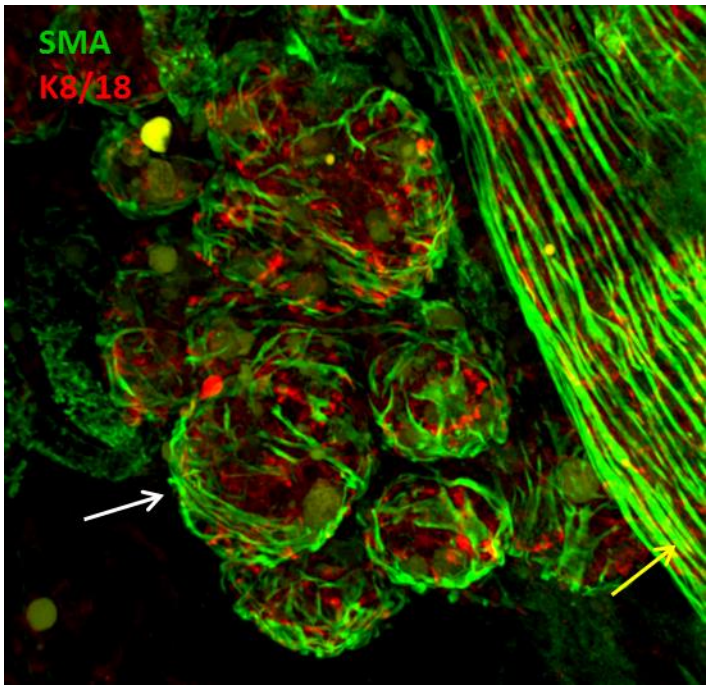

Figure 1l Myoepithelial cells have different morphology in alveoli compared to ducts

Mammary gland of a c57 mouse a post-involution stained for smooth muscle actin (green), keratin 8/18 (red). Alveoli (white arrow) have myoepithelial cells with a stellate morphology, loosely packed around luminal cells (red) whereas ductal ME cells (yellow arrow) are linear along the length of the duct.

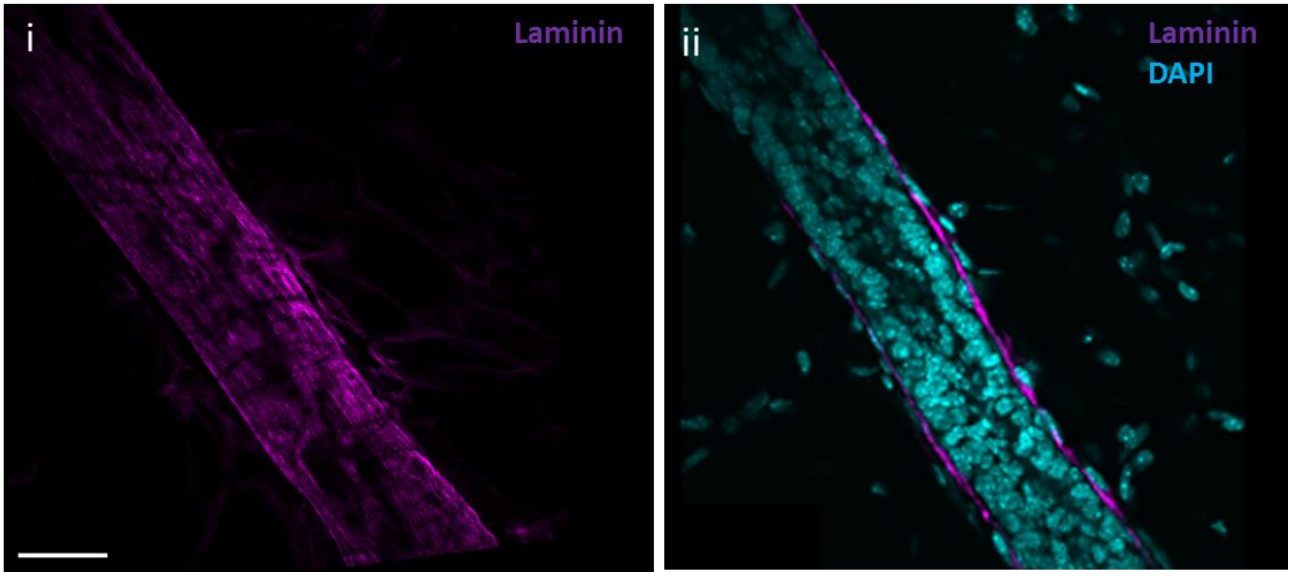

Figure 1m The basement membrane sits closely to myoepithelial cells in the mammary duct

3D rendered mammary gland of a p5 c57 mouse stained for i) laminin (magenta) and DAPI. The striations along the length of the duct are evidence that the basement membrane wraps tightly around myoepithelial cells. ii) shows a cross section of the duct, indicating laminin deposition is specifically basal to the duct. Image acquired on x60 lens, scale bar 33um, pixel size 0.41um, Z-step size 200nM.

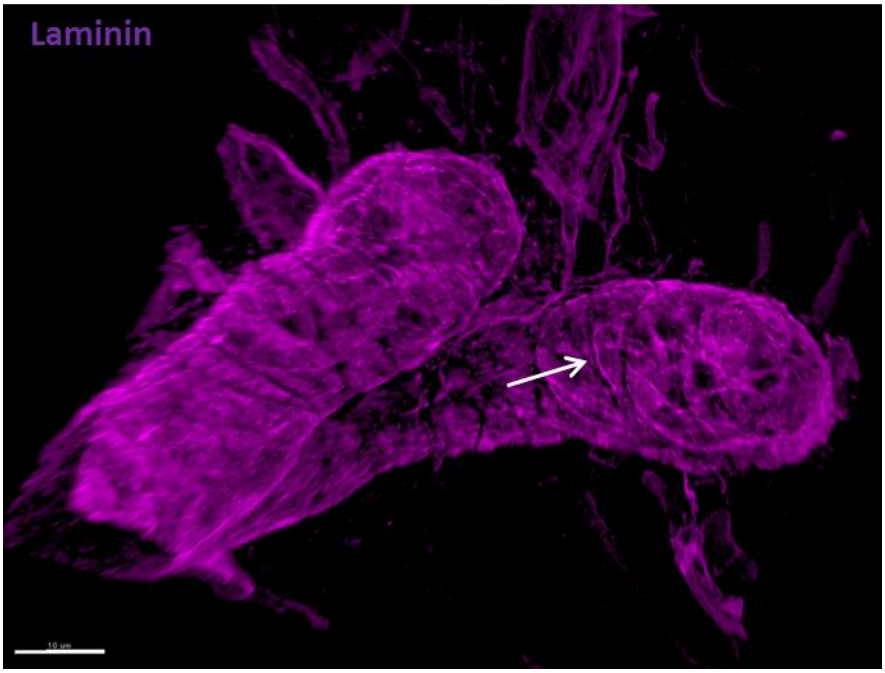

Figure 1n In developing ducts the basement membrane conforms to myoepithelial cells, which appear to be orientated orthogonally to the length of the duct

Mammary gland of a p5 c57 mouse stained for laminin (magenta) showing a bifurcating duct. White arrow shows the basement membrane wrapping around ME cell shapes. Direction of growth is from left to right. Image acquired on x60 lens, scale bar 10um, pixel size 0.41um, Z-step size 200nM.

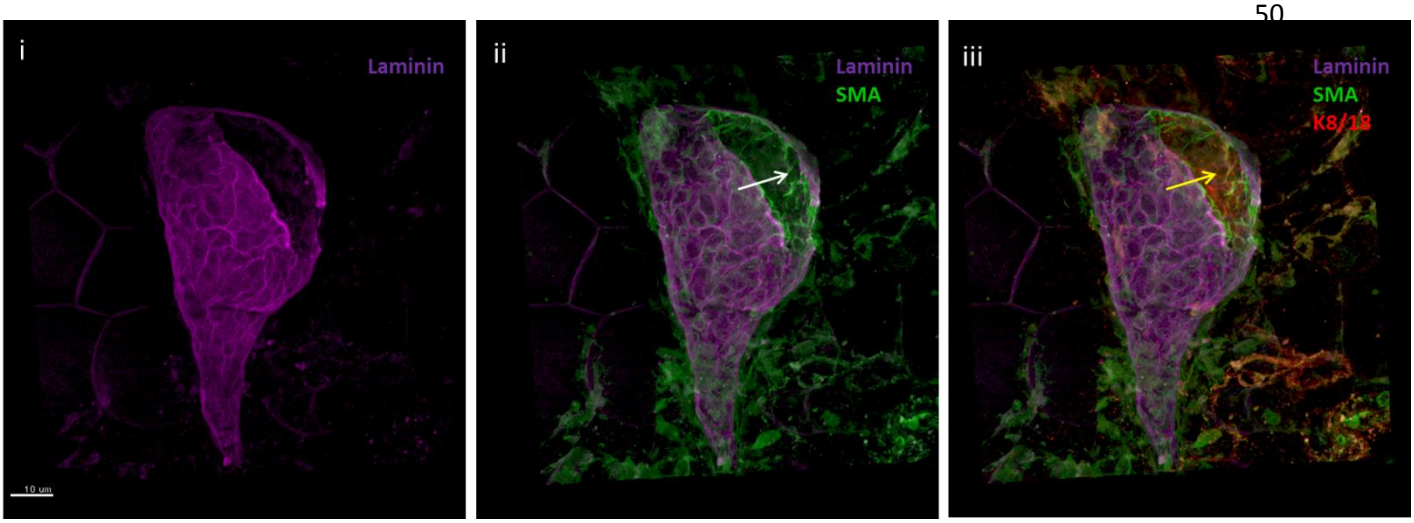

Figure 1o Incomplete basement membrane coverage of a developing alveolus in a 5 day pregnant mouse

3D reconstruction of a p5 c57 mouse mammary gland stained for SMA (green), keratin 8/18 (red) and laminin (magenta) showing a developing alveolus with incomplete basement membrane coverage. iii) At the top of the image there are visible luminal cells (yellow arrow) which are partially subtended by ME cells (ii, white arrow) which are yet to secrete a laminin basement membrane (magenta). Image acquired on x60 lens, scale bar 10um, pixel size 0.41um, Z-step size 200nM.

1.5 Thin Section Staining reveals Luminal Cell – ECM Contact

In order to observe the interactions between cell types in the mammary gland, we stained thin frozen mammary gland sections. This method offers a higher resolution and less light scattering or penetrance issues compared to 3D whole mount imaging. **Figure 1p** shows cross sections of 3 mammary ducts from a 12 week old mouse, with SMA containing ME cells wrapped very closely around the luminal epithelial cells of the duct.

During mammary gland development, luminal cells contact the ECM, which through integrin signalling, specifies the basal membrane. Polarity is transduced throughout the cell by microtubule mediated transport of apical components to the opposite membrane (Akhtar and Streuli, 2013). Due to the ME cell barrier between luminal cells and the basement membrane and ECM, it is unclear whether luminal epithelial cells in mature ducts make contacts with the ECM. β1 integrins are required during normal development for the establishment of apico-basal polarity and lumen formation in the developing mammary gland. In mice with cre recombinase driven in luminal cells only during pregnancy, β1 integrin gene deletion resulted in polarity defects of luminal cells in mature adult ducts (Akhtar personal communication). This suggests that LE cells constantly maintain their apico-basal polarity as a result of ECM-LE cell signalling through integrins. We investigated whether LE cells do contact the ECM or basement membrane in the mature duct.

By staining the basement membrane in 13 week old virgin mice, we showed that in some cases, epithelial cell protrusions may bypass the ME layer to contact the basement membrane (**Figure 1q**). If mature luminal epithelial cells do receive signalling from the basement membrane, this suggests that loss of Luminal cell/ECM interaction, for example through aberrant integrin signalling, results in defects in apico-basal polarity.

In summary, we have developed a whole mount imaging technique of mammary epithelia which can be rendered in 3D to reveal details about mammary structure in great detail. This includes the polarisation of ME cells which subtend the duct, compared to the less densely distributed stellate ME cells of alveoli, observed in many examples. Preliminary data suggests that the basement membrane configures closely to ME cell arrangements on ducts and alveoli, and show an example of possible incomplete basement membrane deposition during epithelial morphogenesis. As well as optimising imaging techniques and attempting

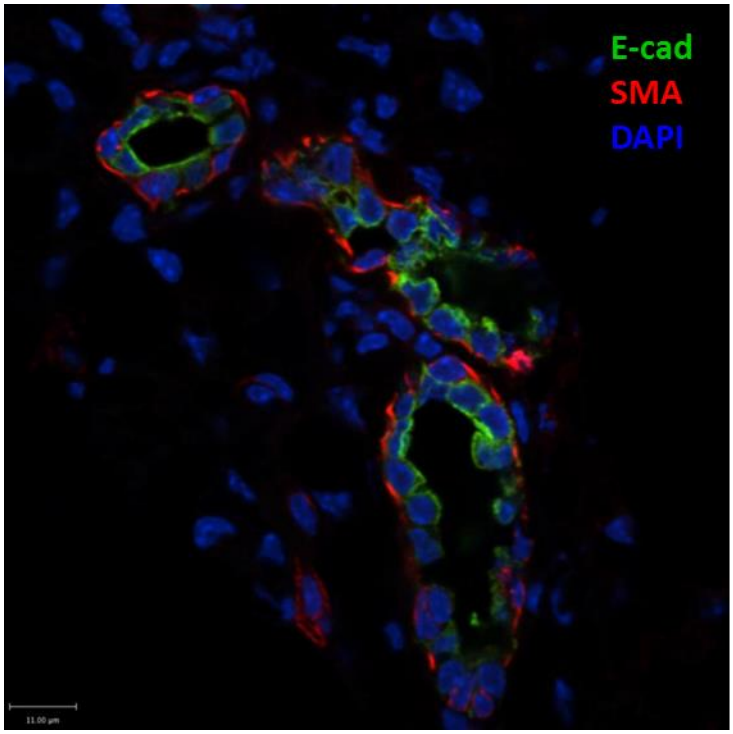

Figure 1p 10uM frozen section of a virgin 12 week old c57 mouse

Immunofluorescent staining of a 12 week old c57 mouse 10uM frozen mammary gland section stained for smooth muscle actin (red), e-cadherin (green) and nuclei (blue). Scale bar 11um.

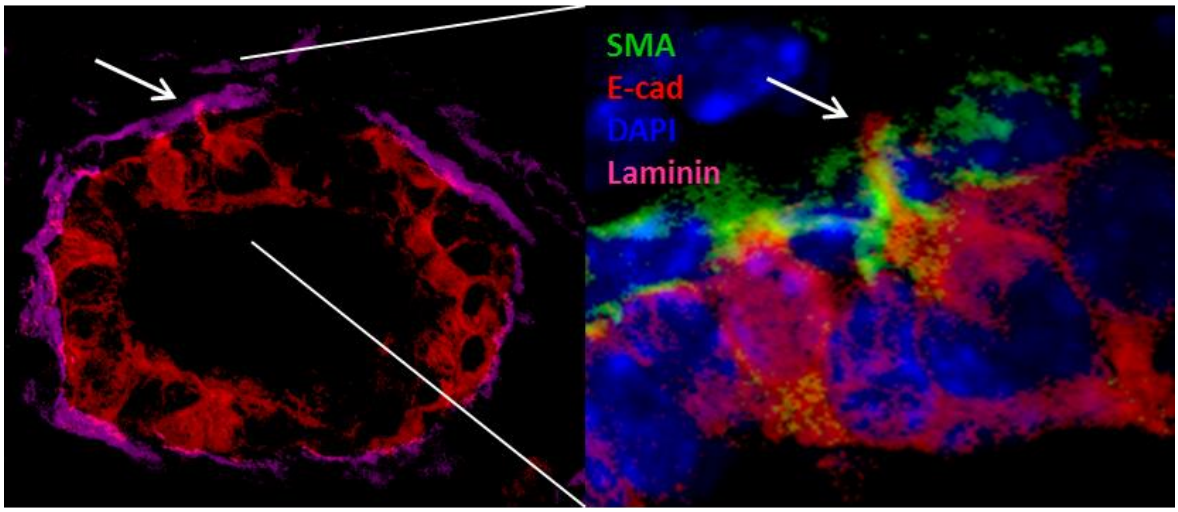

Figure 1q Luminal epithelial cells contact the basement membrane by protrusions passing the myoepithelial layer

Immunofluorescent staining of a 13 week old c57 mouse 10uM frozen mammary gland section stained for smooth muscle actin (green), e-cadherin (red), laminin (magenta) and nuclei (blue). Note the luminal epithelial cell protrusion contacting the basement membrane (white arrows).

LSFM, we have shown that the ME cell barrier may not be complete, with evidence in mature ducts of contact between luminal epithelial cells and the basement membrane.

With further improvement of this technique, planar polarised processes could be studied and imaged at various developmental stages. For example, good tubulin staining would reveal the axis of spindle poles in dividing cells, revealing whether cells are polarised to divide along the axis of mammary ducts. Staining for PCP proteins such as Vangl2 would also reveal how polarised or asymmetric distribution of these components contributes to epithelial morphogenesis. Finally, mammary gland structure and aforementioned planar polarity can be compared in tissue taken from PCP mutants, for example the *Looptail* (Vangl2 mutant) or *Crsh* (Celsr1 mutant) mice.

1.6 Light Sheet Fluorescence Microscopy

While most images presented in this study were taken using a Nikon confocal microscope, this type of image acquisition has limitations. Samples can only be imaged in one plane, although 3D structures can be reconstructed by combining individual slices from multiple Z-stacks. Each Z-stack image is taken sequentially which is time consuming, requiring up to 40 minutes to image a large duct. A consequence of long imaging time is bleaching of fluorophores in the sample leading to signal loss. To address this issue, some samples were mounted in 8% agarose and imaged on a Zeiss Light Sheet Fluorescence Microscope (LSFM). This allows rotation of the sample around 360° and a much quicker imaging speed. However, due to the lower laser power used in LSFM, light was unable to penetrate adipose tissue and only physically exposed mammary gland tissue was detectable, with a high level of light scatter (**Figure 1r**). Images taken with LSFM are of lower resolution in x, y and z axes, with maximum optical magnification of 20x and minimum spacing of 375nm between Z-stacks, compared to 200nm used to capture confocal images. However higher image quality could be achieved in areas with minimal adipose tissue, as actin staining in **Figure 1s** shows the long elongated ME cells around the outside of the duct.

Optical sample clearing by incubation with urea did not increase light penetrance, nor did sample mounting in Matrigel or polyacrylamide. Further optimisation of whole mount preparation for LSFM would include attempts to remove obstructive tissue using fat

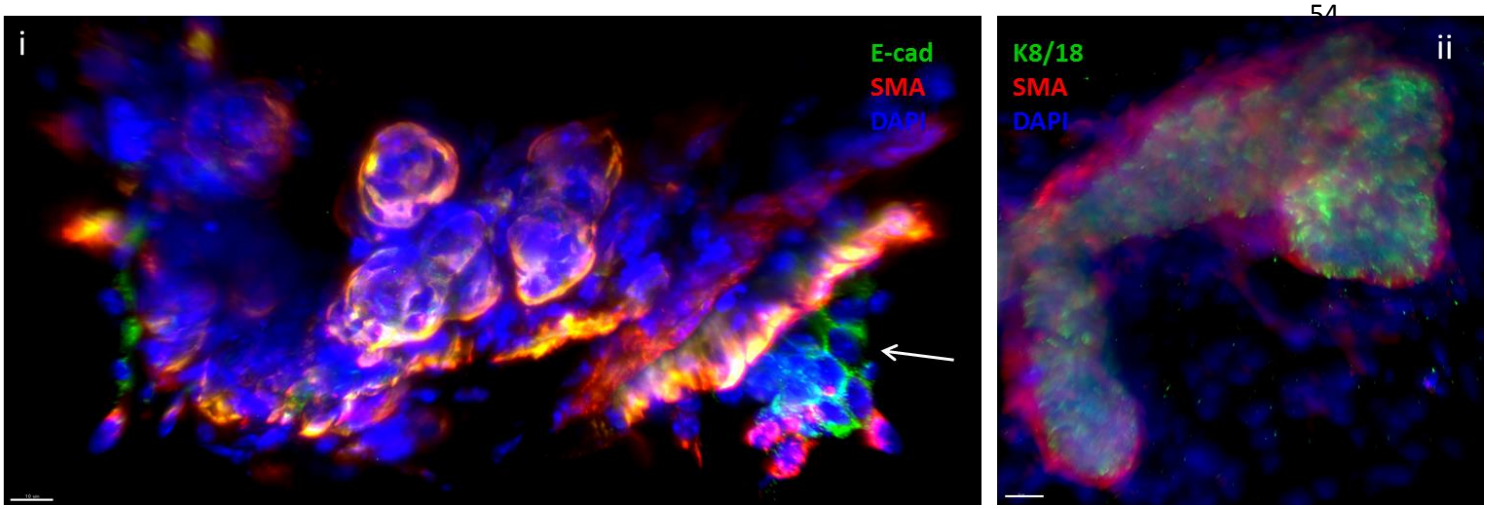

Figure 1r Light Sheet Fluorescence Microscopy of a 5 day pregnant mouse mammary gland

Mammary gland of a 5 day pregnant c57 mouse imaged by LMSF, stained for SMA (red), e-cadherin (green) and nuclei (blue). i) Note the exposed epithelia in the bottom right showing the luminal cell membranes in green. In the middle of the image, adipose tissue refracts and reflects fluorescent light, obscuring epithelial tissue deeper in the tissue. Scale bar 10um. Ii) LSFM image of the same sample in a clearer region, both ME cells (red) and LE cells (green) can be distinguished, however light is scattered through the tissue. Scale bar 20um. Image acquired on x20 lens, Z-step size 375nM.

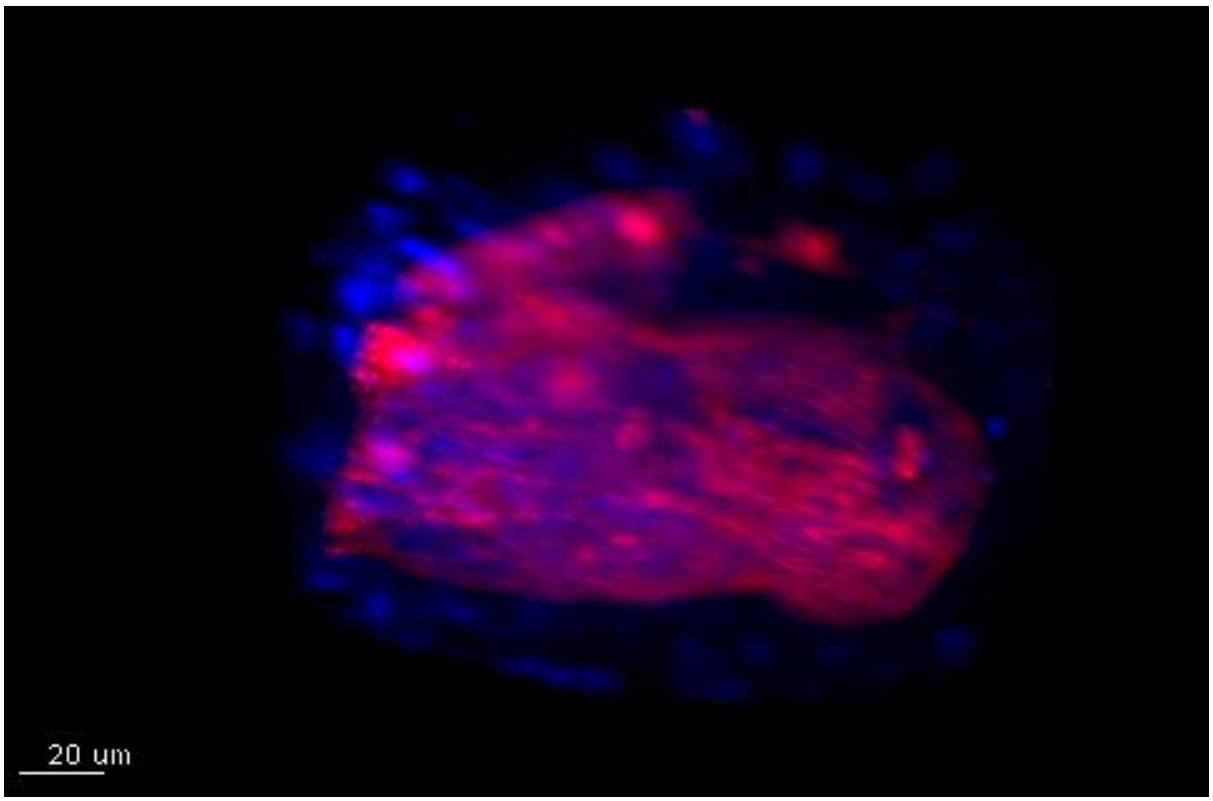

Figure 1s LSFM of a mature mammary duct

Mammary gland of a post-involution mammary gland of a c57 mouse stained for actin (red) and nuclei (blue). This 3D maximum projection image shows the outer layer of ME cells polarised along the length of the duct. Scale bar 20um.

solvents such as xylene. However, it is important to consider the structural impact which removing fat from adipocytes may have on the sample.

We conclude that while light sheet microscopy is advantageous in imaging of some tissues, it is not a reliable method of imaging whole pieces of mammary tissue in 3D, and confocal microscopy should be considered in this application.

In conclusion, we developed an immunofluorescence staining technique of whole mount mammary tissue, which produced high quality 3D images of mammary epithelial structures at various stages of development. Using markers which denoted different mammary cell types including myoepithelial cells and luminal epithelial cells, we showed that ME cells are have differing morphology and orientation depending on whether they line the mature duct, developing duct or alveoli. Furthermore we provided clear images of the laminin basement membrane surrounding the duct in 3D, and suggested possible interaction luminal epithelial cells in the mature duct.

This technique may be used in the future to observe the difference in epithelial structure in mutants, for example Looptail mice, to show the effect of Vangl2 mutations on development. Furthermore staining for other proteins could be provide valuable insight into development, for example a-tubulin to show the angle of cell division in growing mammary epithelia.

2. Vangl2 Expression in the Mammary Gland

We aimed to analyse the expression and localisation of PCP proteins in vivo, to gain insight into their roles during development of the mammary gland. We predicted this may be the case, as development of epithelial structures including the lungs and kidneys are abrogated in PCP mutants (Yates et al., 2010, 2010b). We used mammary tissue dissected from mice at various stages of development, including throughout puberty, when most branching morphogenesis occurs. We initially focussed on expression and localisation of Vangl2, using techniques including western blotting and immunofluorescence and confocal microscopy. This required the optimisation of these protocols, to validate the specificity of antibodies against Vangl2.

2.1 Characterisation of Vangl2 antibody

i) immunoblotting

To characterise the role of planar cell polarity pathways in the morphogenesis of mammary tissue, it is important to understand at which time PCP proteins are expressed, in which cell type and their localisation. Due to the lack of antibodies against mammalian PCP homologues which produce reliable staining and western blotting, we faced the challenge of testing commercially available antibodies. Analysis focussed on Van Gogh-like 2 (Vangl2), a mammalian *Strabismus* homologue, as this is the best studied mammalian PCP protein including in lung development (Yates et al., 2010), inner ear polarity (Montcouquiol, 2006) and convergent extension (Kibar et al., 2001). Therefore we tested Vangl2 antibodies to check that they specifically recognised Vangl2 expression in cells and tissues by Western Blotting, and by immunofluorescence. This would also be important to validate Vangl2 shRNA knockdown.

Firstly, we tested a commercially available Vangl2 antibody which recognises an N-terminal portion of the protein in mice (Santa Cruz N-13 antibody, 46561), which had been previously shown to bind endogenous Vangl2 in brain tissues by western blotting (Nagaoka et al., 2014). Vangl2 expression was analysed in two cell lines: Swiss 3T3 cells and Eph4 cells, a mouse mammary epithelial cell line. Mammary gland tissues dissected from c57 mice during puberty were also analysed.

Figure 2a shows 3T3, Eph4 and 5.5wk c57 mammary gland lysates ran on an SDS-page gel and blotted for E-cadherin, Beta-catenin, Vangl2 and ERK2. The blot shows that a protein band just above 58kD is recognised by the Vangl2 N-13 antibody. A second blot was run in parallel without incubation with the Vangl2 antibody to confirm that bands recognised were due to primary antibody binding only. Another Vangl2 antibody purchased from R&D systems (AF4815) has been shown to recognise overexpressed Vangl2 by western blotting and immunofluorescence. However this antibody (Vangl2 RnD) did not recognise any protein in 3T3 or Eph4 cell lines or mammary tissue (**Figure 2b**).

To obtain more evidence that the band recognised by the Vangl2 N-13 antibody is specific to Vangl2 protein, HeLa cells transfected with hVangl2 cDNA were analysed. Vangl2 overexpression using this cDNA has previously been shown to cause convergent extension phenotypes in Xenopus and Zebrafish (Park and Moon, 2002). By transfecting hVangl2 and Vangl2-GFP into HeLa cells, we showed that the N-13 Vangl2 antibody specifically recognises overexpressed Vangl2 (**Figure 2c**)**.** However, Vangl2-GFP (Kallay et al., 2006) is not recognised, possibly due to GFP masking the N-13 binding site. In this experiment, there was no band at ~65kD in Eph4 cell lysates, suggesting that Vangl2 is either not expressed or unspecific antibody binding to a protein at ~80kD occurred. To support evidence that Vangl2-N13 antibody recognises Vangl2 in pubertal mammary tissue as well as 3T3 and Eph4 cell lines, HeLa-hVangl2 samples were ran alongside and Vangl2-N13 antibody used at 1 in 500 dilution showed that bands are recognised at the same size (around 65kD) in all tissues, including a double band in mammary gland tissue (**Figure 2d**).

A lower signal in Eph4 and 3T3 cells compared to those observed in **Figure 2a** may be due to the lower protein volume loading of 10ul in **2d** compared to 15ul in **2a**.

No signal was present if no primary antibody was used. These optimisation experiments showed that immunoblotting using Vangl2-N13 antibody recognises overexpressed Vangl2 protein, and therefore may recognise endogenous protein.

Characteristics of PCP proteins in many tissues include their asymmetric localisation in cells, for example in a repeated pattern as in *Drosophila* wing cells (Strutt, 2001) or differential expression between cells of growing epithelia like during embryonic lung development (Yates et al., 2010). It is therefore important to reliably visualise the localisation of PCP

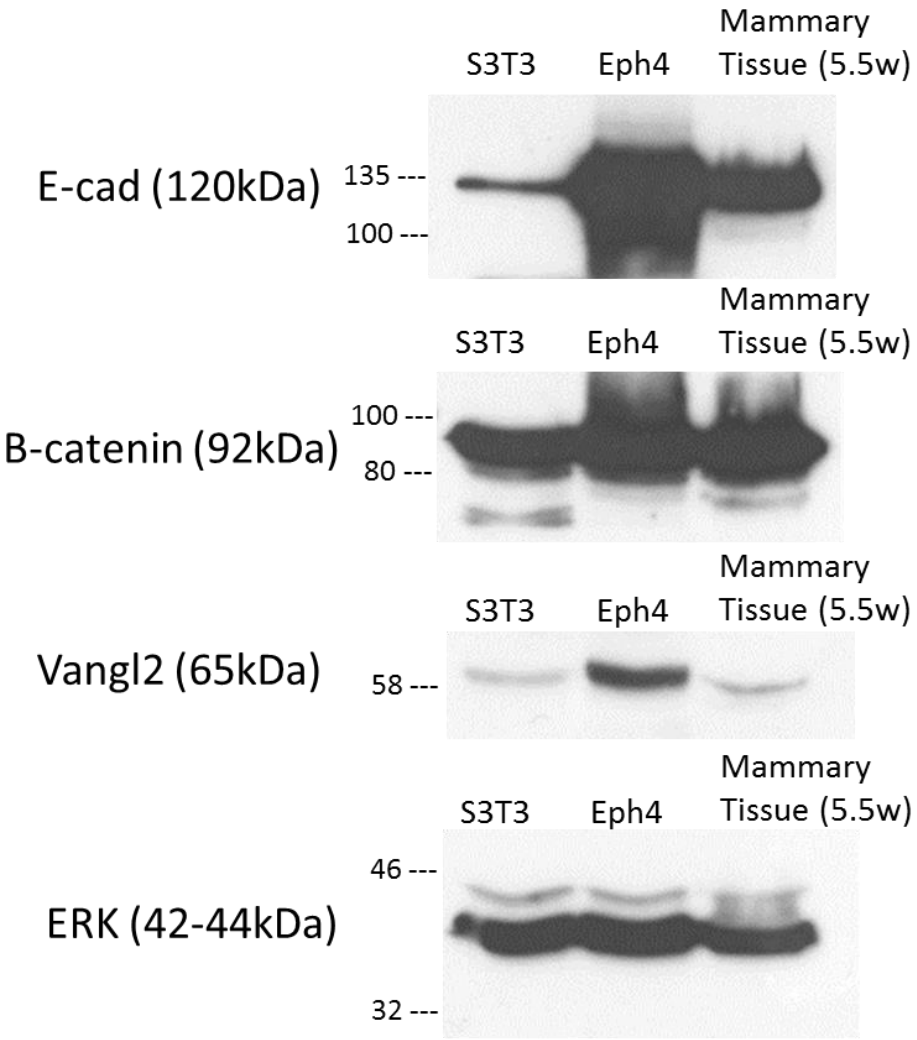

Figure 2a Vangl2 N-13 antibody western blot optimisation

Western blot analysis of lysates of Swiss 3T3 cells, Eph4 cells and 5.5 week mammary epithelia blotted for Vangl2 and tissue controls. Protein amounts were not normalised. A band at the correct size is apparent in all tissue types which is not present when not incubated with Vangl2 N-13, suggesting the Vangl2 N-13 does recognise Vangl2.

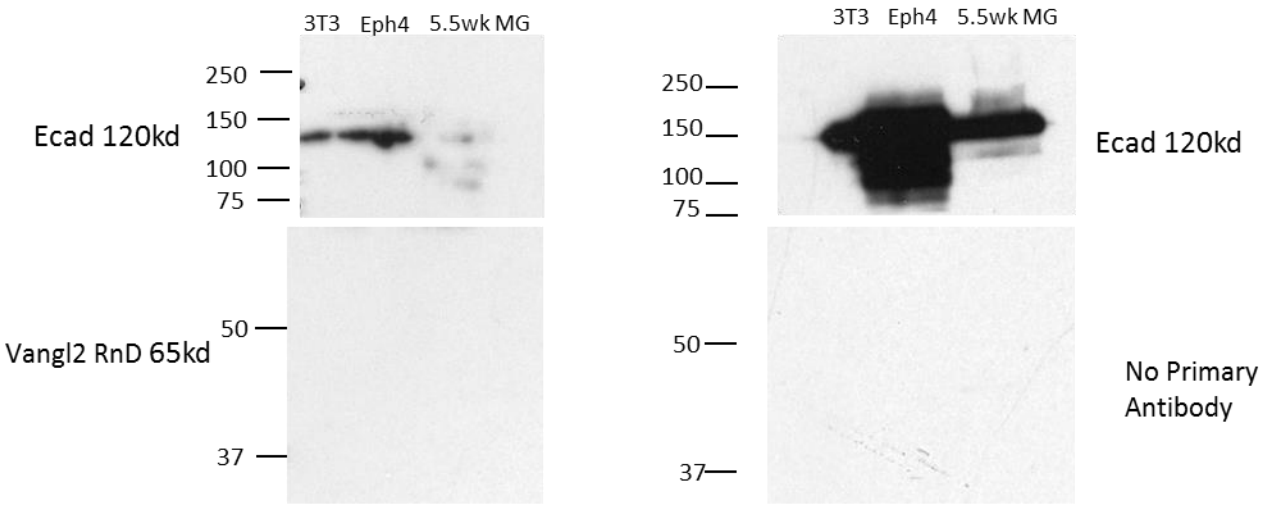

Figure 2b Vangl2 RnD antibody western blot optimisation

Western blot analysis of lysates of Swiss 3T3 cells, Eph4 cells and 5.5 week mammary epithelia blotted for Vangl2 and tissue controls. Protein amounts were not normalised. The blot on the left was incubated with Vangl2 RnD antibody at a dilution of 1:500 but no signal was detected, as in the secondary only control.

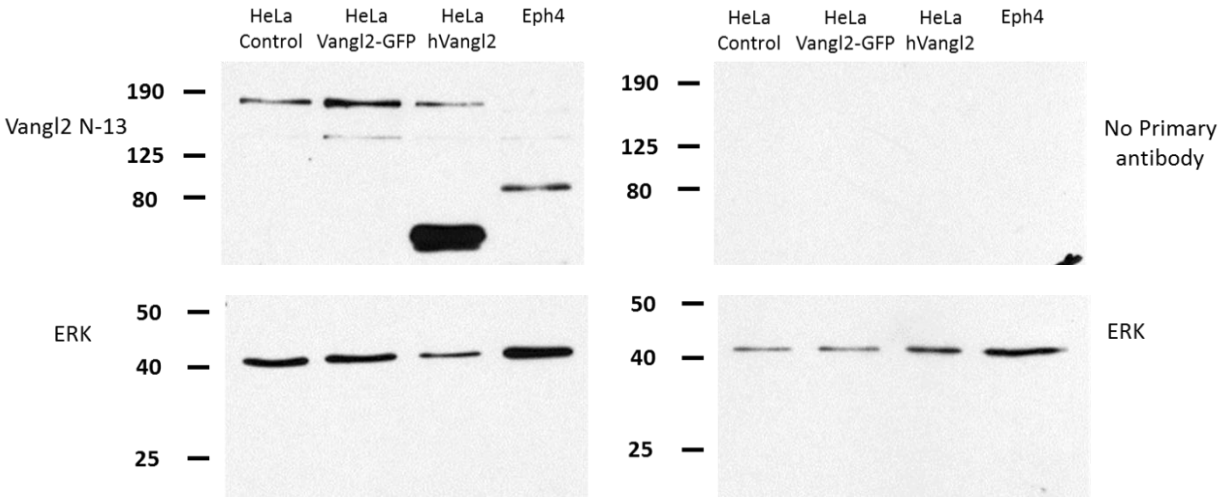

Figure 2c Vangl2-N13 antibody recognises overexpressed Vangl2 in HeLa cell lysates

Western blot analysis of Vangl2 expression in HeLa cell lysates expressed with Vangl2 cDNAs and Eph4 cell lysate. A large band is apparent at around 65kD (left) in hVangl2 transfected HeLa lysates, showing specificity of the N-13 antibody (at 1 in 500 dilution) for Vangl2 which is absent when the sample was not probed with primary Vangl2 antibody.

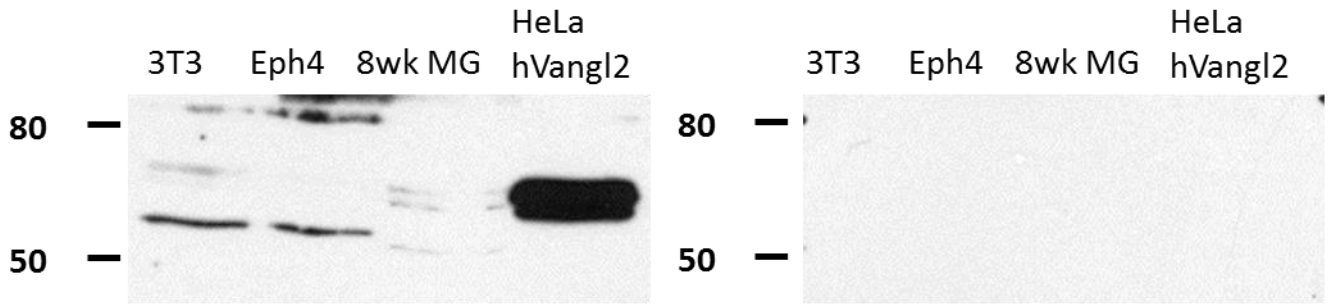

Figure 2d Western blot of cell lines, mammary tissue and overexpressed Vangl2 with Vangl2-N13 antibody

Western blot analysis of 3T3, Eph4 and mammary tissue from an 8 week old c57 mouse, ran alongside lysate of HeLa cells with overexpressed hVangl2. Vangl2 N-13 antibody dilution was 1 in 500 (left) and that bands recognised in 3T3 and 8 week mammary tissue are the same size as overexpressed hVangl2. These bands are not present if N-13 antibody is not used (right, negative control).

proteins, which can be achieved through immunofluorescent labelling and confocal microscopy. There are no published images of Vangl2 localisation in mammary tissue, therefore we directed focus toward finding good antibodies and optimising to specifically recognise Vangl2.

The first antibody tested (RnD Systems, AF4815) has previously been shown to stain endogenous Vangl2 protein in HEK293T and MDCK cell lines (Lindqvist et al., 2010) and in mouse embryo visceral endoderm (Trichas et al., 2011). This antibody was tested by staining thin OCT sections of mammary gland tissue at a 1 in 100 dilution with and without primary antibody and showed membrane staining in epithelial tissue which was weaker in the secondary only control (**Figure 2e**). To identify whether antibody staining specifically targeted Vangl2, Vangl2-GFP was overexpressed in Eph4 cells and stained with Vangl2 (RnD, AF4815). This Vangl2-GFP cDNA construct was designed by Kallay et al. (2006) and was shown to colocalise with Scribble basally and at cell junctions in MDCK cells. Transfected cells have high green fluorescence, due to cytoplasmic localisation of Vangl2-GFP. If the antibody was specific, higher Vangl2 staining (red) would be present in transfected cells. However, as **Figure 2f** shows, the antibody did not recognise overexpressed Vangl2-GFP, which may be due to masking of the antibody binding region by GFP.

hVangl2 cDNA was transfected into HeLa cells and stained using the Vangl2 (RnD AF4815) antibody (**Figure 2g**). Some cells show higher staining than most other cells, suggesting that this antibody may be specific to Vangl2, however without a positive control (like GFP) we were unable to confirm this. We were therefore unable to confirm that the Vangl2 RnD antibody can reliably identify localisation of endogenously expressed Vangl2.

We acquired a monoclonal Vangl2 (2G4) antibody which can specifically recognise Vangl2 in developing heart cells and recognises the Vangl2 peptide sequence CLAKKVSGFK-VYSLGEENST (Ramsbottom et al., 2014). HeLa cells were transfected with both hVangl2 and Vangl2-GFP cDNA and stained with Vangl2-2G4 antibody at 1:100 dilution overnight at 4°c. Cells transfected with Vangl2-GFP showed high signal when stained with Vangl2 2G4 antibody (**Figure 2h**). hVangl2 transfection also resulted in some cells with high Vangl2 staining, which we assume is due to increased Vangl2 expression in these cells (**Figure 2i**)**.**

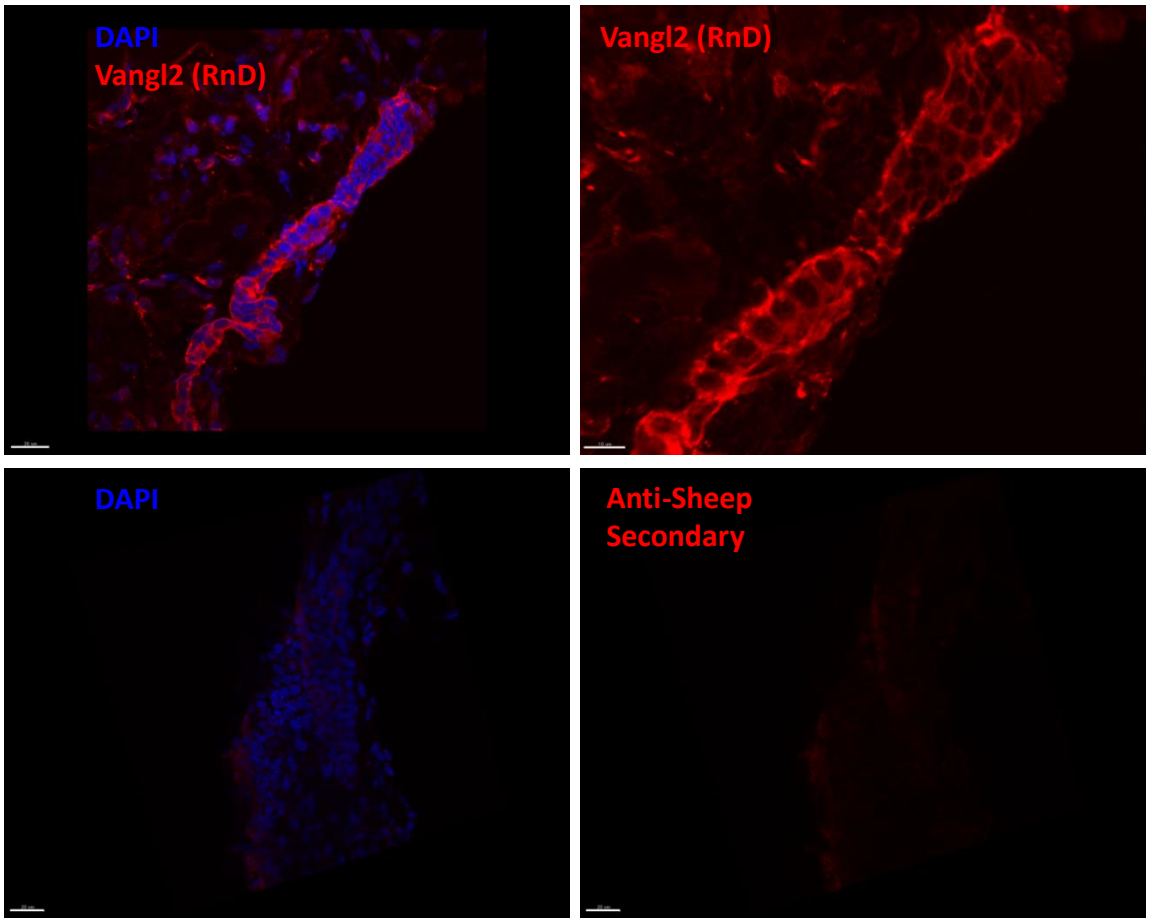

Figure 2e Immunofluorescent staining of thin mammary sections with Vangl2 (RnD AF4815) antibody

10uM OCT sections of a 17 week c57 mouse was stained with (top) or without (bottom) Vangl2 (RnD AF4815) antibody at 1:100 dilution overnight at 4°c and DAPI to stain nuclei. Staining with the antibody shows strong membrane staining in areas of epithelial tissue (large nuclei close together). Some background membrane staining of epithelial tissue is also evident in the secondary (anti-sheep, 1 in 500) only control. Images were taken with the same settings and processed identically. Scale bar 10uM.

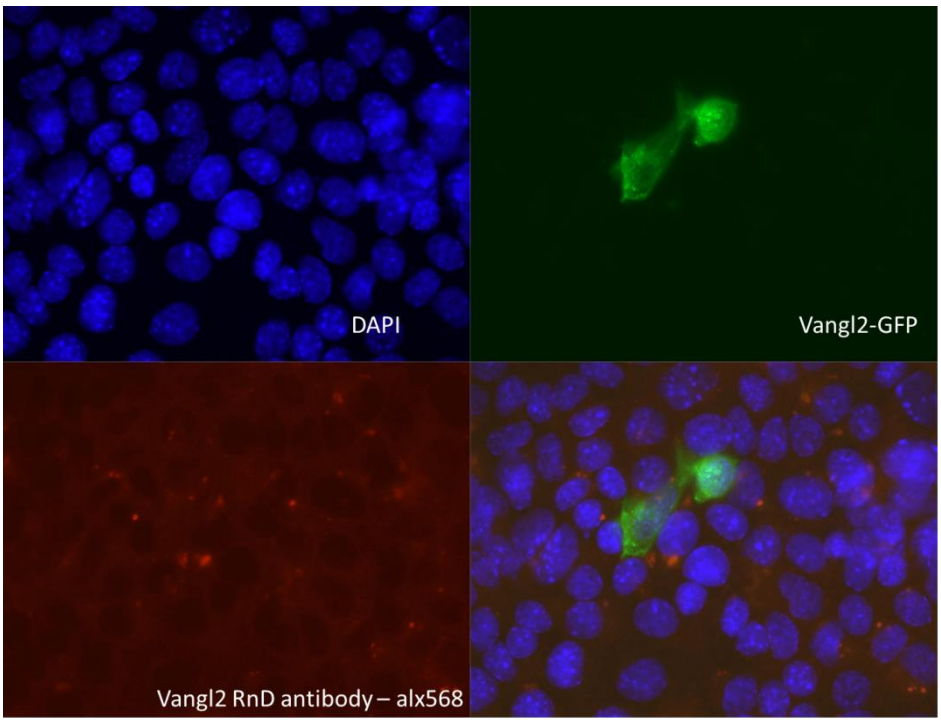

Figure 2f Vangl2 (RnD AF4815) staining of Eph4 cells transfected with Vangl2-GFP cDNA

Vangl2 (RnD AF4815) antibody does not recognise overexpressed Vangl2-GFP in Eph4 cells. Cells were transfected with Vangl2-GFP cDNA and after 48 hours stained with Vangl2 antibody overnight at 4°c. Transfected cells can be seen in green, however there is no increased red signal (Vangl2 antibody), suggesting this antibody does not recognise Vangl2 specifically.

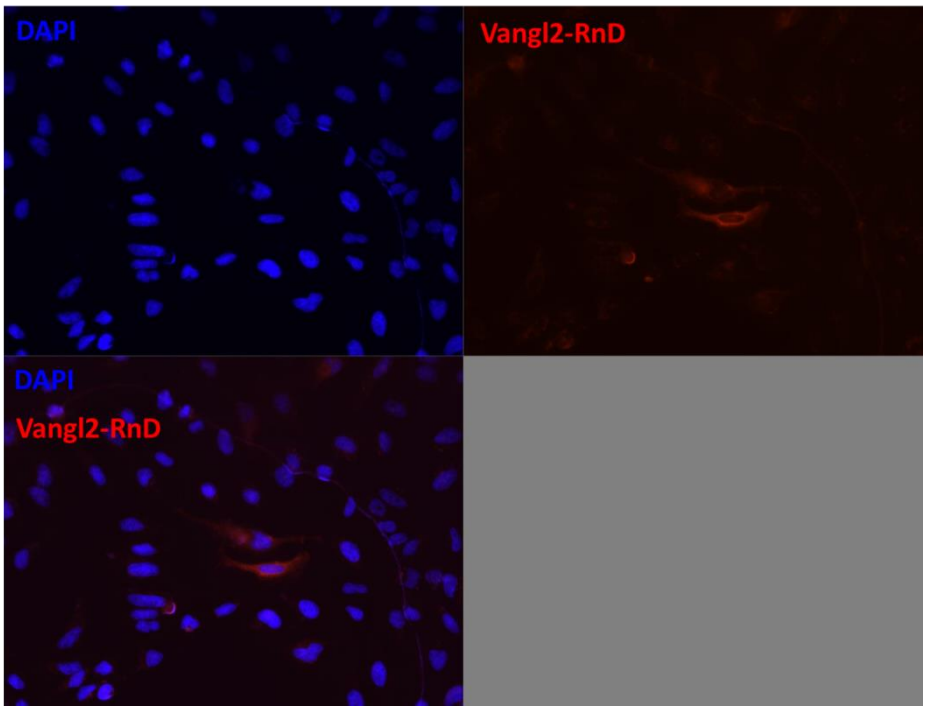

Figure 2g Vangl2 (RnD AF4815) staining of HeLa cells transfected with hVangl2 cDNA

Vangl2 (RnD AF4815) binds to cells overexpressing hVangl2. Cells were transfected with hVangl2 cDNA and after 48 hours stained with Vangl2 antibody overnight at 4°c. Cells with higher signal may be overexpressing Vangl2 however we are unable to confirm this.

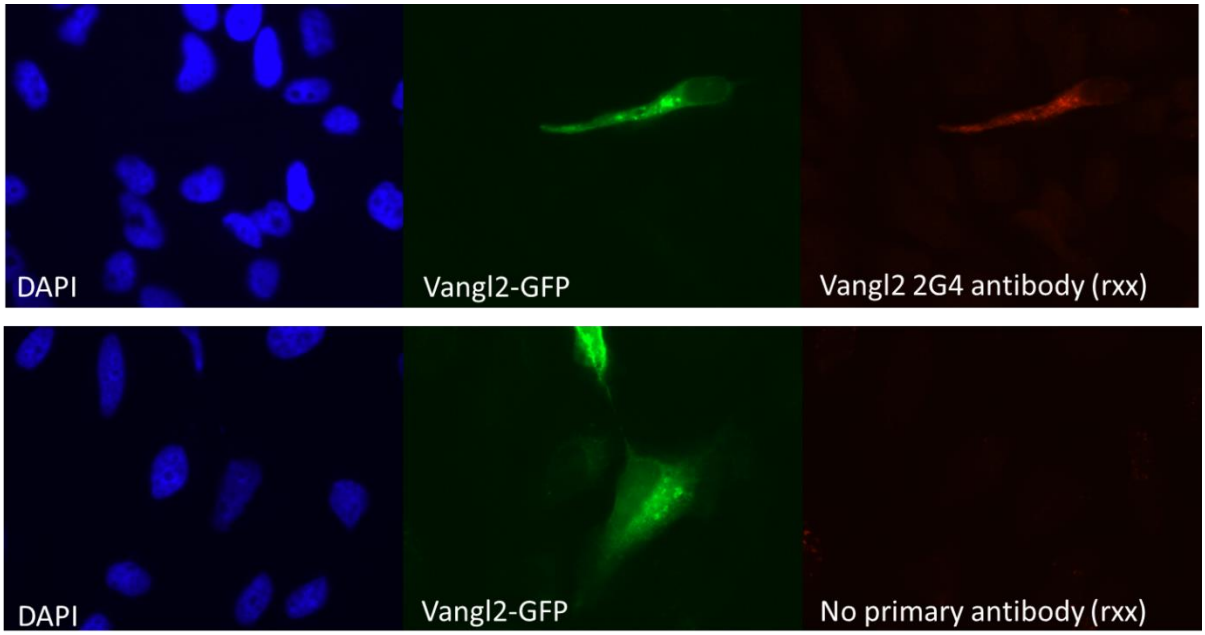

Figure 2h Vangl2 2G4 antibody stains HeLa cells transfected with Vangl2-GFP cDNA

HeLa cells were transfected with Vangl2-GFP cDNA and after 24 hours fixed and stained with Vangl2 2G4 antibody at 1:100 dilution, 4°c overnight (top), or secondary only control (bottom). Positive signal upon Vangl2 2G4 staining suggests that this antibody does recognise overexpressed Vangl2, and is not due to fluorescent bleed-through as a secondary antibody control does not show signal.

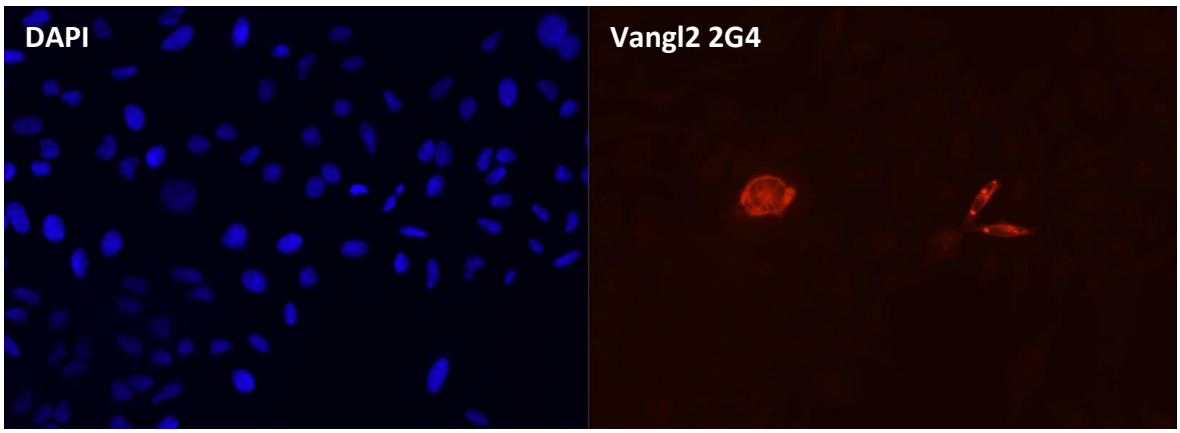

Figure 2i Vangl2 2G4 antibody stains HeLa cells transfected with hVangl2 cDNA

HeLa cells were transfected with hVangl2 cDNA and after 24 hours fixed and stained with Vangl2 2G4 antibody at 1:100 dilution at 4°c overnight. High signal in some cells suggests these cells have higher Vangl2 expression as a result of transfection which is recognised by the Vangl2 2G4 antibody. Images were taken with the same settings and processed identically.

These results suggest that the Vangl2 2G4 antibody can specifically recognise Vangl2 and could be used to reliably localise endogenous Vangl2 in tissue staining.

Imaging mammary gland sections from 8 week old c57 mice showed Vangl2 staining around epithelial cell membranes using the Vangl2 2G4 antibody at 1:100 dilution for 2 hours at room temperature. This is significant compared to the near absence of signal when stained using only the secondary antibody at 1:500 dilution as shown in **Figure 2j**. We concluded that the Vangl2 2G4 antibody can be used to reliably localise endogenous Vangl2 in thin sections of mammary epithelia.

2.2 Expression of Vangl2 in pubertal mammary gland development

Planar Cell Polarity pathways are mostly active during embryonic development in mammals, including in the lung, kidney (Yates et al., 2010, 2012) and cochlear (Montcouquiol et al., 2003). Evidence suggests that in these tissues PCP pathways regulate epithelial morphogenesis, with mutants showing defects in branching and tube diameter. An advantage of studying epithelial morphogenesis of the mammary gland is that most development occurs during puberty, therefore tissues can be easily dissected from mice at any stage of development. We dissected whole mammary glands from CD1 mice at 4, 6, 8, 10 and 12 weeks of age (n=3). Glands 2 and 3 were removed and immediately frozen in liquid nitrogen for protein expression investigation by western blot. Contralateral glands 2 and 3 were either frozen in optimal cutting temperature medium to make thin sections for staining and imaging, or fixed in formalin to embed in wax. Glands 4 were either flash frozen for future RNA analysis, or mounted whole on slides to be imaged. In this section we focus on the protein expression studies performed on these tissues of the mammary gland at every stage of puberty.

Prior to adolescence, each mammary gland consists only of a few rudimentary ducts which grow at the same rate as the animal, and occupy only a small part of the fat pad. At the onset of puberty, at around 4 weeks in mice, terminal end buds (TEBs) form at the end of the ducts and penetrate into the fat pad under hormone control. Over the next few weeks, TEBs branch forming secondary ducts and side branches, as further elongation results in an extensively branched mammary gland. By 8 to 10 weeks, further side branching occurs until

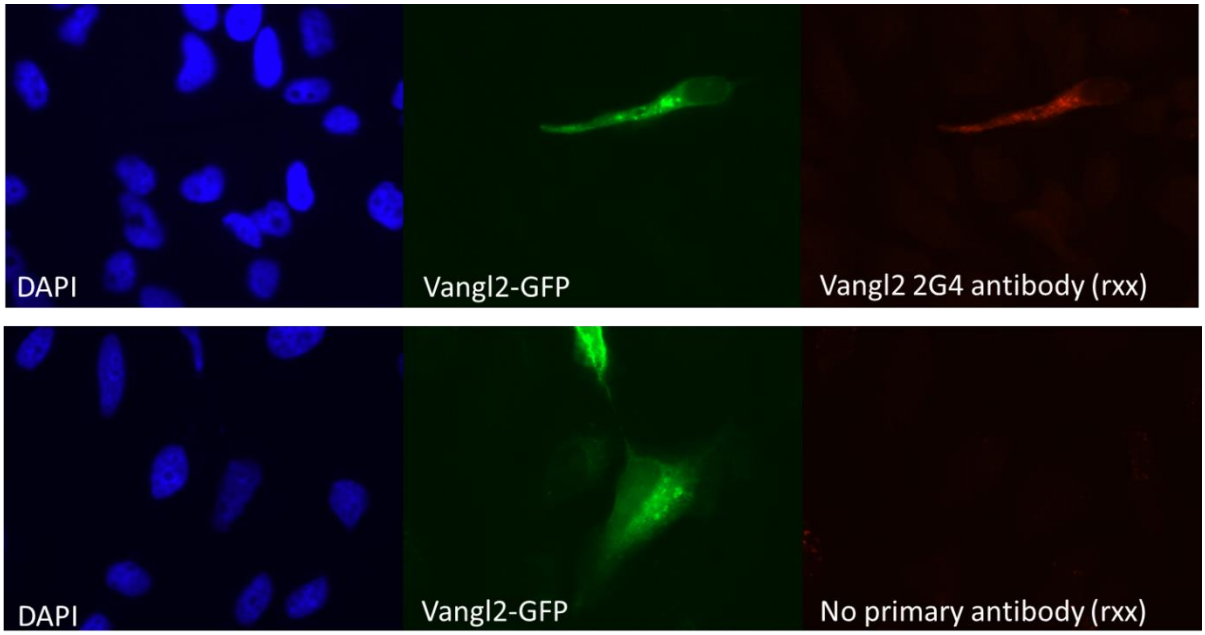

Figure 2h Vangl2 2G4 antibody stains HeLa cells transfected with Vangl2-GFP cDNA

HeLa cells were transfected with Vangl2-GFP cDNA and after 24 hours fixed and stained with Vangl2 2G4 antibody at 1:100 dilution, 4°c overnight (top), or secondary only control (bottom). Positive signal upon Vangl2 2G4 staining suggests that this antibody does recognise overexpressed Vangl2, and is not due to fluorescent bleed-through as a secondary antibody control does not show signal.

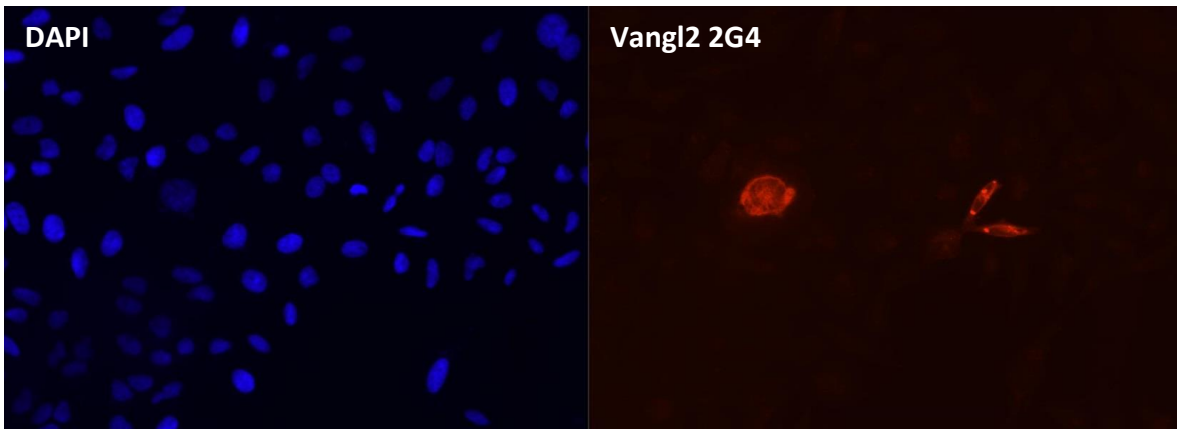

Figure 2i Vangl2 2G4 antibody stains HeLa cells transfected with hVangl2 cDNA

HeLa cells were transfected with hVangl2 cDNA and after 24 hours fixed and stained with Vangl2 2G4 antibody at 1:100 dilution at 4°c overnight. High signal in some cells suggests these cells have higher Vangl2 expression as a result of transfection which is recognised by the Vangl2 2G4 antibody. Images were taken with the same settings and processed identically.

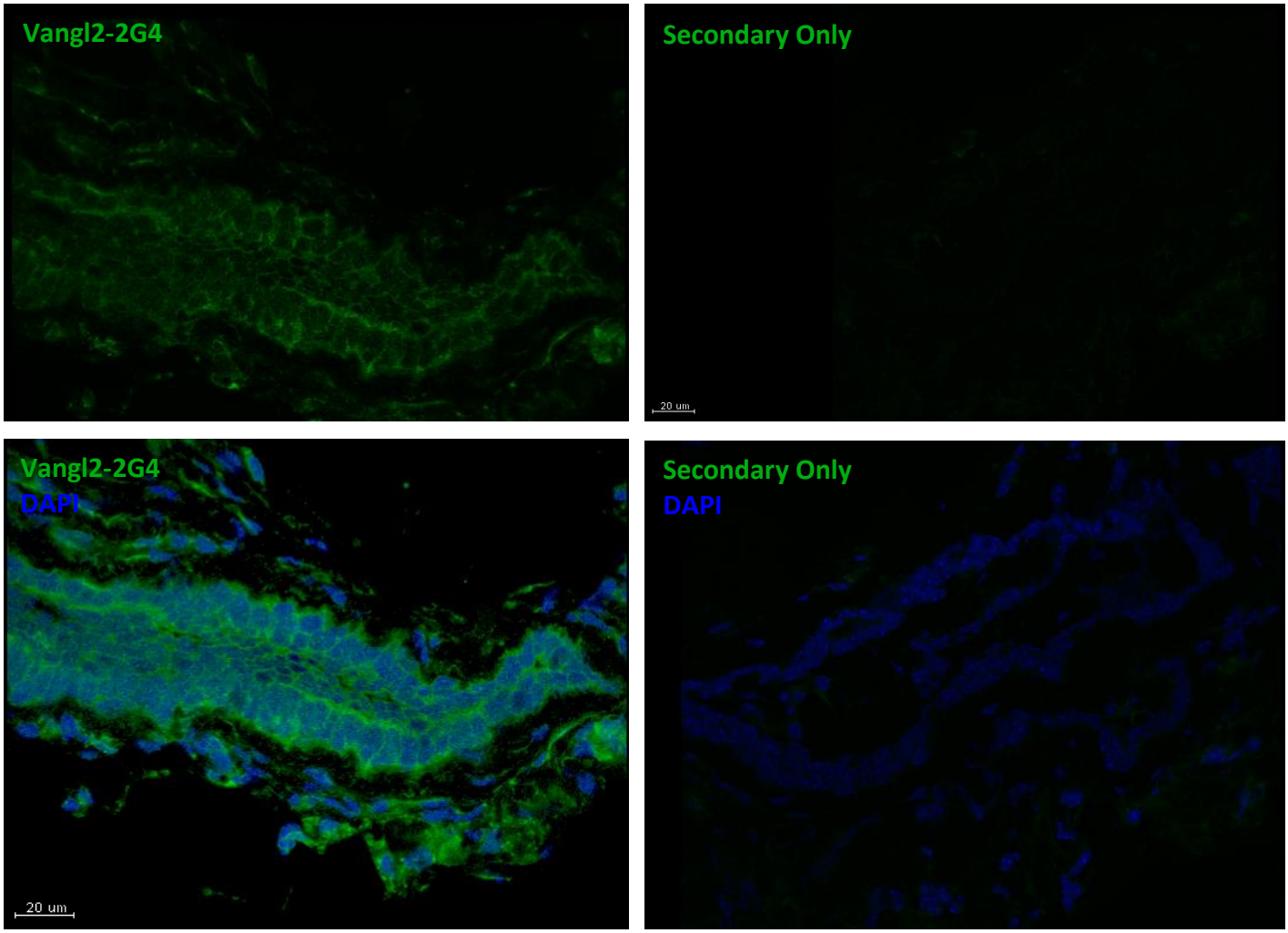

Figure 2j Vangl2-2G4 antibody stains mammary epithelia of an 8 week old c57 mouse

10uM OCT sections of 8 week old c57 mouse mammary epithelia were stained either with Vangl2-2G4 antibody in goat serum at 1:100 dilution for 2 hours at room temperature (left) or with just secondary anti-rabbit antibody at 1:500 dilution and DAPI. Much stronger staining of epithelia and stroma is visible when stained using Vangl2-2G4 antibody, suggesting that Vangl2 is present in 8 week old mammary epithelia. Scale bars 20uM. Images were taken with the same settings and processed identically.

adulthood, around 12 weeks, when branching ceases, ducts reach the end of the fat pad, and the gland grows concurrently with the animal (reviewed in Sternlicht, 2006).

Frozen mammary gland sections were crushed and lysed in lysis buffer with protease inhibitors and phosphatase inhibitor (sodium orthovanadate). To analyse the relative levels of PCP proteins expression in mammary tissue, overall protein levels need to be normalised to epithelium, as most mammary gland mass is made up of stroma and adipocytes, as well as blood vessels, immune cells and collagen. Therefore mammary gland lysates were normalised to levels of e-cadherin, a component of adherens junctions specific to epithelial cells. This was achieved by measuring e-cadherin amounts in the lysates by western blot, and manually altering protein amounts until e-cadherin levels are all the same within each set of samples. **Figure 2k** shows a western blot of sample set #1 normalised to e-cadherin.

After samples were normalised to epithelium, they were blotted for Vangl2 using the previously optimised Vangl2 N-13 antibody. Sample set 2 shows that Vangl2 expression is lowest at 4 weeks, before puberty (**Figure 2l**), if this band is truly specific for Vangl2 protein. Vangl2 protein amount peaks at 6 and 8 weeks, at a time when most branching and elongation occurs, before decreasing again at 10 to 12 weeks.

This experiment was performed in triplicate, with 3 mice at each age analysed. Quantification of Vangl2 expression relative to e-cadherin expression in **Figure 2m** reveals a trend that Vangl2 protein levels are highest on 6 weeks and lowest at 10 and 12 weeks. The difference between Vangl2 expression between 6 and 10 weeks is statistically significant ($p=0.035$). These results suggest that Vangl2 and therefore PCP pathways play roles specifically in the development of mammary gland epithelia when most branching and elongation occurs, but less after branching morphogenesis or during adulthood.

As highest Vangl2 expression is suggested to occur at around 8 weeks in the developing mammary gland, we decided to investigate its localisation using the Vangl2 antibody, Vangl2 2G4 (**Figure 2n**).

Vangl2 staining appears to be limited to lateral and basal cell junctions in 8 week mammary epithelia (**2nii**), with some cells showing higher Vangl2 expression than others. Vangl2 also appears to localise in puncta at junctions between cells and at apico-lateral membranes

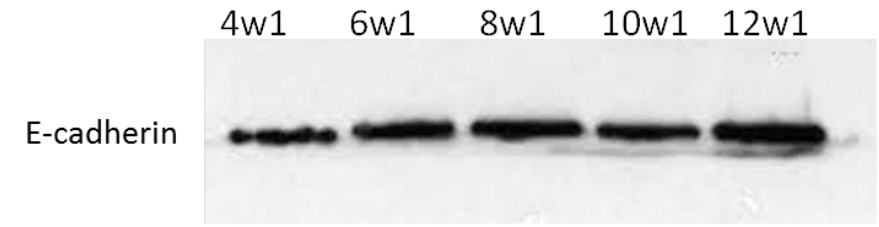

Figure 2k Normalisation of mammary gland tissue to epithelium

Western blot of c57 mouse mammary gland lysates. Samples were ran on a 10% acrylamide SDS-Page gel and blotted for e-cadherin at 1 in 10,000 dilution. E-cadherin levels here are similar, indicating that similar amounts of epithelium were loaded on the gel.

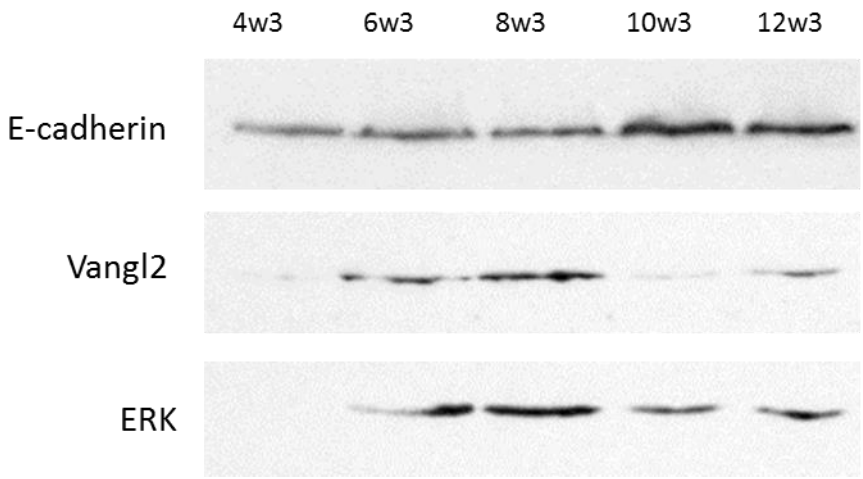

Figure 2l Vangl2 expression appears highest during the branching stages of mammary development

Sample set 3 were normalised to e-cadherin and then Vangl2 and ERK expression levels were measured by western blot. Vangl2 (N-13 antibody) dilution was 1 in 200. Vangl2 expression is lowest at 4 weeks, increases at 4 and 6 weeks and decreases at 10 and 12 weeks, relative to epithelial tissue.

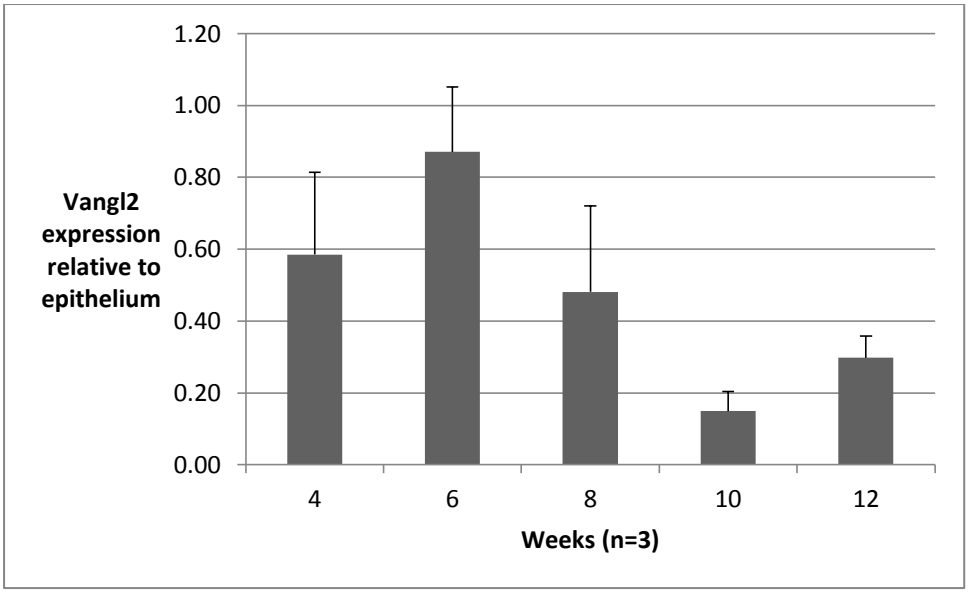

Figure 2m Vangl2 protein expression in mammary epithelia during puberty

This graph shows that Vangl2 expression in epithelia increases from 4 to 6 weeks as mammary gland morphogenesis progresses. This decreases at 8 weeks and is lowest at 10 and 12 weeks when pubertal mammary gland morphogenesis slows down. Western blot bands were quantified on ImageJ. All e-cadherin bands were normalised to 1 on a single blot, so that E-cadherin intensity was level in all subsequent western blots. Vangl2 band intensity was then divided by e-cadherin intensity in the same sample, and then normalised to 1 for comparison. n=3. 3 mice per age were dissected, and all results were combined into the above graph. Error bars show standard error of the mean across 3 sample sets. Difference between Vangl2 expression at 6 and 10 weeks by a one way ANOVA test is p=0.035

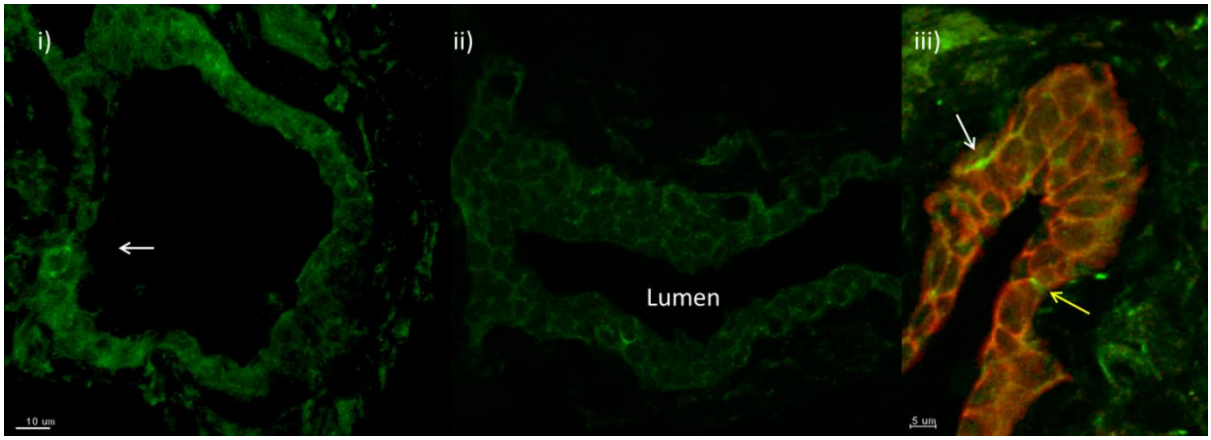

Figure 2n Vangl2 has distinct cellular localisations in 8 week old mammary epithelia

10uM sections of 8 week old mammary tissue stained for Vangl2 using 2G4 antibody at 1:100 dilution for 2 hours at room temperature. i) Strong Vangl2 signal is present in a single rounded cell, with localisation at opposite ends of the cell. As this is a cross section of a duct, Vangl2 localisation may be circumferential, perpendicular to the apico-basal axis. ii) Long section of a duct showing that Vangl2 staining is strongest at cellular junctions, rather than at the apical membrane where no staining is present. iii) Double staining with E-cadherin (red). Enriched Vangl2 staining is visible at the basal membrane (white arrow) in some locations, and in puncta at lateral cell junctions (yellow arrow). Small puncta are also visible at apico-lateral junctions at several points in this image. Scale bars i) 10um and iii) 5um.

(2niii). Interestingly, Vangl2 appears to localise to opposite poles of one large rounded cell, which suggests that it may be undergoing cell division, whereas surrounding cuboidal cells are not. This may provide evidence that supports the theory of PCP pathway roles in directing cell division orientation, localising mitotic spindle machinery to opposite ends of the cell during metaphase (Starzyński et al., 2012).

These images suggest that Vangl2 may be functioning in a similar manner to in other tissues, with activity focussed at lateral cell junctions, and asymmetric localisation in some highly expressing individual cells. However, specific protein localisation in this tubular tissue would be much clearer to visualise in 3D whole mount tissue, as thin 2D sections only show localisation in a single plane, depending on the direction of section. Future work may involve investigating Vangl2 localisation using the previously described 3D whole mount method.

In conclusion, we validated anti-Vangl2 antibodies for identification and quantification of endogenous Vangl2 expression in the developing mammary gland. This was achieved by comparing the signal of endogenous Vangl2 in mammary tissue with over-expressed Vangl2 in cell lines. We subsequently identified that Vangl2 expression in mammary epithelia during development mirrors the periods of most active branching morphogenesis; most strikingly that expression is highest at 6-8 weeks.

We also optimised immunofluorescence staining of Vangl2 in sectioned mammary epithelia in order to detect Vangl2 localisation, and subsequently infer function. To achieve this we tested multiple Vangl2 antibodies under various staining conditions, and tested them against overexpressed h-Vangl2 and Vangl2-GFP in cell lines. We identified the antibody which produced the strongest signal, and staining in sections of glands taken from 8 week old mice show strong signal in some cell membranes. As we are interested in the 3D distribution of PCP proteins in epithelia, Vangl2 localisation in whole mount mammary glands would provide better suggestion of its function in developing epithelia than in 10um sections.

3. Developing 3D Mammary Cell Culture Technology to Analyse Planar Polarised Cell Behaviour in Morphogenesis

The chemical and mechanical events which drive morphogenesis of most tissues have until recently been unobservable. This is as most development occurs early in an organism's life and deep within tissues. In previous decades, most insight into these processes have been deduced from analysis of fixed tissues, which only reveal snapshots in time of dynamic events; or study of organism physiology.

More recently thanks to developing microscopy technology, including the ability to image organisms and tissues in real time in 3D, we are able to observe the development of tissues and organs at high spatial and temporal resolution. The use of fluorescently conjugated proteins is a cornerstone of live imaging, and gives us the tools to follow structures like cell membranes or nuclei, cell populations expressing (or lacking) genes of interest, or follow protein dynamics. Through use of these tools the development of many 'lower' organisms like Drosophila, zebrafish and nemotode have been mapped and studied in depth. By permanently or temporarily deleting genes using techniques such as RNA interference (RNAi), or study of mutant animal lines, the specific roles of proteins in various processes can be dissected. Furthermore, advances in image analysis techniques and mathematical modelling, imaging data of protein dynamics and cell shape changes or movements can be analysed and quantified to produce fascinating insights into the functions of many components of morphogenesis.

2D cell culture techniques have been an essential tool to reveal biochemical and mechanical detail of various pathways important to life; however tissue morphogenesis occurs in specialised environments and multiple cell types exchanging specific signals are required to maintain survival and promote proper growth. Typically attempts to culture ex vivo tissues fail due to the inability to maintain differentiation or produce correct tissue architecture in foreign environments. These problems have been circumvented by development of 3D cell culture, which allows differentiated cells taken from organisms to develop in a similar environment as in vivo, and produce correct function and architecture. With the advent of organoid technology, live imaging, fluorescent protein labelling and gene knockdown, morphogenesis research is no longer limited to the study of lower organisms.

Above other epithelial organs, the mammary gland is advantageous to study as its two main developmental stages occur during adolescence and pregnancy, so tissues undergoing morphogenesis can be easily removed and studied. Whereas ex vivo 2D cell cultures lose differentiation, transplantation of cells into gland-free fat pads of mice develop into a tubed network well (Daniel and Deome, 1965). This showed that components of the microenvironment are essential to development. Furthermore, culture of ex vivo mammary cells in collagen gels produced secretory structures which could secrete milk (Emerman et al., 1997), and mixed cultures of luminal cells and myoepithelial cells are capable of producing their own laminin basement membrane (Streuli et al., 1991). 3D matrices commonly used to facilitate mammary organoid growth include Matrigel, a protein mixture extracted from Engelbreth-Holm-Swarm (EHS) mouse sarcoma cells, containing ECM components.

Primary organoid cultures are grown from mammary epithelial cells which are freshly dissected from either virgin or pregnant murine mammary glands. Glands are minced and mammary epithelial cells are dissociated using digestion with collagenase and trypsin. Cell fractions are isolated through serial centrifugations to separate from other tissues and cell types, and then cultured onto Matrigel (Summarised from Fata et al., 2007).

Like experiments in Drosophila and zebrafish, organoid cultures can be experimentally manipulated to study morphogenesis and molecular pathways. Fluorescent labelling of proteins either through the germ line, transfected fluorescent proteins or live stains can be utilised to follow cell dynamics in real time by imaging organoids during growth. Immunofluorescent staining of fixed organoids can reveal high resolution protein dynamics and morphology information which is difficult to achieve by staining whole tissue samples. Functional studies can also be performed by growing organoids from mutant mice, or knocking down proteins in wild type cultures using lentiviral shRNA infection. Small molecule inhibitors of common molecular pathways, or transfection with dominant negative protein variants have also been used to study effects on morphogenesis.

Organoid cultures could be an excellent system to study planar polarised processes and specifically whether PCP pathways control these processes. For example, movies of

elongating ducts would be analysed to give insight to whether collective cell movements occur, and quantified to suggest whether they are planar polarised. Furthermore, incorporation of fluorescently tagged histones allowing nuclei tracking can show orientations of cell division. This could suggest whether planar polarisation of cell division along the duct regulates ductal elongation.

An important tool to confirm importance of PCP pathways in these processes would be to knock down the pathways through shRNA technology. Organoid formation would then be analysed and compared to wild type, clearly showing differences in cell movements, division orientation, cell shape changes and remodelling compared to wild type. More large scale effects such as impacts on branching events and tubule diameter, which is abrogated in some PCP mutant mice lung and kidneys, could also be measured.

The microenvironment plays an essential role in development of epithelial organs, providing both signalling cues which stimulate development and the mechanical scaffold to support tissue architecture. 2D cell culture techniques usually involve mono-layers of adhesive cells while 3D culture of cells in an environment similar to those in vivo allow some recapitulation of morphology and cell function, and so is an improved experimental model in many cases.

For example, culture of primary mouse luminal epithelial cells in 3D laminin matrix but not 2D stimulates production of milk proteins including WAP and β-casein, due to the polarising effect of laminin (Barcells-Hoff et al., 1989; Streuli et al., 1991). Polarisation of epithelial cells in cultures is important as it allows the basal side of cells to receive signals from the basement membrane, ECM and myoepithelial cells, while the apical membrane secretes milk into the lumen.

3D organoid culture experiments involve growth of ex-vivo mammary cells in 3D extracellular matrix medium derived from mouse EHS cells; however this technique is expensive and labour intensive. Alternatively, Eph4 cells are an immortal non-tumourigenic cell line originally isolated from mid-pregnant mice which share characteristics with mammary luminal epithelial cells (Reichmann et al., 1989). It has previously been shown that Eph4 cells form acini with a lumen and apico-basal polarity when cultured in 3D gels.

Branching structures have also been observed in Eph4/K6 variant cell line cultures treated with growth factors (Niemann et al., 1998), however these structures were irregularly shaped and thin compared to proper ducts formed in vivo or primary organoids.

In these experiments we aimed to test whether 3D culture of mammary epithelial cells could mimic mammary development observed in vivo and in primary organoid cultures.
We show in this section that Eph4 cells cultured in 3D matrix can arrange into 3D acinar structures, however stimulation with FGF2 does not stimulate ductal morphogenesis. Whereas FGF2 stimulation of primary organoid cultures does drive ductal morphogenesis, co-culturing Eph4 cells with a mouse fibroblast cell line did not provide structural or signalling support for ductal growth. Finally we test the behaviour of exogenous Vangl2-GFP in 2D Eph4 cultures compared to 3D cultures.

3.1 Eph4 cells cultured in 3D Matrigel form acini but not ducts

When cultured in 2D in a plastic flask, Eph4 cells form adherens junctions with each other in a monolayer, as shown in **Figure 3a**. Within days of plating onto Matrigel, cells invade into the gel until they are surrounded on all sides. This may be in response to signalling of ECM components like laminin and collagen specifying the basal domain of Eph4 cells. Some clusters of cells also specify continuous apical domains, resulting in generation of a central lumen surrounded by a single layer of epithelial cells (**Figure 3b**). iii) shows a single z-stack image taken on a confocal microscope showing a small acinus surrounded by a single layer of Eph4 cell nuclei. Immunofluorescent e-cadherin staining shows localisation at all lateral membranes and some horizontal membranes suggesting incomplete epithelial polarisation. Co-staining for Vangl2 did not show specific Vangl2 localisation in Eph4 cells, however background fluorescence or staining is evident in the middle of the cells in v). This cluster has failed to polarise or generate a lumen, which is evident from nuclei present in the centre of the cluster.

Whereas Eph4 cells can form polarised structures in 3D culture with similar polarity to in vivo, whether these acini can be stimulated to produce elongated ductal structures is unknown. Primary organoid cultures can be stimulated to produce ductal trees with

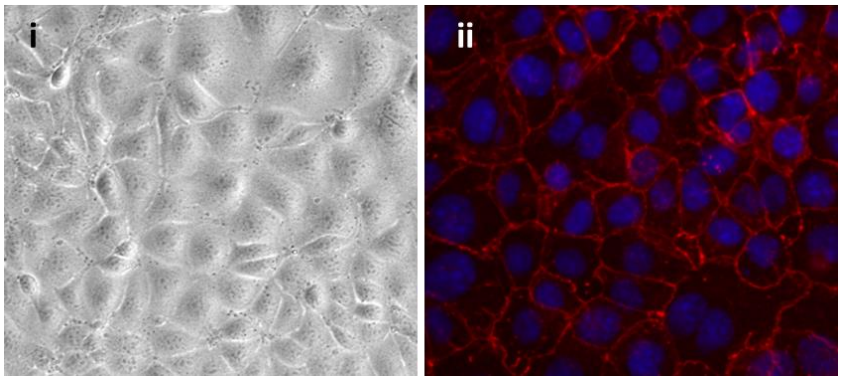

Figure 3a Eph4 cells form a monolayer with adherens junctions in 2D culture

Eph4 cells cultured in plastic flasks in complete DMEM/F12 media. i) Phase contrast image of live Eph4 cells, ii) immunofluorescent staining of Eph4 cells showing beta catenin (red) denoting adherens junctions at cell boundaries and nuclei (blue).

structurally similar terminal end buds by addition of 2.5nM fibroblast growth factor 2 (FGF2) (Ewald et al., 2008). Growth is not directionally controlled in Matrigel cultures, unlike in vivo where collagen fibres are suggested to guide mammary branching and elongation. Indeed synthesising oriented collagen fibres in Matrigel cultures is sufficient to guide mammary gland growth (Brownfield et al., 2013). Eph4 cells cultured in cavities of moulded collagen gel formed hollow tubes conforming to collagen cavities, and under stimulation with epidermal growth factor (FGF) or hepatocyte growth factor (HGF) could undergo branching morphogenesis into surrounding collagen (Nelson et al., 2006).

Ductal morphogenesis of Eph4 cells may be achievable in the absence of long collagen fibres in 3D cultures. Niemann et al., 1998 showed that Eph4 cultures in Matrigel can be stimulated with hepatocyte growth factor (HGF) to form branched tubules. Whereas these tubules appear to have a continuous lumen, their morphology is irregular, unlike the straighter consistently sized ducts which develop in vivo or primary organoid cultures. Additionally there is no evidence of directed growth from a multi-layered epithelium like the TEB. We hypothesised that like primary organoids in Matrigel, Eph4 cell cultures in the presence of FGF2 would form elongated ductal structures which we could use to study planar polarised cell behaviours in epithelial morphogenesis. Eph4 cells were plated onto Matrigel and cultured in either minimal DMEM/F12 media or minimal media with FGF2 at 2.5, 5, 7.5 or 10nM concentrations. Cultures were checked every day and while FGF2 caused increased Eph4 cell proliferation compared to controls, no branching structures were detected as shown in **Figure 3c**.

3.2 Luminal Mammary Cell 3D co-cultures

Eph4 cells alone may lack the ability to produce proper mammary gland morphology as in vivo they are supported by myoepithelial cells, stromal fibroblasts and adipocytes. Primary organoid cultures are able to form ductal morphologies with only two cell types: Luminal Epithelial (LE) cells and Myoepithelial (ME) cells. We hypothesised that when co-cultured with a supporting cell type, Eph4 cells may be able to arrange into a ductal morphology. MCF10A cells, a human mammary epithelial cell line, are able to form functionally differentiated structures when co-cultured with human fibroblasts and adipocytes on a silk

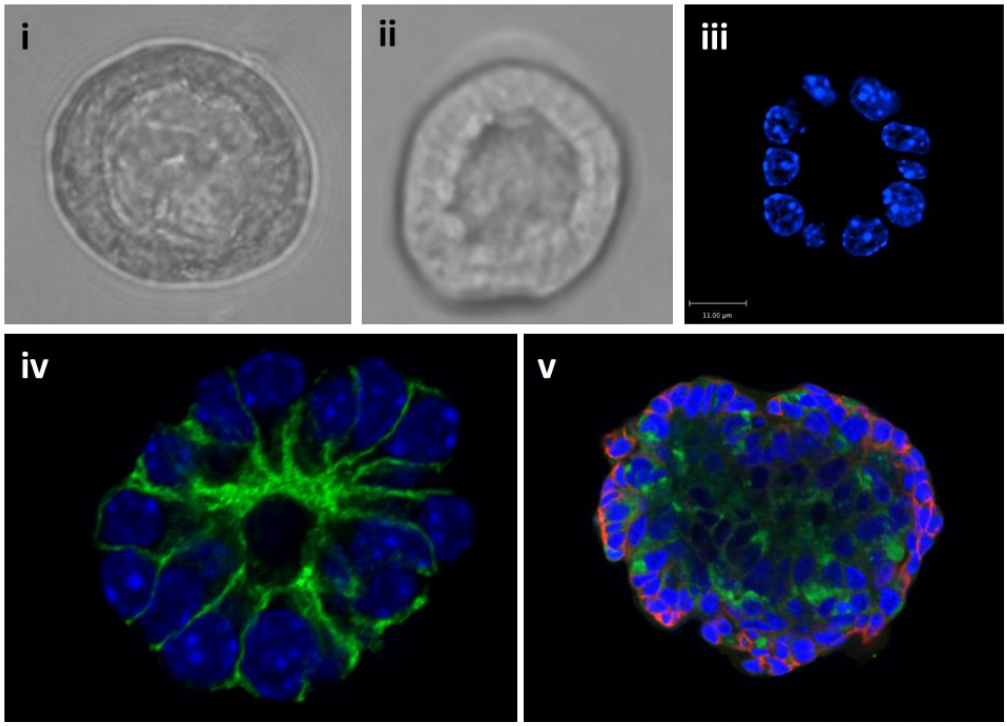

Figure 3b Eph4 cells form hollow acini when cultured in a 3D extracellular matrix

Eph4 cells were seeded onto set Matrigel at $2x10^5$ cells per well in complete DMEM/F12 culture media. Phase contrast images were taken of live cultures at i) 2 days and ii) 4 days and show formation of hollow balls with a single lumen. Organoids were fixed, stained and imaged by confocal microscopy, iii) shows a single z-stack through the centre of an Eph4 acinus, with one single layer of Eph4 cell nuclei (blue) around a central lumen (blank) scale bar 11um. iv) 3D cultures were also stained with antibodies against e-cadherin (green) which show lateral cell junctions and a central lumen in formation. v) shows a large EPh4 cell cluster stained for e-cadherin (red) which is localised around membranes of outer cells and Vangl2 (green) which gave unspecific background signal in all cells.

substrate (Wang et al., 2010), suggesting that fibroblasts rather than only ME cells may be sufficient to arrange luminal cells. Therefore we cultured Eph4 cells with Swiss 3T3 cells, a mouse fibroblast cell line, in a 2:1 or 1:2 cell ratios in Matrigel. After 3 days in 3D culture, phase contrast and immunofluorescent confocal images were taken (**Figure 3d**). Rather than growing in 3D, most cells adhered to the coverslip; however were still under influence of signalling molecules present in the Matrigel. When Eph4 cells outnumber 3T3 cells (i), 3T3 cells appear to surround Eph4s and protrude away from Eph4 cells which cluster together. Interestingly, when 3T3 cells outnumber Eph4s, 3T3 cells form an elevated barrier surrounding Eph4 cells (ii). Immunofluorescent microscopy shows that Eph4 cells express e-cadherin which localises to cell junctions (white arrows), and interact closely with Swiss 3T3 cells (yellow arrows) which do not express e-cadherin (iii and iv). Staining for smooth muscle actin (red) was not specific as it is not expressed by either cell type.

3.3 Eph4 cell sub-populations

In 3D primary mammary organoid cultures, proliferating cells differentiate into subpopulations including luminal and myoepithelial cells. These cell types have different gene expression profiles: luminal epithelial cells express keratin 8/18 (K8/18) and myoepithelial cells express keratin 14 (K14) (reviewed in Inman et al., 2015). This differentiation is essential in mammary gland development, therefore evidence of Eph4 cell differentiation would suggest they are capable of reconstituting mammary morphology under correct conditions. We stained Eph4 cell cultures with antibodies against K14 and K8/18 (**Figure 3e**). Interestingly, we observed that between cells, expression differs to varying degrees. Large populations of cells express K14 (magenta) whereas some cells express virtually no K14 and high levels of K8/18 (green) as shown in i). Conversely, ii) shows a single cell which expressed both K8/18 and K14 (white), while surrounding cells express neither marker. Staining for Smooth Muscle Actin (SMA) appeared unspecific. These results suggest that Eph4 cells may have the multipotency to differentiate into different cell types and so could possibly be used to form morphogenetically sound mammary ducts. However, as far as we know, Eph4 cells are not able to fully convert into myoepithelial cells which may be required to facilitate proper organoid growth in 3D cultures (Ewald et al., 2008).

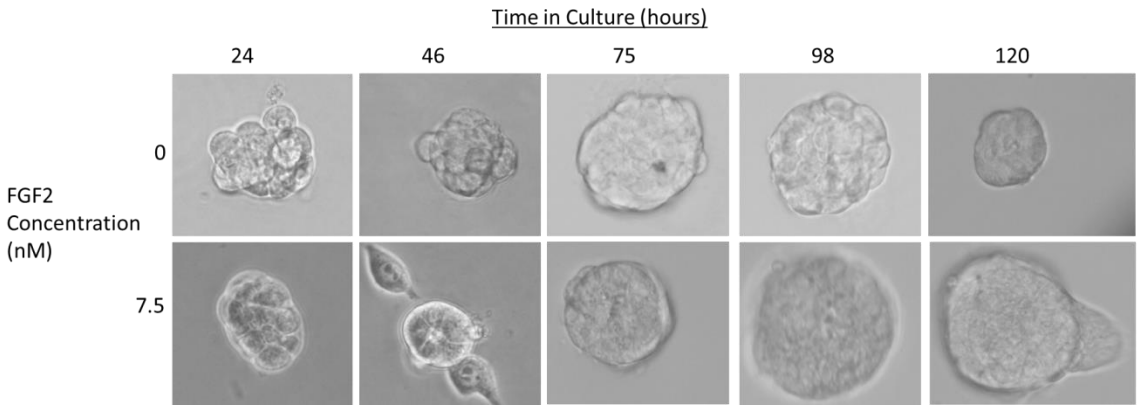

Figure 3c 3D Eph4 cell cultures do not develop ducts upon FGF2 stimulation

Eph4 cells were suspended in either minimal media (top row) or minimal media supplemented with FGF2 at 2.5, 5, 7.5 or 10nM and plated onto Matrigel. This figure shows phase contrast images taken every day for 5 days after plating. Images do not show the same cells. Sizes are all directly comparable. Although increased Eph4 proliferation and a larger number of polarised structures were observed as a result of FGF2 addition, no branching structures developed.

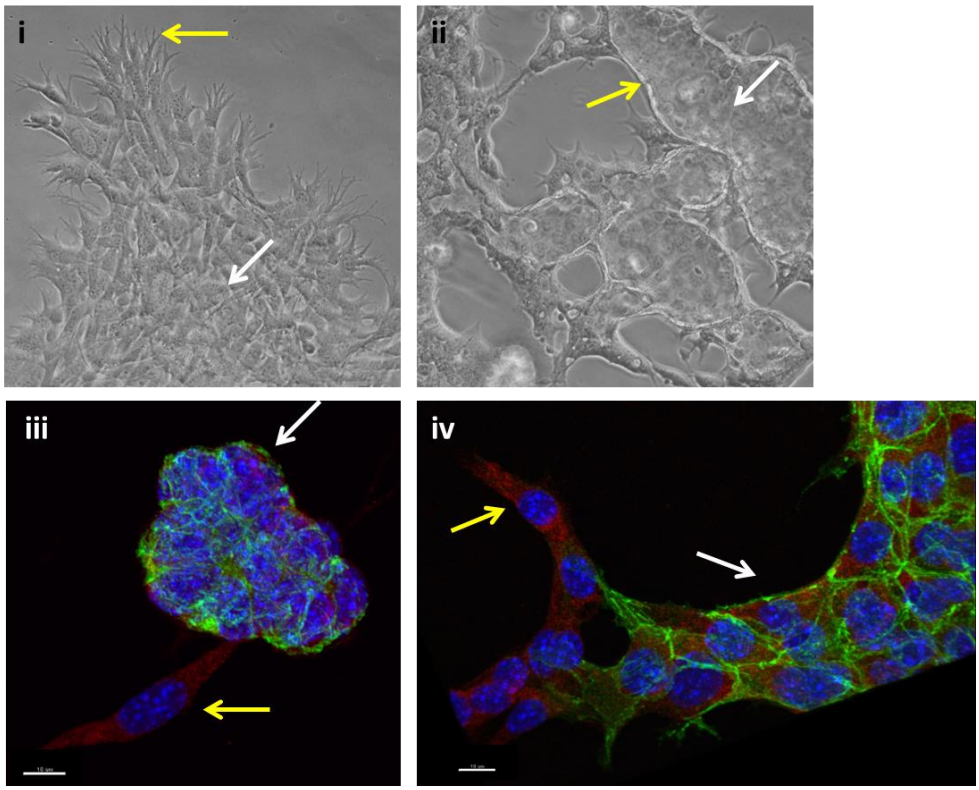

Figure 3d Eph4 and Swiss 3T3 3D co-culture does not facilitate duct development

Mixing Eph4 and Swiss 3T3 cells in complete DMEM/F12 media before plating on Matrigel did not produce ductal structures. Phase contrast images show cells growing on the coverslip although they may still be altered by the extracellular environment of Matrigel. i) Eph4 and 3T3 cells mixed at a 2:1 ratio resulted in 3T3 cells around the outside with long protrusions (yellow arrow) while Eph4 cells clustered centrally (white arrow). ii) Eph4 and 3T3 cells mixed at a 1:2 ratio, appears to show 3T3 cells (yellow arrow) form an elevated barrier around Eph4 cells (white arrow). iii) Eph4/3T3 3D co-culture stained for e-cadherin (green) and smooth muscle actin (red). 3T3 cells (yellow arrows) do not express e-cadherin. Scale bars 10um.

3.4 Vangl2-GFP overexpression in 3D Eph4 cultures

We had previously shown that exogenously expressed Vangl2-GFP shows perinuclear cytoplasmic localisation in 100% of transfected Eph4 cells cultured on plastic in 2D (n=17) (**Figure 3f** i), similar to overexpression in SKBR7 cells, a basal mammary epithelial cell line (Puvirajesinghe et al., 2016). As Eph4 cells cultured in 3D extracellular matrix rather than 2D plastic initiate pathways which establish apico-basal polarity, we asked whether 3D culture also impacts upon planar polarity pathways. To test this, we transfected Eph4 cells with Vangl2-GFP cDNA and after 24 hours, plated these cells onto Matrigel. 3 days later, cultures were fixed and imaged by confocal microscopy. Strikingly, we observed that in 3D culture, Vangl2-GFP localises to cell contacts as shown in ii) and iii). This suggests that establishment of apico-basal polarity in Eph4 3D cultures may act upstream of planar cell polarity pathways. However, due to low transfection efficiency in Eph4 cells, we were unable to observe fully polarised Eph4 acini with lumens which also expressed Vangl2-GFP. Therefore the 3D culture in **Figure 3f** ii) and iii) is incompletely polarised, however it is likely that ECM contacting membranes have begun to respond to signals driving polarisation through integrins (Akhtar and Streuli, 2013), which at some point causes Vangl2-GFP membrane localisation. Conversely, alternate pathways responding to ECM components but not normal culture media could direct Vangl2 to the membrane. Vangl2 adopts asymmetric localisation in some tissues including in developing mouse cochlear cells (Montcouquiol et al., 2006). In **Figure 3f,** Vangl2 is equally distributed around every membrane, suggesting that other planar polarising cues, for example asymmetrically localised Frizzled or Prickle may not be present in the same cell or neighbouring cells. For example, Frizzled at a neighbouring cell membrane may increase Vangl2 localisation at adjoining cell membranes.

Future experiments may also co-transfect Frizzled-RFP to analyse whether Frizzled and Vangl2 adopt planar polarity by localising to opposite sides of the cell as observed by Frizzled and Strabismus in Drosophila pupal wing cells (Strutt, 2001; Bastock et al., 2003). While more components of the core PCP pathway are necessary to achieve polarisation, this experiment could suggest whether PCP mechanisms can produce asymmetry in mammary cultures as they do in other tissues.

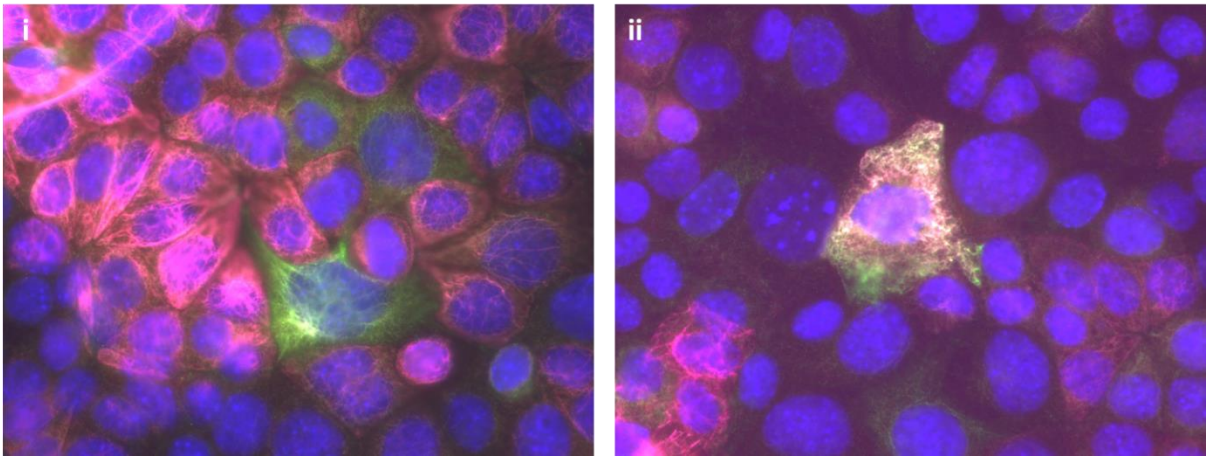

Figure 3e Eph4 cell monocultures partially differentiate to different mammary cell lineages

2D Eph4 cell cultures were fixed 2 days after seeding and stained for Keratin 14 (magenta), Keratin 8/18 (green) and DAPI (blue).

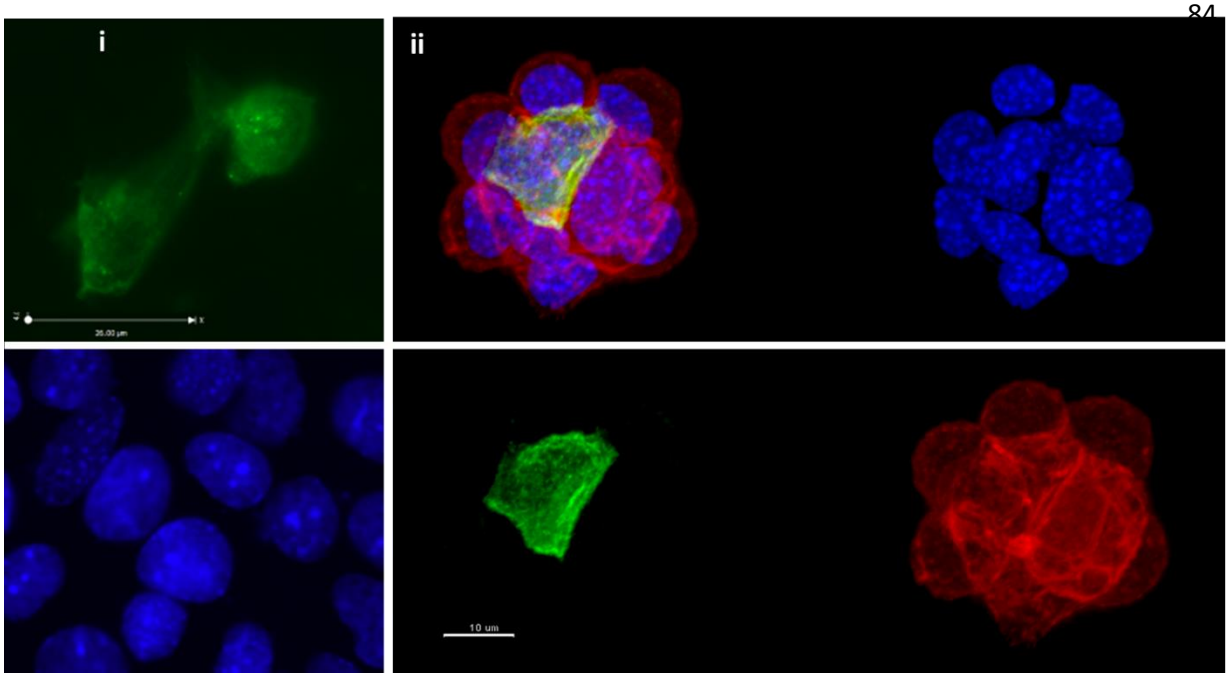

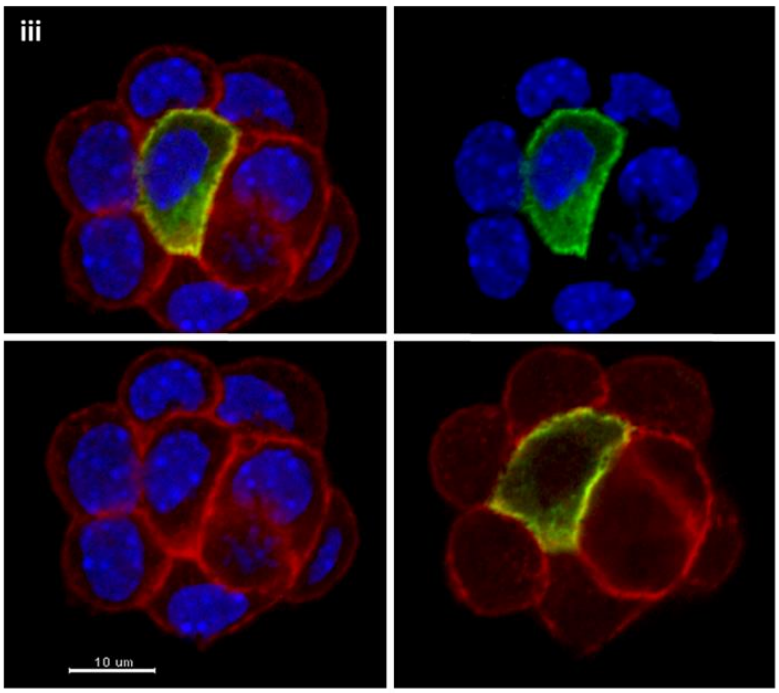

Figure 3f Vangl2-GFP localises to Eph4 cell junctions in 3D culture

Eph4 cells transfected with Vangl2-GFP and cultured i) on plastic in 2D for 24h or ii) and iii) in 3D Matrigel (fixed 4 days after transfection). ii) shows 3D rendered Eph4 cultures fixed after 4 days and stained with phalloidin to show actin (red) and DAPI to show nuclei (blue). iii) is a single Z-stack taken through the middle of a 3D Eph4 acinus. **Scale bars i) 20um, ii)10um.**

We showed in this section that stimulation of 3D Eph4 cultures with FGF2 is insufficient stimulate ductal morphogenesis, in contrast to FGF2's action on primary organoid cultures (Ewald et al., 2008).

Co-culture experiments of Eph4 cells with a mouse fibroblast cell line did not provide structural or signalling support to stimulate ductal growth, suggesting that myoepithelial cells may be necessary. Finally we showed that whereas overexpressed Vangl2-GFP in 2D cultures adopts cytoplasmic localisation, in 3D cultures Vangl2-GFP appears to localise more at cell contacts.

4. Generating tools to analyse PCP pathways in mammary organoids

To study planar cell polarity pathways in epithelial morphogenesis, we planned to analyse the collective cell behaviour in mammary organoid cultures, and observe effects after knockdown of the planar cell polarity pathway activity. shRNAs against Vangl2 were designed, which could be delivered to mammary cultures using lentiviral infection and effects of PCP pathway loss could be analysed. These include the polarised collective migration of cells, the cell shape regulation which drives tube formation, elongation and branching, and effects on lumen diameter and shape which is abrogated in Vangl2 mutant mouse lungs and kidneys (Yates et al., 2010, 2010b). Orientation of cell division is a planar polarised process which we hypothesise drives elongation of the mammary gland. Therefore we incorporated fluorescent histones using a H2B-RFP gene cloned into the lentivirus transfer vector, which labels nuclei red. Consequently, live imaging of organoids could be analysed to measure cell division angles relative to the long axis, and the effect of PCP knockdown can be observed. This chapter describes the generation of Vangl2 shRNA tools, nuclei labelling, and their validation in cell lines. Overall, we aimed to generate tools used to analyse the roles of PCP pathways in developing primary mammary organoids by knocking down the activity of PCP proteins.

4.1. shRNA cloning into 2nd generation lentivirus vector

We aimed to knock down PCP pathways in mammary organoid cultures to observe their function in epithelial morphogenesis. Typically, knockdown of one core PCP protein disrupts the whole pathway, so in theory Vangl2 knockdown would be sufficient to disrupt planar polarity. An effective method of knockdown in organoid cultures is through short hairpin RNA (shRNA) interference, a method to silence target gene expression continually. shRNAs are transcribed from DNA and cleave target RNA through the RNA-induced silencing complex (RISC). An advantage of shRNAs over small interfering RNAS (siRNAs) is that shRNAs can be continually produced from DNA by the cells RNA transcription pathway, whereas siRNAs are short-lived. shRNAs are usually delivered to cell cultures through transfection, however primary organoids are difficult to transfect. Therefore lentiviral delivery of shRNAs is used to knock down targeted proteins, as lentiviruses a) infect cells at a high efficiency, and b) DNA is inserted into transcriptionally active host chromatin, so shRNAs are passed on

to progeny cells, which is advantageous for experiments with a time course over days. The 2nd generation lentiviral 'transfer vector' we selected to use was pLVTHM, a plasmid in which shRNAs can be cloned into downstream of a H1 promoter (Addgene, 12247). pLVTHM also has GFP, which allows identification and isolation of infected cells. **Figure 4a** shows a schematic diagram of pLVTHM and its elements.

Three different shRNAs against Vangl2 were selected from previously published literature. Vangl2 shRNAs 1 and 2 were selected from Nagaoka et al., 2014. The sequences were used to knock down rat and human Vangl2 in hippocampal neuron cultures. Vangl2 shRNA sequence 3 was selected from Shafer et al., 2011, which knocked down Vangl2 in HEK293 cells. BLAST sequence analysis (blast.ncbi.nlm.nih.gov) showed that all sequences also recognised mouse Vangl2, and did not recognise any other proteins. Oligonucleotides were designed to include ClaI and MluI restriction sites to facilitate cloning into the pLVTHM vector. Also integrated to the design was a hairpin site (TTCAAGAGA, in green) and spacers (CCCC or GGGG, highlighted), as shown in **Figure 4b**. One Scrambled shRNA was designed to use as a negative control in knockdown experiments.

shRNA oligonucleotides were annealed together and ligated into the digested pLVTHM vector, then transformed into bacteria and plated. Colonies were picked and ran in a PCR reaction using primers of sequences either side of the shRNA insert site and ran on a 2.5% agarose gel. Colonies containing pLVTHM plus Vangl2 shRNA inserts produced a fragment size of 310bp, while pLVTHM without the insert gave a 248bp fragment. **Figure 4c** shows a colony PCR of colonies transformed for Vangl2 shRNA1 and shRNA2. Upward shifted bands show that the PCR products are larger, indicating successful integration of Vangl2 shRNA sequences. Some positive colonies were selected and grown in liquid culture containing carbenicilin overnight, then pLVTHM-Vangl2 shRNAs were purified using Qiagen miniprep kits. Diagnostic digests were performed to confirm the shRNAs were correctly integrated using XbaI and EcoRI for 1 hour at 37°c. Digest products were ran on a 1.5% gel and correct shRNA insertion was indicated by a shift from 492 to 549bp (**Figure 4d**). To confirm there were no mutations in Vangl2 shRNA sequences, shRNAs were sequenced using primers flanking insert regions.

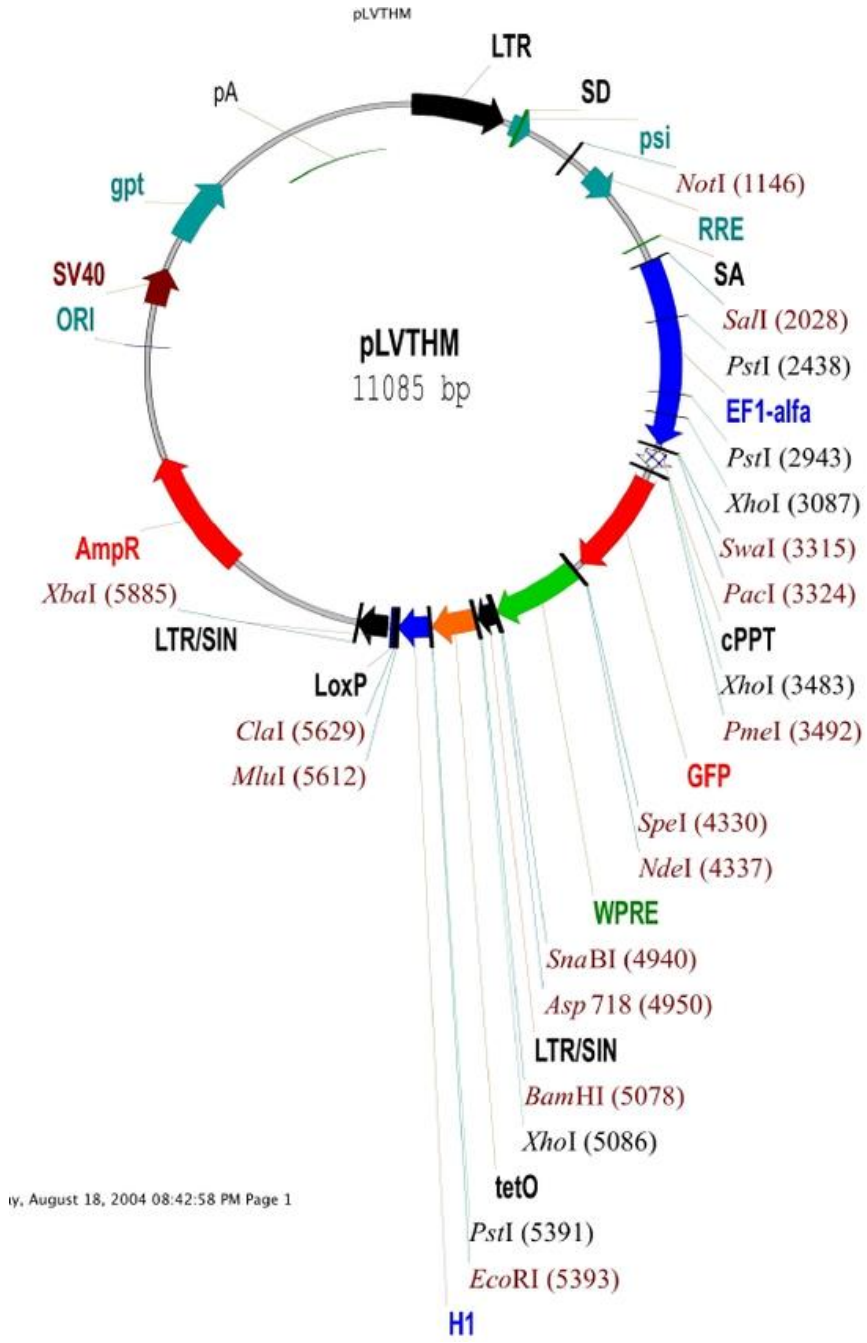

Figure 4a Schematic diagram of pLVTHM vector

pLVTHM is a 2nd generation lentiviral transfer vector. shRNAs are cloned in using the restriction sites ClaI and MluI, downstream of a H1 promoter (blue). Transfected cells express GFP (red, right), and transformed bacteria are resistant to ampicillin due to an ampicillin resistance gene (red, left). Long Terminal Repeats (LTRs) facilitate integration into the host genome. (Addgene, 12247)

Vangl2 shRNA1

Sense

5'-CGCGTCCCCGAGATAAATCAGTGACGATTTCAAGAGAATCGTCACTGATTTATCTCTTTTTGGAAAT-3'

Antisense

5'-CGATTTCCAAAAAGAGATAAATCAGTGACGATTCTCTTGAATCGTCACTGATTTATCTCGGGGA-3'

Vangl2 shRNA2

Sense

5'-CGCGTCCCCTGGGAGTCGTGGAGATAAATTCAAGAGATTTATCTCCACGACTCCCATTTTTGGAAAT-3'

Antisense

5'-CGATTTCCAAAAATGGGAGTCGTGGAGATAAATCTCTTGATTTATCTCCACGACTCCCAGGGGA-3'

Vangl2 shRNA3

Sense

5'-CGCGTCCCCGGGAGAAACAACAACGGTGTTCAAGAGACACCGTTGTTGTTTCTCCCTTTTTGGAAAT-3'

Antisense

5'-CGATTTCCAAAAAGGGAGAAACAACAACGGTGTCTCTTGAACACCGTTGTTGTTTCTCCCGGGGA-3'

Scrambled1 shRNA

Sense

5'-CGCGTCCCCGCCTGGACAAGCAGGGCAATTCAAGAGATTGCCCTGCTTGTCCAGGCTTTTTGGAAAT-3'

Antisense

5'-CGATTTCCAAAAAGCCTGGACAAGCAGGGCAATCTCTTGAATTGCCCTGCTTGTCCAGGCGGGGA-3'

Figure 4b Oligonucleotides designed to clone Vangl2 shRNAs into pLVTHM

shRNA sequences (black) are complimentary to fold and bind into a hair-pin around the hinge region (green) when transcribed into RNA. Spacers are included to separate shRNA sequences from restriction sites (yellow highlight and blue). Restriction sites are in red: MluI (Sense A^CGCGT); ClaI (Sense AT^CGAT). shRNA sequences were ordered from Integrated DNA Technologies and resuspended at 50mM in TE buffer.

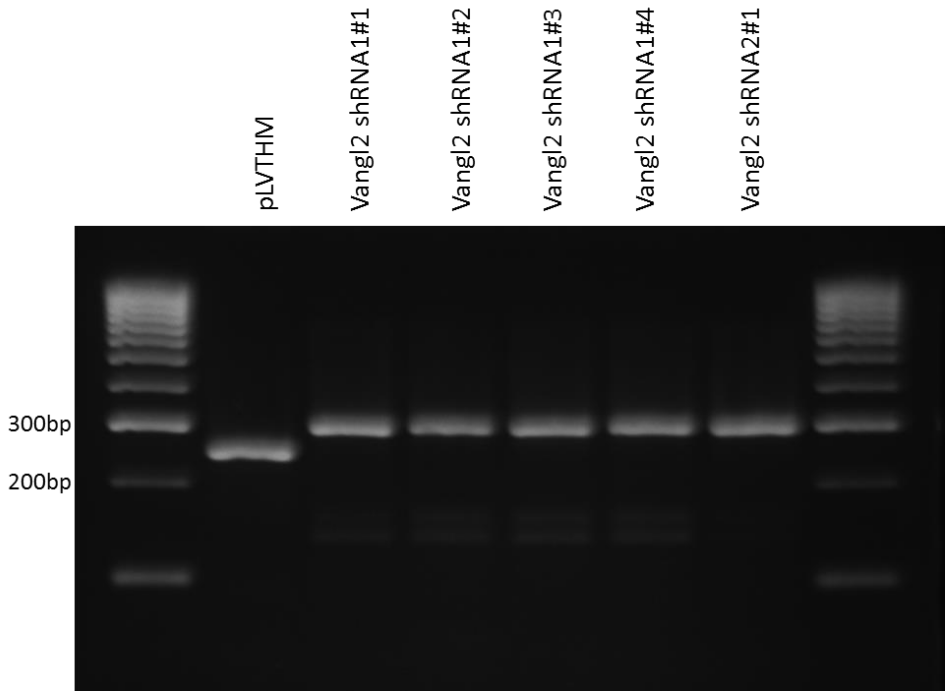

Figure 4c Colony PCR of pLVTHM + Vangl2 shRNAs transformed a-select bacteria

pLVTHM plus Vangl2 shRNAs were transformed into bacteria and plated on agar plates with ampicillin. Colonies were picked and ran on a PCR. Higher bands compared to pLVTHM indicate pLVTHM is larger after integrating shRNAs.

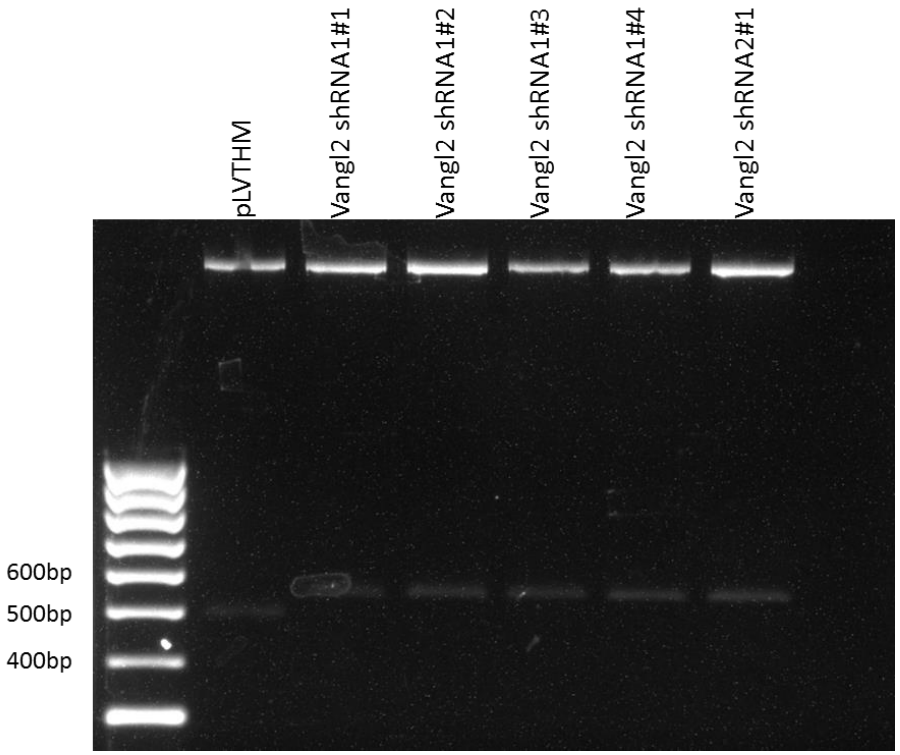

Figure 4d pLVTHM diagnostic digests with XbaI and EcoRI

Purified cDNA was digested with XbaI and EcoRI and ran on a 1.5% agarose gel. Upward shifts indicate shRNA integration into pLVTHM.

4.2 H2B-RFP cloning into pLVTHM vector

Cells which have successfully been infected with pLVTHM express GFP as a positive marker. One hypothesis we wanted to test was that orientations of cell divisions in developing mammary epithelia are oriented along the length of the duct. Therefore to test this by analysing cell division orientation, we swapped the GFP in pLVTHM with a gene for fluorescent histones, H2B-RFP. This involved removing a H2B-RFP gene from an unknown plasmid we acquired, and cloning this into pLVTHM in place of GFP. As the H2B-RFP vector plasmid was unknown, primers were designed to sequence outwards in both directions from H2B and the plasmid was sequenced. After 2 rounds of primer designs and sequencing, the DNA sequence of H2B-RFP and surrounding sequences was determined. Two unique restriction sites either side of GFP in the pLVTHM plasmid were selected, PmeI (forward) and SpeI (reverse). **Figure 4e** shows the difference in pLVTHM sequence before and after RFP-H2B cloning.

After H2B-RFP sequence was elucidated, primers were designed to remove the H2B-RFP while adding PmeI and SpeI restriction sites, without shifting the gene out of frame in relation to the upstream Ef1a promoter in pLVTHM. Some PCR product was ran on a 1.2% agarose gel and purified using a Qiagen PCR purification column. An expected fragment of 1.14kb was confirmed (**Figure 4f**).

Both pLVTHM and RFP-H2B fragments were digested for 3 hours at 37°c with PmeI and SpeI restriction enzymes and immediately ran on a 1.2% agarose gel. Fragment sizes expected for pLVTHM were 10244bp and 841bp (GFP), and digested RFP-H2B was expected to be 1131bp (**Figure 4g**). Digested DNA bands were extracted and purified using a Fermentas gel extraction kit.

Digested pLVTHM and H2B-RFP were ligated overnight at 4°c at a 5x insert to vector ratio, transformed into a-silver select cells and cultured overnight at 37°c on agar plates with ampicillin. Four colonies were inoculated and DNA was purified the next day. To confirm that H2B-RFP was ligated into pLVTHM, a diagnostic digest with PmeI and SpeI showed bands at the correct sizes for all colonies, as shown in **Figure 4h**. To test correct function, pLVTHM-H2B-RFP was transfected into Eph4 cells. Red fluorescence of some nuclei indicated that GFP was successfully swapped out for H2B-RFP (**Figure 4i**).

i) pLVTHM (with GFP)

ttaaaagaaaaggggggattgggggtacagtgcaggggaaagaatagtagacataatagcaacagacatacaaactaaagaattacaaaaacaaattacaaaaattc
aaaattttccgatcacgagactagcctcgaggtttaaactacgggatcttcgaaggcctaagcttacgcgcgcgtcctagcgctaccggtcgccaccatggtgagcaa
gggcgaggagctgttcaccggggtggtgcccatcctggtcgagctggacggcgacgtaaacggccacaagttcagcgtgtccggcgagggcgagggcgatgccacct
cggcaagctgaccctgaagttcatctgcaccaccggcaagctgcccgtgccctggcccaccctcgtgaccaccctgacctacggcgtgcagtgcttcagccgctaccc
cgaccacatgaagcagcacgacttcttcaagtccgccatgcccgaaggctacgtccaggagcgcaccatcttcttcaaggacgacggcaactacaagacccgcgccga
ggtgaagttcgagggcgacaccctggtgaaccgcatcgagctgaagggcatcgacttcaaggaggacggcaacatcctggggcacaagctggagtacaactacaacag
ccacaacgtctatatcatggccgacaagcagaagaacggcatcaaggtgaacttcaagatccgccacaacatcgaggacggcagcgtgcagctcgccgaccactacca
gcagaacaccccatcggcgacggccccgtgctgctgcccgacaaccactacctgagcacccagtccgccctgagcaaagaccccaacgagaagcgcgatcacatggt
cctgctggagttcgtgaccgccgccgggatcactctcggcatggacgagctgtacaagtccggactcagatctcgatagctagtagctagctagctagtcgagctcaa
cttcgggg actagt catatgataatcaacctctggattacaaaatttgtgaaagattgactggtattcttaactatgttgctccttttacgctatgtggatacgctgc
tttaatgcctttgtatcatgctattgcttcccgtatggctttcattttctcctccttgtataaatcctggttgctgtctctttatgaggagttgtggcccgttgtcag

ii) pLVTHM-H2B-RFP

aaaattttccgatcacgagactagcctcgaggtttaaacCACCATGCCAGAGCCAGCGAAGTCTGCTCCCGCCCCGAAAAAGGGCTCCAAGAAGGCGGTGACTAAGGC
GCAGAAGAAAGGCGGCAAGAAGCGCAAGCGCAGCCGCAAGGAGAGCTATTCCATCTATGTGTACAAGGTTCTGAAGCAGGTCCACCCTGACACCGGCATTTCGTCCAA
GGCCATGGGCATCATGAATTCGTTTGTGAACGACATTTTCGAGCGCATCGCAGGTGAGGCTTCCCGCCTGGCGCATTACAACAAGCGCTCGACCNNCNNNNNNAGGGA
GATCCAGACGGCCGTGCGCCTGCTGCTGCCTGGGGAGTTGGCCAAGCACGCCGTGTCCGAGGGTACTAAGGCCATCACCAAGTACACCAGCGCTAAGGATCCACCGGT
CGCCACCATGGTGTCTAAGGGCGAAGAGCTGATTAAGGAGAACATGCACATGAAGCTGTACATGGAGGGCACCGTGAACAACCACCACTTCAAGTGCACATCCGAGGG
CGAAGGCAAGCCCTACGAGGGCACCCAGACCATGAGAATCAAGGTGGTCGAGGGCGGCCCTCTCCCCTTCGCCTTCGACATCCTGGCTACCAGCTTCATGTACGGCAG
CAGAACCTTCATCAACCACACCCAGGGCATCCCCGACTTCTTTAAGCAGTCCTTCCCTGAGGGCTTCACATGGGAGAGAGTCACCACATACGAAGACGGGGGCGTGCT
GACCGCTACCCAGGACACCAGCCTCCAGGACGGCTGCCTCATCTACAACGTCAAGATCAGAGGGGTGAACTTCCCATCCAACGGCCCTGTGATGCAGAAGAAAACACT
CGGCTGGGAGGCCAACACCGAGATGCTGTACCCCGCTGACGGCGGCCTGGAAGGCAGAAGCGACATGGCCCTGAAGCTCGTGGGCGGGGGCCACCTGATCTGCAACTT
CAAGACCACATACAGATCCAAGAAACCCGCTAAGAACCTCAAGATGCCCGGCGTCTACTATGTGGACCACAGACTGGAAAGAATCAAGGAGGCCGACAAAGAGACCTA
CGTCGAGCAGCACGAGGTGGCTGTGGCCAGATACTGCGACCTCCCTAGCAAACTGGGGCACAAACTTAATTGAGCAGactagtcatatgataatcaacctctggatta

Figure 4e the fluorescent marker in pLVTHM, GFP was swapped for H2B-RFP

i) pLVTHM contained a sequence for GFP (green) which is expressed in transfected or infected cells. Unique restriction sites were selected either side: PmeI (blue) and SpeI (peach). ii) GFP was digested out and replaced with a H2B-RFP gene. H2B (orange), RFP (red).

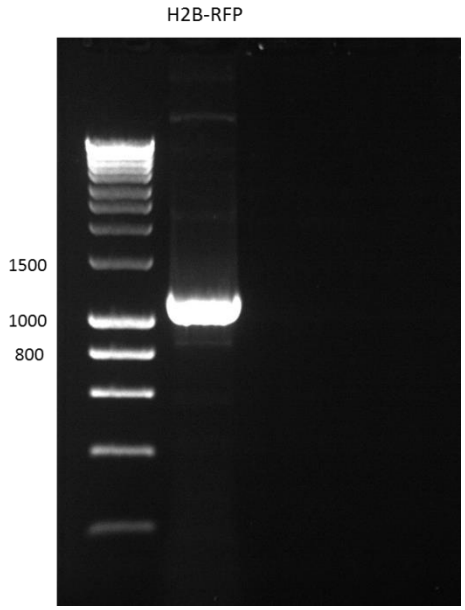

Figure 4f PCR product of H2B-RFP isolation

H2B-RFP was isolated from an unknown plasmid using primers designed against flanking regions of the gene, plus added PmeI and SpeI restriction sites. A fragment of 1.14kb was identified on an agarose gel.

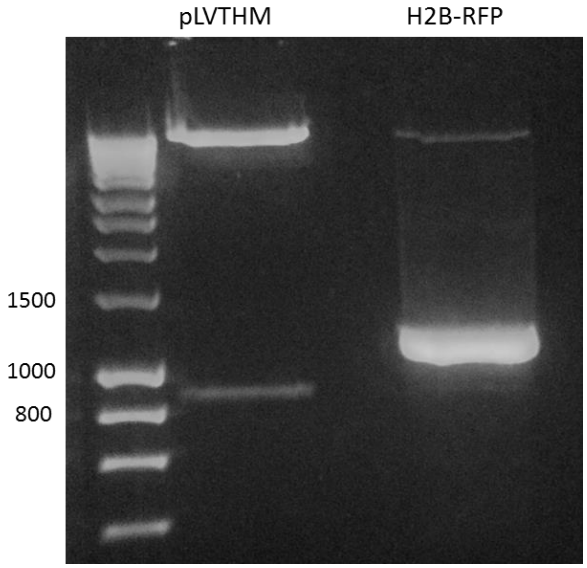

Figure 4g pLVTHM and H2B-RFP restriction digests with PmeI and SpeI

Restriction digest were ran on an agarose gel with Sybr-Safe to confirm correct fragment sizes. The desired bands, 10kb for pLVTHM and 1.1kb H2B-RFP, were extracted using a scalpel and DNA was isolated using a Fermentas gel extraction kit.

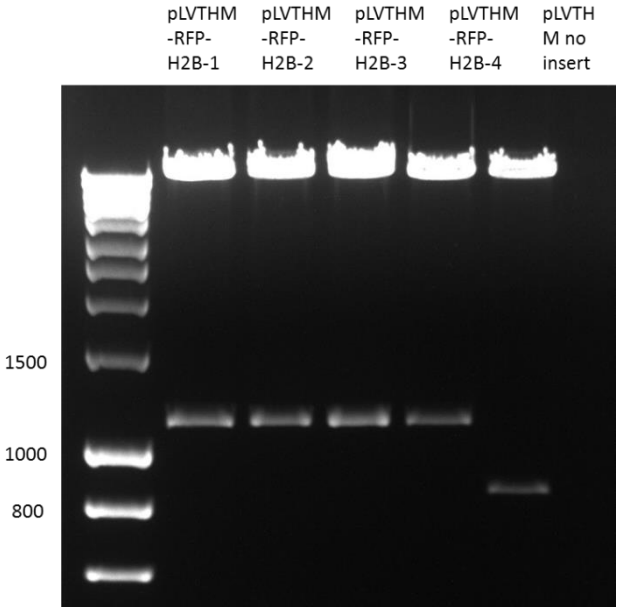

Figure 4h Diagnostic digest of pLVTHM-RFP-H2B with PmeI and SpeI

Purified pLVTHM-H2B-RFP cDNA was digested with PmeI and SpeI and ran on a 1.2% agarose gel. All pLVTHM-RFP-H2B colonies have inserts at 1126bp, compared to an 841bp insert without inserted H2B-RFP (right lane).

4.3 Analysis of WPRE in pLVTHM vector

The 2nd generation lentiviral transfer vector we selected to use, pLVTHM cDNA contains a Woodchuck Hepatatis Virus Posttranscriptional Response Element (WPRE), an untranslated DNA sequence which when inserted into the untranslated region of viral transfer vectors increases transgene expression 5 to 8 fold. In this case, the WPRE increases shRNA expression (Zufferey et al., 1999). There were biological safety concerns over a truncated 'Protein X' being expressed from the WPRE sequence, which has been reported to have oncogenic activity in mouse livers (Kingsman et al., 2005). This required us to prove that Protein X is not expressed in cells transfected with pLVTHM.

To analyse whether Protein X is expressed, primers were designed against 5' and 3' regions of truncated protein X cDNA, which would be produced through reverse-transcription PCR (RT-PCR) on isolated RNA samples. pLVTHM was transfected into Swiss 3T3 cells using lipofectamine 3000 and incubated for 32 hours. 3T3 cells were lysed and RNA was extracted using a Trifast, phase separation and RNA precipitation method. RNA concentrations were measured on a Nanodrop machine to confirm RNA isolation. In order to test that RNA samples were pure and free of DNA contamination, a PCR cycle was ran on RNA samples using primers against Protein X. Untransfected 3T3 cell lysates were ran as a negative control, while pLVTHM cDNA was included as a positive control for the Protein X sequence. We aimed to prove that truncated Protein X RNA was not transcribed in pLVTHM transfected cells; however a band at around 200bp was detected as shown in Figure 4j. This result was due to pLVTHM cDNA remaining in the sample, therefore we decided to ensure pLVTHM cDNA is totally removed from RNA extractions.

DNA removal involved treatment with DNAse I and clean-up using Qiagen RNeasy spin columns. Samples were then ran again on a PCR using primers against truncated Protein X, however a band still appeared in pLVTHM transfected 3T3 RNA extracts (**Figure 4k**). It is possible that DNAse treatment failed to remove pLVTHM cDNA, therefore RT-PCR could not be performed. To avoid potential safety issues we decided to swap to a 3rd generation lentivirus system using pLKO.3G as a transfer vector. Further safety issues with the use of a 2nd generation lentiviral vector in our laboratory meant we took the decision to abandon

use of the pLVTHM in favour of a 3rd generation lentivirus system using pLKO.3G as a transfer vector.

4.4 shRNA cloning into 3rd generation lentivirus vector

The components of lentivirus production are split between 3 or 4 plasmids in order to increase virus safety. These include the transfer plasmid, the envelope plasmid and one or two packaging plasmids. 3rd generation lentivirus systems are safer than 2nd generation, as packaging components encoding Rev, Gag and Pol are split between two plasmids. Importantly, the lentiviral transfer vector we selected to express shRNAs, pLKO.3G (addgene 14748), does not have a protein X sequence in the WPRE. Therefore we re-designed Vangl2 shRNA oligonucleotides to be cloned into pLKO.3G and repeated cloning with similar steps.

Restriction sites either side of the shRNA insert site in pLKO.3G are EcoRI (forward) and PacI (reverse). Therefore we re-designed oligonucelotides for Vangl2 shRNAs to be cloned in to pLKO.3G using these restriction sites (**Figure 4l**). Oligonucleotides were annealed together and ligated into digested pLKO.3G. Ligated cDNA was transformed into DH5a cells and plated onto agar plates with ampicillin. Plates were incubated overnight at 37°c and colonies were checked the next morning. pLKO.3G-shRNA colonies were picked and vortexed in 50ul autoclaved ddH20. PCR was performed on these samples, using 5ul of colony solution in 25ul PCR reactions and primers designed against pLKO.3G regions either side of the shRNA insert site.

PCR products were ran on 2% agarose gels with Sybrsafe, and pLKO.3G colonies with successfully inserted shRNA sequences produced amplified regions with size shifted from 257bp to 287bp as shown in **Figure 4m**. pLKO.3G-shRNA cloning was shown to be complete and absent of deletions or mutations through sequence analysis.

4.5 shRNA validation via transfection

Before cloning into a lentivirus to knock down Vangl2 in mammary organoid cultures, shRNAs need to be validated to ensure that they knock down their target at sufficient levels. We aimed to do this by transfecting Vangl2 shRNAs into cells and analysing knockdown by either western blot or immunofluorescence.

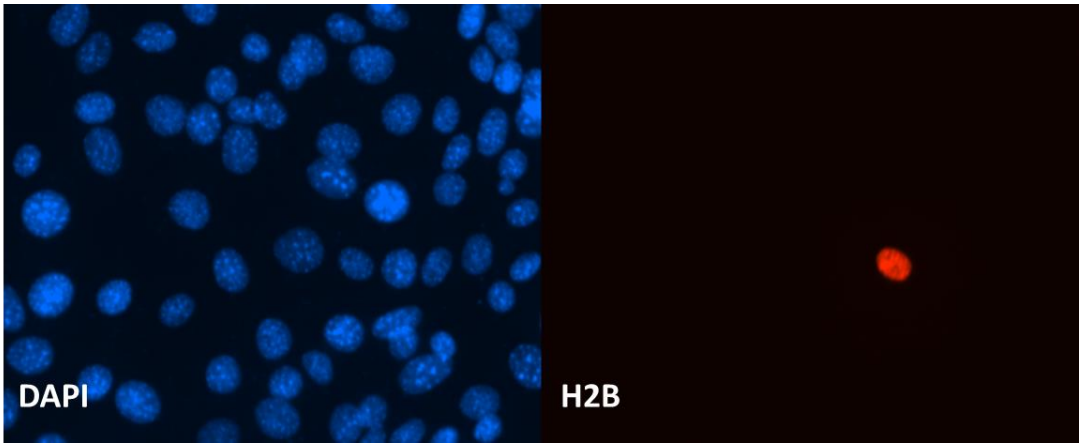

Figure 4i Eph4 cells transfected with pLVTHM-H2B-RFP

Red fluorescence indicates pLVTHM transfected cells express H2B-RFP instead of GFP.

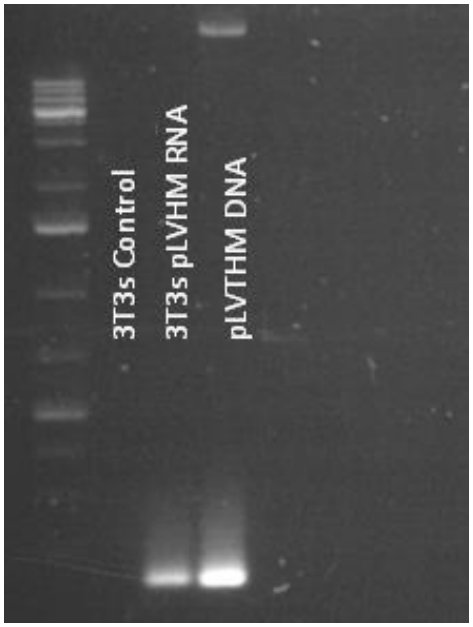

Figure 4j RNA extracts analysed for Protein X RNA expression

Swiss 3T3 cells, or 3T3 cells transfected with pLVTHM cDNA were lysed and RNA was extracted. Samples were run in PCR using primers against truncated Protein X and ran on a 2% agarose gel. pLVTHM cDNA was also used as a positive control. A band is present in the middle lane at around 200bp, indicating a region of Protein X sequence was recognised and amplified in the RNA extract.

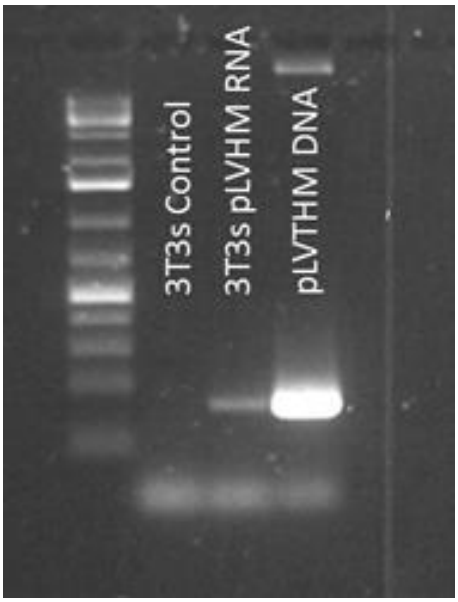

Figure 4k Protein X is still amplified in pLVTHM transfected 3T3 RNA samples

3T3 RNA lysates were treated with DNaseI to remove pLVTHM cDNA, however truncated Protein X was still amplified by PCR.

Vangl2-shRNA1
Sense
AATT GAGATAAATCAGTGACGAT CTCGAG ATCGTCACTGATTTATCTC TTTTTTTAT
Antisense
AAAAAAA GAGATAAATCAGTGACGAT CTCGAG ATCGTCACTGATTTATCTC

Vangl2-shRNA2
Sense
AATT TGGGAGTCGTGGAGATAAA CTCGAG TTTATCTCCACGACTCCCA TTTTTTTAT
Antisense
AAAAAAA TGGGAGTCGTGGAGATAAA CTCGAG TTTATCTCCACGACTCCCA

Vangl2-shRNA3
Sense
AATT GGGAGAAACAACAACGGTG CTCGAG CACCGTTGTTGTTTCTCCC TTTTTTTAT
Antisense
AAAAAAA GGGAGAAACAACAACGGTG CTCGAG CACCGTTGTTGTTTCTCCC

Vangl2-scrambled-shRNA1
Sense
AATT GAATCATACGGTTAAGAGA CTCGAG TCTCTTAACCGTATGATTC TTTTTTTAT
Antisense
AAAAAAA GAATCATACGGTTAAGAGA CTCGAG TCTCTTAACCGTATGATTC

Figure 4l Oligonucleotides designed to clone Vangl2 shRNAs into pLVTHM

Oligonucleotide sequences containing shRNA sequences (blue – Vangl2 or red – scrambled), and a hairpin region (green). EcoRI and PacI restriction sites are either side (orange).

Swiss 3T3 cells are an adhesive mouse fibroblast cell line which is commonly used to validate RNA knockdown efficiency due to their high transfection efficiency potential. Therefore we used Lipofectamine 2000 reagent to transfect pLVTHM-Vangl2shRNA cDNA into Swiss 3T3 cells. Transfection efficiency can be measured by microscopy as transfected cells express large amounts of GFP. One day prior to transfection, 3T3 cells were plated onto nitric acid treated coverslips so that they would be 50% confluent the next day. Several transfection attempts using pLVTHM cDNA and following manufacturer's instructions only produced very low transfection efficiency at <5% (**Figure 4n**). Transfection efficiency was not improved by altering lipofectamine amounts between 4 and 12ul, or increasing cDNA amounts from 2ug to 8ug.

An alternate transfection method was attempted, using calcium phosphate. Mixture of plasmid DNA with calcium phosphate produce DNA-calcium ion mixtures and bind to cell monolayers, which enhances uptake (Graham et al., 1973) through endocytosis. However, we were unable to successfully transfect any Swiss 3T3 cells using the CaPO4 transfection method.

Transfection was also tested using Lipofectamine 3000 reagent in both Swiss 3T3 cells and HeLa cells. Experiments were performed in a 24 well plate using 0.5ug pLVTHM cDNA and 4.5ul lipofectamine 3000 per well. After 24 hours, cells were fixed, DAPI stained and imaged on a widefield microscope. Lipofectamine 3000 produced a much higher transfection efficiency, which when quantified reached 22% in Swiss 3T3 cells and 20% in HeLa cells (**Figure 4o**). Increased transfection efficiency was not due to the change in plate size from 12 to 24 well, as transfection using Lipofectamine 2000 in a 24 well plate produced efficiency less than 1%. Likewise, the use of different types of sterile Eppendorf tubes did not affect transfection efficiency efficiently.

Unfortunately, 20% transfection efficiency is not high enough to validate Vangl2 knockdown by western blot. Additionally, immunofluorescence and microscopy cannot be used to confirm knockdown as Vangl2 has no obvious localisation in Swiss 3T3 cells which could be reliably detected using the antibodies available.

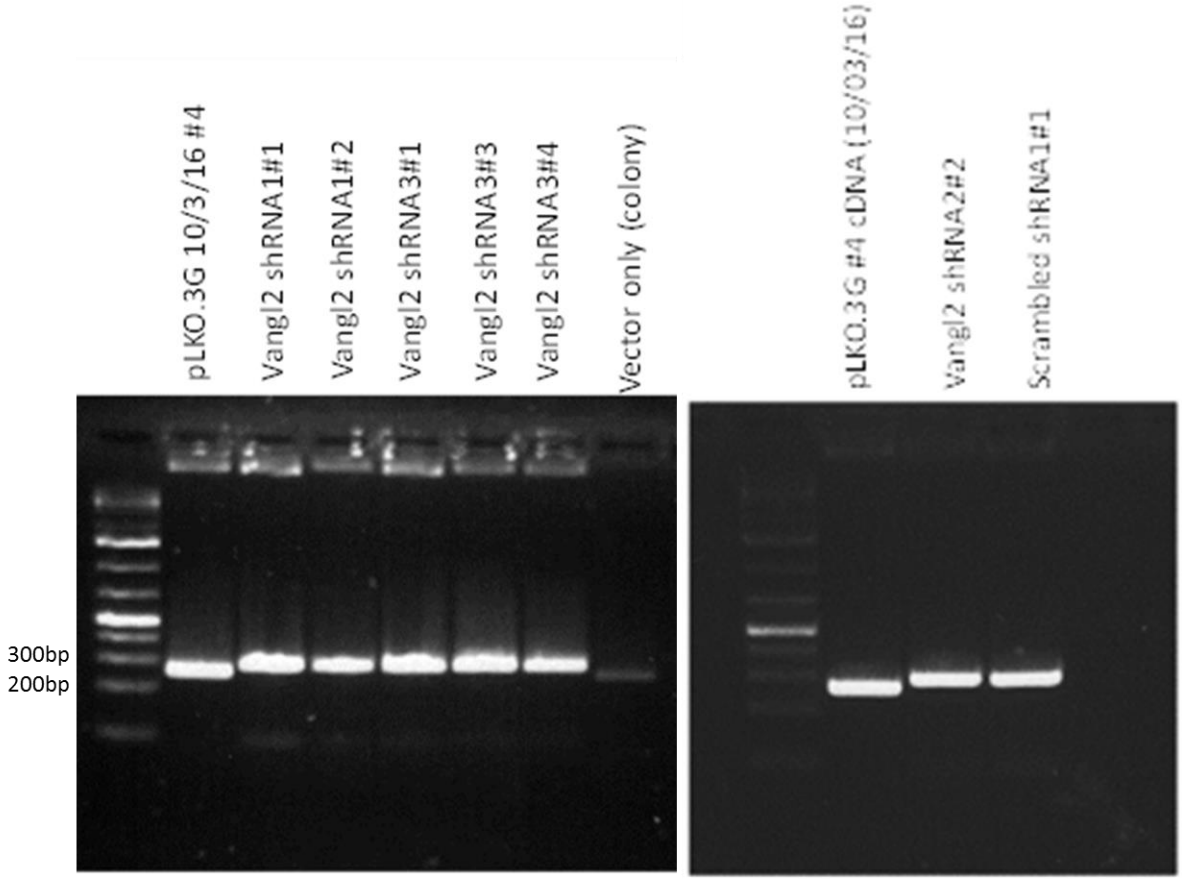

Figure 4m Colony PCR showing completed shRNA cloning into pLKO.3G

pLKO.3G-shRNA cDNA transformed colonies were picked and the region of the shRNA insert site was amplified. Upward shifts were observed in bands amplified from Vangl2-shRNA and scrambled-shRNA colonies compared to colonies of pLKO.3G only, or pLKO.3G cDNA.

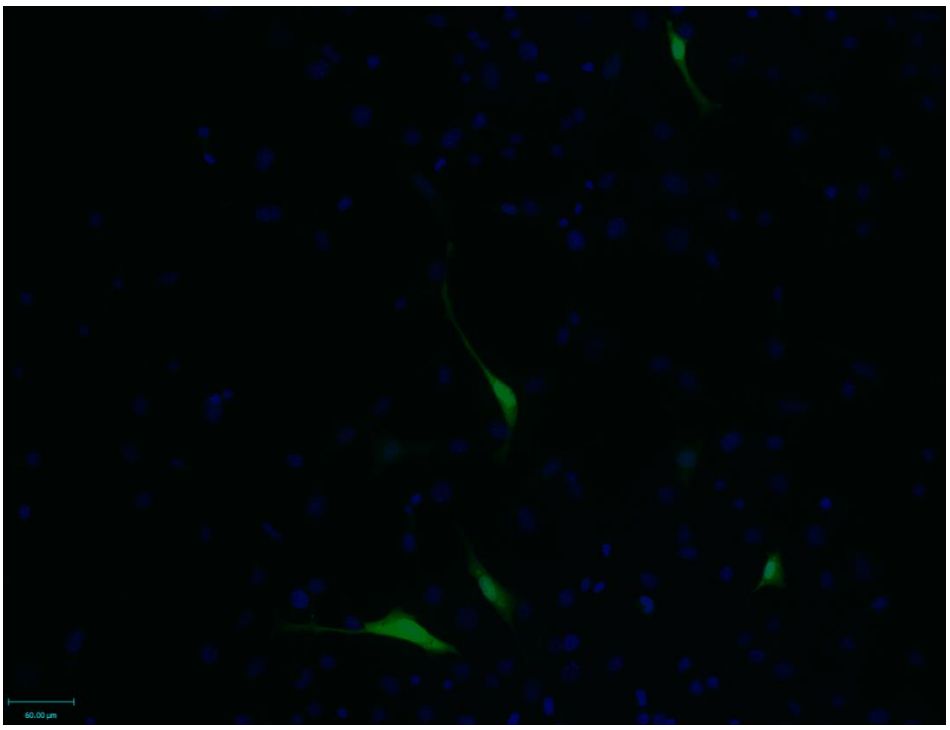

Figure 4n Swiss 3T3 cells transfected with pLVTHM cDNA

3T3 cells were transfected with 2-8ug pLVTHM cDNA using lipofectamine 2000 reagent and fixed after 24 hours. Transfected cells are green, nuclei are blue. Scale bar 60um.

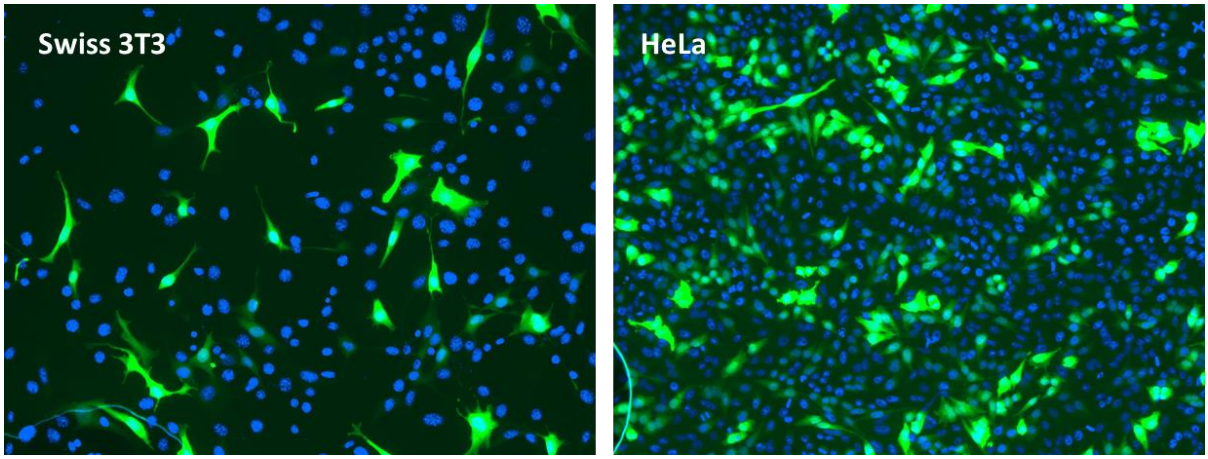

Figure 4o 20% transfection efficiency was achieved using Lipofectamine 3000

Swiss 3T3 and HeLa cells transfected with 0.5ug cDNA using 4.5ul lipofectamine 3000 per well in a 24 well plate. After 24 hours, cells were fixed and imaged on a widefield microscope. Transfection efficiency was calculated using a self-written script using Volocity imaging software (PerkinElmer). Transfected cells are green, nuclei are blue.

Therefore we made the decision to only validate Vangl2 shRNAs after they were grown into lentivirus particles, as viral infection produces a much higher DNA uptake efficiency than plasmid transfection.

In conclusion, we generated plasmid vectors containing shRNAs against Vangl2 in both pLKO.3G (for generation of 3rd generation lentiviruses), and pLVTHM (to be used in 2nd generation lentiviruses). Additionally, we replaced the GFP marker expressed by pLVTHM infected cells to express H2B-RFP. This could then be used to identify and quantify the angle of cell division in developing mammary organoids by the red fluorescence of cell nuclei in infected cells. Together, these would allow us to knock down Vangl2 in primary mammary organoids, and observe the effects of knockdown on epithelial structure, for example collective cell migration, orientation of cell division and regulation of cell shape.

Discussion

How epithelial tissues develop through the coordinated growth, rearrangement and shape changes of thousands of cells is a fundamental question in biology. Through recent developments in biomedical research including live imaging and organoid cultures, as well as analysis of fixed tissues and biochemical analysis, we can begin to piece together the individual processes which combine to produce different tissues with their own characteristic shapes and functions.

We aimed to understand the collective cell behaviours which drive the morphogenesis of epithelial tubes, and gain insight into how several organs develop and what can go wrong in disease. Most human cancers are of epithelial origin which arise as either a reversal of developmental processes, for example epithelial-mesenchymal transition (EMT) to mesenchymal-epithelial transition (MET) in cancer; or the reactivation of development pathways at the wrong time and place. Identification of proteins and pathways which contribute to disease opens the door to development of treatments, like small molecule pathway inhibitors.

We hypothesise that correct epithelial development is achieved through three processes which guide collective cell behaviours. These include collective cell migration directed by planar polarised movement of cells; cell divisions oriented to occur predominantly along the plane of a tissue; and control of cell shape changes through cytoskeleton and cell junction remodelling which collectively produce a properly shaped tissue.

Through our research we show imaging and biochemical evidence that some collective cell behaviours contribute to the morphogenesis of the mammary gland, which may be regulated by the core planar cell polarity pathway. These include different behaviours of cells in the mammary gland and the interactions between different compartments and the ECM; expression and localisation of a planar cell polarity protein during development; and limitations of mammary cell lines in 3D cultures.

3D Whole Mount Mammary Gland Imaging

Microscopic analysis of mammary gland development has largely been provided through histological staining of mammary tissue, or immunofluorescent staining of thin sections.

Here we developed a whole mount staining technique to visualise morphology at developmental stages including mature ducts and development during early pregnancy. Previous double immunofluorescent staining of whole mammary tissue pieces showed that ME cells are polarised along the length of the duct, while alveolar ME cells have a stellate morphology (Moumen et al., 2011). Here we showed this structural feature in excellent detail, for example Figure 1D.

In addition, a snapshot of the elongating duct showed an orthogonal ME cell arrangement which was not previously clear. Here, ME cells have a linear morphology and are arranged orthogonally to the duct (Figure 1F), suggesting that this arrangement may provide the mechanical force to mould the bulbous end into a more tubular shape, which is probable as ducts lacking ME cells do not form to the correct diameter. A main function of myoepithelial cells is their oxytocin induced contraction which forces milk through lactating ducts (reviewed in Murrell, 1995), although whether ME cell contraction is required to physically mould mammary ducts during elongation is unknown. Contraction is mediated by highly expressed smooth muscle actin (SMA) and heavy-chain myosin proteins in ME cell cytoplasm (Lazard et al., 1993), and mice lacking alpha-SMA suffer reduced lactation, although unimpaired duct development (Haaksma et al., 2011). Further research is required to establish whether ME cell contraction occurs to produce mammary ductal structure.

Myoepithelial cells, which differentiate from progenitors in the basal TEB, have been suggested to drive mammary duct branching by obstructing the migration of luminal cells through the ECM (Ewald et al., 2008). The SMA+ ME cell present in the apical region of the developing duct suggests however that differentiation is not limited to cells contacting the ECM. Furthermore, branching may be caused by the inhibitory effect of ME cells on LE cell growth, a mechanism suggested as ME cells are known to have tumour suppressing potential as an anatomical border, restricting Ductal Carcinoma In Situ (DCIS) from forming invasive cancers (reviewed in Barsky and Karlin, 2006).

Ewald et al., 2008 showed using primary organoid cultures that LE cells proliferate and migrate into gaps in ME cell coverage, followed by ME cell migration which separates LE cells and ECM. While our images of fixed elongating ducts are unable to corroborate this

observation (Figure 1n), recording these dynamic events would require live imaging of developing glands.

Unpublished evidence showed that LE cells require β1-integrin to maintain an open lumen in the mature duct, suggesting direct contact with the ECM (Akhtar personal communication), however they are thought to be separated by a continuous layer of ME cells. Figure 1Q suggests that LE cells may have protrusions which bypass the ME cell layer to contact the ECM, thus maintaining apico-basal polarisation.

Development of this whole mount staining and imaging technique provides a good foundation for future research, including potential to study the orientation of cell divisions in the duct and developing epithelia using antibodies against cell division machinery. However, α-tubulin antibody staining produced no clear signal; therefore this staining would require further optimisation. This technique could also be used to analyse cell behaviours and planar polarity manifestation in PCP mutant mammary glands. This is particularly possible using glands taken from Looptail (Vangl2) and Crsh (Celsr) mutant strains. We might expect to observe in these mutants abrogated polarity of ME cells along the duct, disorganisation of epithelial cell layers, or changes in diameter and branching patterns as observed in mutant kidney and lung (Yates et al., 2010, 2010b).

Whole mount staining would also allow observation of adherens junctions in mutant tissues by staining for proteins such as e-cadherin. Junction disruption could be expected as Vangl2 under or overexpression in MDCK cells impairs adherens junction formation (Lindqvist et al., 2010).

Yates et al., 2012 also observed that in PCP mutants, the sub-apical actomyosin ring which regulates lung lumen diameter, is incomplete and unpolarised. This important structural feature may also be required for mammary gland development, and the role of PCP pathways in its establishment could be clarified using this staining technique.

Finally we showed that confocal microscopy is a preferable method for imaging thick mammary gland tissue, as LSFM lacks the laser penetration and resolution to view epithelial structures due to the light scattering adipose tissue in the mammary stroma. Removal of fat

tissue using clearing solvents such as xylene before antibody staining may allow imaging at higher resolution by LSFM.

Vangl2 protein expression during mammary gland development

Due to the morphogenetic defects observed in multiple tissues in planar cell polarity mutant mice, it is strongly suggested that PCP pathways are active in mammalian morphogenesis. In Vangl2 and Celsr1 heterozygote mutant mice, abnormal lung and kidney development produces epithelia with inconsistent diameter, reduced branching events and loss of cortical actin organisation (Yates et al., 2010, 2010b).

We showed that Vangl2 expression in the mammary gland mirrors the phases of its development during puberty, with highest Vangl2 protein expression at 6 weeks when most ductal elongation and branching occurs. Higher Vangl2 protein expression coinciding with increased growth strongly suggests that PCP activity is important in driving cell behaviours which produce structure in the mammary gland. For example, Vangl2 may play roles in regulating actin dynamics during cell migration. Collective cell migration has been suggested to be partly controlled by the PCP pathway in kidney tubule morphogenesis (Karner et al., 2009), and in gastrulation (Wei et al., 2001). Rho Kinases (ROCK) and RhoGTPases are some factors which mediate cytoskeletal remodelling, with ROCK inhibition causing reduction in lung branching (Moore et al., 2002). ROCK is also essential for correct mammary gland development, as its inhibition reduces apical epithelial cell adhesion in organoid cultures (Ewald et al., 2012). Control of actin dynamics through RhoA and ROCK has been linked to PCP signalling in both flies and mammals. Planar cell polarity signalling regulates actin dynamics driving omatidial rotation through Drosophila Rho Kinase (Drok) by phosphorylation of non-muscle myosin regulatory light chain (Winter et al., 2001). The RhoA-ROCK polarising axis drives directed cell migration in many tissues, including in myocardium cells during heart development. In looptail +/- mice, RhoA localisation at the leading edge and filopodia of migrating cells is lost, with cells retaining normal cortical actin and failing to migrate (Phillips et al., 2005), suggesting Vangl2 is required to polarise actin dynamics machinery driving collective cell migration. All together published data and our observation of increased Vangl2 expression during pubertal mammary branching and

elongation suggests that PCP pathways may play a polarising role in directing collective cell migration.

Correlation between Vangl2 expression and epithelial morphogenesis events supports evidence that increased Vangl2 RNA and protein levels in breast cancer samples lead to a tumourigenic state. Cell proliferation, differentiation and disorganisation in cancer development has long been linked to resurgent activity of developmental signalling pathways in the wrong time or place, for example Wnt-Hedgehog signalling in the colonic epithelium causing colorectal cancer in adulthood (Bertrand et al., 2012), the second leading cause of cancer death worldwide (American Cancer Society, Colorectal Cancer Facts & Figures, 2011). Identification of oncogenic proteins increases our knowledge of potential targeted treatments for such diseases.

Strictly controlled cellular localisation of proteins regulating cell migration and shape is essential to restrict their actions to only parts of the cell, for example proximal strabismus in Drosophila pupal wing cells restricts actin polymerisation which ensures trichome development only in the distal part of each cell (Strutt and Warrington, 2008).

This is also true for Vangl2 in animal tissue development, with Vangl2 activity at anterior cell borders necessary for myosin II mediated contraction during xenopus convergent extension (Ossipova et al., 2015).

Although no trend appears in Vangl2 localisation to asymmetric membranes (e.g. proximal or distal) in 8 week old developing mouse mammary glands, punctal Vangl2 was observed at some cell membranes (Figure 2n). Highly stable punctal organisation of PCP core proteins including Frizzled and Strabismus at lateral junctions has been studied in the developing *Drosophila* wing, an important event in establishment of asymmetry and planar cell polarity (Strutt et al., 2011). Clustering of Vangl2 into membrane subdomains could suggest that Vangl2 in mice may function similarly to strabismus in *Drosophila*, with similar interactions between other members of the PCP core pathway. This could be tested by immunostaining for proteins such as mammalian homologues of *frizzled*, *prickle* or *flamingo* and looking for co-localisation in puncta at lateral membranes.

Surprisingly, we observed that when Vangl2-GFP is expressed in Eph4 cells and cultured in 3D Matrigel, Vangl2-GFP localises to cell membranes, in comparison to 2D adhesive cultures where cytoplasmic localisation is observed. These cells do form adherens junctions as shown by beta-catenin staining (Figure 4a).

Significant differences exist between 2D and 3D cultures which may cause this difference. Cells cultured in Matrigel are exposed to extracellular matrix components such as basement membrane proteins, collagen, proteoglycans and growth factors; as well as the opportunity for cells to make contacts on every membrane rather than only lateral membranes. We predict that in response to these factors, Vangl2 is preferentially recruited to cell contacts.

Vangl2's recruitment may coincide with apico-basal polarisation in 3D cultures, as Eph4 cells respond to laminin in Matrigel to specify their basal and apical domains. This may not be completely true as 2D cultured Eph4 cells secrete their own basement membrane, so may partially establish apico-basal polarity. Although crosstalk between apico-basal polarisation and PCP is limited, it has been shown that Frizzled activity is restricted by atypical protein kinase C (aPKC) at apical membranes in Drosophila eye cells (Djiane et al., 2005), and at the basolateral membranes of MDCK cells, overexpressed Vangl2 selectively binds to Scribble (Kallay et al., 2006). Basolateral targeting of Vangl2 may explain some basal localisation observed in mammary tissue (Figure 2n iii). Alternatively membrane targeting of Vangl2 may result from the increased time Vangl2 could be expressed and sorted in cells: 2D cells were fixed 24 hours after transfection, compared to 4 day in 3D culture.

Vangl2 functions in some tissues consisting of a single polarised epithelial layer, including *Drosophila* wing, trachea, mouse cochlear, lungs and kidneys. Furthermore activity in many of these tissues is observed at lateral cell junctions rather than apical or basal membranes. It is therefore likely that a degree of apico-basal polarisation is necessary for Vangl2 recruitment to cell junctions in this 3D Eph4 model. However it is clear that in *Drosophila* pupal wing cells, localisation to lateral membranes is first established by homophilic *flamingo* binding at junctions, followed by recruitment of other core proteins.

As well as analysis of other PCP proteins in mammary development by immunofluorescence and immunoblotting, RNA expression levels could be measured by quantitative PCR (qPCR)

to clarify whether PCP expression profiles mirror pubertal development in a similar manner to Vang2 protein expression.

3D Cell Culture Methods to study Epithelial Morphogenesis

Recent advancements in 3D cell and organoid culture techniques and ability to live-image morphogenesis using dyes and proteins with fluorescent conjugates has allowed us to observe some cell behaviours which drive epithelial development. These include ex-vivo organoid cultures of stem cell populations from the mammary glands and pancreas of mice.

Although several publications take advantage of primary 3D mammary organoid cultures, Eph4 mammary cell lines also form into apico-basally polarised acini when cultured in Matrigel and do not require animal culling or cell fractionation which primary cultures do.

While 3D Eph4 cultures stimulated with growth factors such as HGF have developed tubular arrangement (which did not mimic normal ductal morphology observed in tubular epithelia), addition of FGF2 to organoid cultures stimulates elongation and branching of primary organoids in a similar fashion to the Terminal End Bud in vivo. We showed that addition of FGF2 to Eph4 3D cultures does not result in tubulogenesis. Consequently it is not possible to use this model to study morphogenesis of tubular epithelium.

We hypothesised that this may be due to lack of other cell types present in organoid cultures, including myoepithelial cells. We tested Wang et al.'s (2010) evidence that co-culture with fibroblasts may be sufficient to arrange mammary epithelial cell lines into differentiated more tubular structures. However, although Eph4 and Swiss 3T3 cells did interact, no tubulogenesis or repeated 3D interactions were observed. Future experiments may involve co-culture between Eph4 cells and a basal cell line. For example SUM149 cells are a triple negative cell line originally derived from inflammatory breast cancer which shows high Vangl2 expression (Puvirajesinghe et al.,2016). SUM149 may have lost differentiation compared to myoepithelial cells as they are isolated from breast cancer samples, so may not be a good model for their replacement in co-culture experiments.

Inability to form tubes may be a limitation of cell lines: Eph4 cells are highly proliferative and were originally derived from a mid-pregnant mouse when a high rate of mammary development occurs. Contrastingly, fresh mammary stem cell populations which develop

into mammary organoids in culture likely have better potential to differentiate and respond to signalling cues. However, we intriguingly showed that Eph4 cell cultures differ in expression profiles from cell to cell. Some cells show high K14 protein expression (like myoepithelial cells), while most display high K8/18 expression (as seen in luminal epithelial cells). Although K14 expressing cells maintain luminal cell characteristics such as adhesion with neighbouring cells and 'cobblestone' morphology, these results suggest that in the correct environment, Eph4 cells may be capable of further differentiation into myoepithelial lineage.

Therefore while primary organoid cultures probably remains the gold standard for observing morphogenesis in 3D and real time, Eph4 cells show potential in their use for studying epithelial tubulogenesis, however further research into environmental cues and supporting cells is required.

Conclusion

We showed in this thesis a deeper insight into mammary morphogenesis through developing a whole mount imaging technique, evidence that planar cell polarity pathways play a role in pubertal mammary gland development, and studied alternatives to primary organoid cultures in epithelial tubulogenesis. We also developed tools which could be used in the future to analyse planar polarised processes in mammary organoid cultures, including knockdown of Vangl2 using lentiviral delivery of shRNAs and integration of fluorescent-tagged histones.

These tools can be used to show whether PCP pathway knockdown results in abrogated development as observed in other tissues, and in PCP mutant development of lungs and kidneys. For example, questions remain unanswered such as whether polarised cell divisions drive mammary elongation, or whether cells in developing ducts collectively migrate in one direction due to planar polarisation.

Planar cell polarity pathways play essential roles in tissues from flies to mice, and have been studied in development of epithelial organs as well as in early body patterning and development of some sensory organs such as the mouse ear and Drosophila eye. As well as the importance of understanding the mechanics of how PCP is established and manifests in

polarised tissues, how these processes translate to 3D organism development is essential to analyse how human development occurs, and how disease manifests when these processes go awry. Further research is required to confirm the role of PCP pathways in mammary gland development, and how morphogenesis can be observed, experimentally altered and analysed by the most efficient methods.